Dedicated to

*My Parents*

## ACKNOWLEDGEMENTS

I would like to thank my supervisor Dr. Punyabrata Pradhan for his guidance and patience and encouragements. The depth of his insight always motivated me in solving problems. I would also like to thank Dr. Sakuntala Chatterjee and Prof. Subhrangshu Sekhar Manna for their questions, suggestions and encouragements during seminars and conferences. I would like to thank our collaborator Prof. P. K. Mohanty from Saha Institute of Nuclear Physics for suggestions and advices. I acknowledge financial support during 2012-2016 from Council of Scientific and Industrial Research, India [grant No. 09/575(0099)/2012-EMR -I] and S. N. Bose National Centre for Basic Sciences for 2017. I appreciate S. N. Bose National Centre for Basic Sciences for providing facilities for this research work.

I thank Dr. Arup Roy, my teacher and mentor, for his eccentric lessons and motivations. His morality and punctuality inspired me in every sense and enriched me to be a better human being.

I would like to thank my group mates Arghya, Subhadip, Amal, Dhiraj for time to time academic and non academic discussions. I wish Anirban, our new group mate a very good luck.

I would like to thank Biplab, Ashutosh, J.B., Arnab, Debanjan, Ishita, who have been lovely batchmates and cheerful friends. I would like to thank Shauri, Debolina, Chandreyee for many cherishable moments. I am indebted to my senior Rudra Banerjee for his friendship and guidance. Amartya da, Kapil da, Animesh da, Arghya da and Semanti di owe my sincere gratitude for their companionship and support. I must name Debmalya da, whose lively presence and laughter inspire me to stay positive in utmost negative situations.

I would love to thank my juniors Suman, Subrata, Souvanik, Rajkumar, Rakesh, Suchetana, Dipanjan, Tuhin, Shreya for their company.

I have spent a cool time with Yendrembam Chaoba Devi and Sreeraj T. P. during their stay at SNB. I am indebted to this couple for their immense positive energy and optimistic views. They have been bestest friends one could have in life. Chaoba's sisterly love and inspiration is still with me. I thank them and wish their well being all along.

I thank Anirban Samanta, who has been dearest friend from my M.Sc times for his extreme care, support and inspiration.

I thank Subhasish Chakrabarty for being with me for the last six years and bear with my moods.

Finally, I want to *thank* my parents who are by my side every now and then. They have taught me the meaning of punctuality, honesty and simplicity. Their support builds my inner strength in every situation. I am proud to be their daughter. I doubt whether any amount of thanks is enough for them!

Lastly, I wish to thank my life for making me tough for the last few years.

# PUBLICATIONS

## PAPERS TO BE INCLUDED IN THE PH.D. THESIS

- **Gammalike mass distributions and mass fluctuations in conserved-mass transport processes**, Sayani Chatterjee, Punyabrata Pradhan and P. K. Mohanty, Phys. Rev. Lett. **112**, 030601 (2014).

- **Zeroth law of thermodynamics for nonequilibrium steady states in contact**, Sayani Chatterjee, Punyabrata Pradhan and P. K. Mohanty, Phys. Rev. E **91**, 062136 (2015).

- **Hydrodynamics, density fluctuations and universality in conserved Manna sandpiles**, Sayani Chatterjee, Arghya Das and Punyabrata Pradhan *(submitted)*.

## OTHER PUBLICATIONS

- **Additivity property and emergence of power laws in nonequilibrium steady states**, Arghya Das, Sayani Chatterjee, Punyabrata Pradhan, and P. K. Mohanty, Phys. Rev. E **92**, 052107 (2015).

- **Spatial correlations, additivity and fluctuations in conserved-mass transport processes**, Arghya Das, Sayani Chatterjee, and Punyabrata Pradhan, Phys. Rev. E **93**, 062135 (2016).

# CONTENTS

## LIST OF FIGURES

## LIST OF TABLES

# 1

# INTRODUCTION

## 1.1 EQUILIBRIUM SYSTEMS AND ADDITIVITY PROPERTY

Equilibrium systems are characterized by time-stationary state where net energy or particle current is zero. A system is said to be in *mechanical equilibrium* if there is no net force acting on it and, similarly, in *thermal equilibrium* if temperature throughout the system is uniform and takes the same value as that of a surrounding or an environment (also called heat bath or heat reservoir). Likewise, a system is said to be in *chemical equilibrium* if its chemical composition is also the same throughout the system. Thus, when a system is in mechanical, thermal and chemical equilibrium simultaneously, it is called *thermodynamic equilibrium*. Classical theory of thermodynamics deals with macroscopic properties of various states of matter in equilibrium systems, which consist of large degrees of freedom corresponding to the discrete microscopic constituents. On the other hand, the task of statistical mechanics is to provide a framework in terms of microscopic principles, i.e., in terms of properties of the microscopic constituents, where fluctuations can characterized and the laws of classical thermodynamics could be derived.

According to classical thermodynamics, a finite set of thermodynamic variables characterize equilibrium state of a system. There are two types of such variables as following. (i) Extensive thermodynamic variables: These variables are proportional to the volume of the system, e.g., number of particles $N$, internal energy $E$ and various thermodynamic potentials such as entropy $S$ and free energy $F$. (ii) Intensive thermodynamic variables: These variables do not depend on the system size, rather depend on densities; temperature $T$, chemical potential $\mu$, pressure $P$ are examples of such variables. When two systems are put in contact so that they can exchange conserved quantities such as energy, particle or volume and eventually equilibrate to achieve a time-translational invariant state (called steady state), the intensive variables of the individual systems equalize and attain the same value throughout the combined system. Intensive variables are usually functions of energy density and/or number density.

For example, let us consider a gas of molecules. The system is described by the positions and momenta of the constituent molecules. A complete specification of configuration or phase space of the system $C \equiv \{x_i, p_i\}$, where $i$ is particle index, could be given by specifying positions and momenta of all particles. System can evolve through collision, from one configuration or phase space point to another. The statistical description of the system could then be provided in terms of the probability $P(C,t)$ of a configuration $C$ at time $t$. When a system reaches equilibrium, probability $P_{eq}(C)$ of the equilibrium configuration becomes stationary or time independent, i.e., $P_{eq}(C) = \lim_{t\to\infty} P(C,t)$. If the system is kept isolated (no exchange of energy of particles with environment), all configurations are equally probable, i.e,

$$P_{eq}(C) = \frac{1}{\Omega}, \tag{1.1}$$

where $\Omega$ is total number of configurations having a constant energy value. This distribution is known as *microcanonical* distribution. Now, if the system is allowed to exchange energy with a heat reservoir keeping the average energy of itself fixed, the probability of a certain configuration $C$ is given by Boltzmann distribution

$$P_{eq}(C) = \frac{\exp[-\beta E(C)]}{Z}, \tag{1.2}$$

where $\beta$ is inverse temperature of the heat bath/environment and $Z = \sum_C \exp[-\beta E(C)]$ is normalisation constant called the canonical partition function of the equilibrium system. thus, this is the *canonical* description of the system. The canonical or Helmholtz free energy of the system is defined as $F(\beta, N, V) = -\beta \ln(Z)$ and is a function of inverse temperature $\beta$, number of particles $N$ and volume $V$ of the system. Similarly, if this system is also allowed to exchange particle with the environment keeping the average number of particles fixed, the probability of a configuration is given by

$$P_{eq}(C) = \frac{\exp[-\beta E(C) + \beta\mu N]}{\mathcal{Z}}, \tag{1.3}$$

where $\mu$ is chemical potential and $\mathcal{Z}$ is grandcanonical partition function. This description is called *grandcanonical* description of the system. The grandcanonical free energy is written in terms of the partition function as $G(\beta, \mu, V) = -\beta \ln(\mathcal{Z})$ and is a function of inverse temperature $\beta$, chemical potential $\mu$ and volume $V$.

A remarkable feature of systems in equilibrium is additivity property (or simply additivity), which is satisfied irrespective of the details of interactions among the microscopic constituents in the system, provided the interactions are short-ranged. Additivity, a tenet of equilibrium thermodynamics, states that, if a system is divided into many subsystems, total

free energy (or entropy for an isolated system) of the system is sum of the free energies of the individual subsystems. For example, consider a system, kept at temperature $T$, which is divided into two subsystems with masses $M_1$ and $M_2$. Due to exchange of masses between the two subsystems, the subsystem masses $M_1$ and $M_2$ are fluctuating variables, however with total mass $M = M_1 + M_2$ being conserved. Then total free energy of the system can be written as $F(M) = F_1(M_1) + F_2(M_2)$. In other words, the joint probability distribution of the subsystem masses $M_1$ and $M_2$ can be approximately written in a factorized form,

$$\mathcal{P}(M_1, M_2) \simeq \frac{e^{-\beta F_1(M_1)} e^{-\beta F_2(M_2)}}{Z} \delta\left(M_1 + M_2 - M\right), \tag{1.4}$$

where $Z = \exp(-\beta F)$ is normalization constant or the partition sum. Consequently, macrostate, or the most probable state, of the system can be obtained by minimizing total free energy function $F$ with respect to $M_1$ (or equivalently, $M_2$) along with the constraint $M = M_1 + M_2 =$ constant. The minimization leads to the following equality,

$$\mu_1 \equiv \frac{\partial F(M_1)}{\partial M_1} = \frac{\partial F(M_2)}{\partial M_2} \equiv \mu_2, \tag{1.5}$$

which implies that the macrostate of the system is characterized by the condition that chemical potentials $\mu_1$ and $\mu_2$ of the two subsystems must equalize.

Therefore, additivity property leads to equalization of intensive thermodynamic variables such as the above mentioned chemical potential $\mu$ (corresponding to exchange of particles or mass between subsystems) or temperature $T$ (corresponding to energy exchange) and pressure $P$ (corresponding to volume fluctuation), etc. Another consequence of additivity is fluctuation response relation (FR), which relates the fluctuation of the average subsystem mass ($\langle m \rangle$), to the response due to change in chemical potential $\mu$,

$$\frac{d\langle m \rangle}{d\mu} = \sigma_v^2 = \langle m^2 \rangle - \langle m \rangle^2, \tag{1.6}$$

or in terms of density $\rho = \langle m \rangle / v$,

$$\frac{d\rho}{d\mu} = \sigma^2, \tag{1.7}$$

where $\sigma^2 = \lim_{v \to \infty} \sigma_v^2 / v$ is the scaled variance and $v$ is the subsystem size.

Closest counterpart to equilibrium system are those having a nonequilibrium steady state (NESS), which are characterized by a finite steady flux of particle or energy. These systems acquire energy or particle from an external source and dissipate on average, an equal amount of it to the surroundings, thereby maintaining a steady state with a constant mean energy or particle flow. Now, the surroundings or environment has infinite degrees of freedom and

it is impossible to have the knowledge of detailed microscopic description of the environment. Thus the environment/bath is completely stochastic in nature and the dynamics of the system under consideration becomes solely random and probabilistic due to the contact with this stochastic bath. The system now cannot be described by Newtonian Dynamics. We need a stochastic setup to model this kind of systems preserving the dynamics, because, the dynamics is important to determine the steady state of the system. In this thesis, we are going to focus on nonequilibrium systems which evolve obeying markovian dynamics, which is simplest to analyze and could be efficiently simulated in computers. In the next section, Markov process is briefly introduced.

## 1.2 MARKOV PROCESS

A random number or stochastic variable is an object X defined by a set of possible values, which is called "Range" or "Set of States" or "Sample Space" or "Phase Space". This set may be discrete or continuous, e.g., head or tail of coin tossing problem, one velocity component of a Brownian particle ranging from $(-\infty \to +\infty)$. A probability distribution can be associated over this set.

*Markov Property:* A stochastic process has the Markov property if the conditional probability distribution of future states of the process, given the present state and the past, depends only on the present state, i.e. the past is irrelevant as it does not matter how the current state is reached. Let us consider a system having configurations $X(t)$ at time $t = t_0, t_1, t_2, \cdots t_n,$. The time evolution of this system is Markovian if

$$P[(X(t_{n+1}) = i_{n+1}|X(t_n) = i_n, \cdots, X(t_0) = i_0] = P[X(t_{n+1}) = i_{n+1}|X(t_n) = i_n] \tag{1.8}$$

*Markov Chain:* The discrete time Markov process is called Markov chain. Let $X_n$ stands for the state of the system at time $t = n$. The configuration space of the system is denoted by $\mathbb{C}$. The probability that the system is in the configuration $C$ at time $n$ is $P_n(X_n = C)$. The Markov property helps to define the transition probability from one configuration $C$ to another configuration $C'$ as $W(C \to C') = P(X_n = C'|X_{n-1} = C)$.

*Master Equation:* The time evolution of a system obeying stochastic Markovian dynamics can be expressed by master equation. Markov chain is governed by a discrete time master equation as

$$P_{n+1}(C) = \sum_{C'} W(C' \to C) P_n(C') \quad \forall C' \in \mathbb{C}, \quad \forall n. \tag{1.9}$$

The solution of this equation gives the probability of a certain configuration $C$ at time $n$. We can span $P_n$ in a finite dimensional vector space having basis vectors $|C\rangle$ as

$$|P_n\rangle = \sum_C P_n(C)|C\rangle. \tag{1.10}$$

The transition probabilities $W(CC')$ form a matrix which is called transition matrix. The matrix is given by

$$W = \sum_{C,C'} W(C' \to C)|C\rangle\langle C'|, \tag{1.11}$$

where $\langle C'|$ forms the basis of the dual vector space. The bases $|C\rangle$ and $\langle C'|$ satisfy a scalar product relation as $\langle C'|C\rangle = \delta_{C,C'}$. The elements of the $W$ matrix satisfy the following relation

$$\sum_{C'} W(C \to C') = 1, \forall C' \in \mathbb{C}. \tag{1.12}$$

Then, as a direct consequence of the master equation in Eq. 1.9, we can write the time evolution equation in an iterative form as

$$|P_{n+1}\rangle = W|P_n\rangle, \tag{1.13}$$

which implies the following

$$|P_{n+1}\rangle = W^n|P_0\rangle. \tag{1.14}$$

When the system reaches steady state at $t \to \infty$, the steady state probability vector does not change anymore. So, Eq. 1.13 is written as

$$|P_{st}\rangle = W|P_{st}\rangle. \tag{1.15}$$

Thus $|P_{st}\rangle$ turns out to be the eigenvector of $W$ matrix with eigenvalue 1. For systems, which perform a discrete time Markovian dynamics, the steady state distribution can be determined by looking at the normalized eigenvector corresponding to the largest eigenvalue of $W$ matrix, which is always 1. The real part of other eigenvalues are lesser than 1 so that, the eigenvectors corresponding to those eigenvalues cannot represent the steady state probability vector of the system.

For continuous time dynamics, the master equation is given by

$$\frac{\partial|P(C,t)\rangle}{\partial t} = \sum_{C'\neq C}[W_{C'C}|P(C',t)\rangle - W_{CC'}|P(C,t)\rangle] \tag{1.16}$$

$$= \mathbb{W}|P(C,t)\rangle. \tag{1.17}$$

In this case, the elements of the $\mathbb{W}$ matrix obey the following relation

$$W(C\to C) = -\sum_{C',C'\neq C} W(C\to C'). \tag{1.18}$$

The steady state of the system is given by the eigenvector corresponding to the largest eigenvalue 0 of matrix $\mathbb{W}$.

*Detailed Balance:* Before proceeding to our next discussion, we take simple notation for $|P(C)\rangle$ as $P(C)$.

For equilibrium systems, probability of a configuration is time independent and probability current between the elements of every pair of configurations vanishes. So, Eq. 1.16 gives us

$$W_{C'\to C}P(C') - W_{C\to C'}P(C) = 0 \qquad \text{for any pair of } C \text{ and } C'. \tag{1.19}$$

Eq. 1.19 is called *Detailed Balance* condition which is valid only for equilibrium systems. From, Eq. 1.19, we have

$$\frac{P(C)}{P(C')} = \frac{W_{C'\to C}}{W_{C\to C'}} = \exp\left[-\beta\{E(C) - E(C')\}\right], \tag{1.20}$$

where $\exp[-\beta E(C)]$ is the Gibbs Boltzmann factor for equilibrium probability distribution of a configuration $C$ and $E(C)$ is the confirgurational energy of the same. Thus, the transition rate between the configurations $C$ and $C'$ can be written in terms of equilibrium probability distributions of the corresponding configurations. The necessary and sufficient condition to check the validity of detailed balance in an arbitrary stochastic system without using the steady state probability distributions is Kolmogorov loop criterion. For a cycle of $n > 2$ configurations $C_1 \to C_2 \to C_3, \cdots, \to C_n \to C_n$, provided detailed balance in Eq. 1.19 is satisfied, we can write the following,

$$P(C_1) = \frac{W(C_2\to C_1)}{W(C_1\to C_2)}P(C_2,)$$

$$= \frac{W(C_2\to C_1)W(C_3\to C_2)}{W(C_1\to C_2)W(C_2\to C_3)}\cdots\frac{W(C_1\to C_n)}{W(C_n\to C_1)}P(C_1). \tag{1.21}$$

Hence, as an implication of the above equation, we have

$$W(C_1 \to C_2)W(C_2 \to C_3)\cdots W(C_n \to C_1) = W(C_2 \to C_1)W(C_3 \to C_2)\cdots W(C_1 \to C_n). \tag{1.22}$$

Conversely, if the equality in the Eq. 1.22 is valid for every cycle, then detailed balance will be satisfied and the system will be in equilibrium. The Kolmogorov loop criterion is the implication of time reversibility in the equilibrium systems.

On the contrary, for nonequilibrium steady state systems, though probability of a configuration is time independent, probability current between the elements of every pair of configurations is not zero and the time reversibility is violated. So, detailed balance is not satisfied. The steady state is governed by

$$\sum_{C'} W_{C' \to C} P(C') - W_{C \to C'} P(C) = 0, \tag{1.23}$$

where each term in the summation does not vanish. In this case, the solution of the steady state distribution is nontrivial and is not given by the equilibrium Boltzmann-Gibbs distribution. Thus it becomes difficult to calculate the macroscopic observables even at steady states. So, what are the large scale spatial structures in these nonequilibrium steady state systems? Is it possible to have a statistical mechanics framework to characterize the large-scale in the steady state?

In this thesis, to address these questions and investigate the steady state properties of nonequilibrium steady state systems, we explore a broad class of paradigmatic models having a nonequilibrium steady state. These model systems consist of interacting microscopic constituents, called particles or masses in general. These systems are collectively called mass transport processes in literature. Varieties of system in nature involve microscopic dynamics of fragmentation, diffusion and coalescence of masses, e.g., in clouds [1], fluids condensing on cold surfaces [2], suspensions of colloid-particles [3], polymer gels [4], etc. These systems have different nonequilibrium steady states as underlying dynamics are widely varied. To study the statistical properties of these natural processes, physicists have introduced several conserved discrete and continuous mass transport processes on discrete and continuous spatial dimensions with discrete, continuous or mixed update rules [5–14]. These models are easy to define in terms of simple dynamical rules, but contain interesting rich physical structure. In the next section, we briefly introduce some of these models and describe their general structure and common features.

### 1.3.1 *Force fluctuation in granular bead packs:*

To study structure and properties of granular material when external force is applied on it, Liu *et al.* [15, 16] proposed a theoretical model of regular two dimensional lattice systems where each site contains a bead of unit mass. The $i^{th}$ site of layer $D$ is connected to $N$ sites in layer $D+1$. The beads support the beads of upper layers. A random fraction $q_{ij}$ of the total weight $w(D,i)$ supported by $i^{th}$ particle in layer $D$ is transmitted to $j^{th}$ particle in the next layer $D+1$. Thus, $w(D,i)$, satisfies a stochastic equation

$$w(D+1,j) = 1 + \sum_i q_{ij}(D) w(D,i), \tag{1.24}$$

where the random fraction $q_{ij}$s are identical random variables with the force balancing constraint $\sum_j q_{ij} = 1$. For uniform $f(q_{ij})$, the probability of realizing a given set of $q$'s at each site $i$ could be well approximated by a factorized distribution function of the form

$$P(q_{i1}, \cdots, q_{iN}) = \prod_j f(q_{ij}) \delta(\sum_j q_{ij} - 1). \tag{1.25}$$

In this case, under mean field approximation, the probability distribution of scaled force $v = w/D$ for large values of $D$ is shown to be

$$P(v) = \frac{N^N}{(N-1)!} v^{N-1} \exp(-Nv). \tag{1.26}$$

Authors also showed that, under mean field approximation, for any generic continuous density function of $q$, $P(v) \propto v^{N-1} \exp(-Nv)$ as $v \to \infty$ and $P(v) \propto v^{N-1}$ as $v \to 0$. The mean field theory turns out to be exact for uniform $f(q)$. This force fluctuation model is later mapped on to asymmetric mass transfer model for discrete time dynamics by Krug and Garcia [7] and Rajesh and Majumdar [8]. The interesting point is, the granular bead pack system definitely has finite spatial correlations, which is neglected in these studies. Thus there remain open issues to be addressed.

### 1.3.2 *Asymmetric interacting particle system*

J. Krug and J. Garcia [7] studied discrete particle systems on a continuous line keeping total particle number conserved. This model on continuous space appears in applications to traffic systems in cities [17, 18]. Let us consider $N$ particles distributed randomly on continuous one dimensional space of length $L$. The configuration is denoted by the position $x_i$ of the $i^{th}$

particle $C : \{x_i\}$ where $i = 1, 2, \cdots N$. A particle $i$ jumps to its right direction to a position $x_i + \delta_i$, where $\delta_i < (x_{i+1} - x_i)$ with a jump rate $\gamma$. The gap between two particles is denoted as $(x_{i+1} - x_i) = u_i$ and the configuration space could be written in terms of this gap variable $u_i$. So, $\delta_i$ is a random fraction of the gap $u_i$ and has some distribution function

$$f_i(\delta_i) = u_i^{-1} \phi\left(\frac{\delta_i}{u_i}\right). \tag{1.27}$$

The jump rate $\gamma$ could be a function of the gap variable $u_i$, i.e. $\gamma = \gamma(u_i)$. Taking $\phi(y)$ as a uniform distribution and the jump rate $\gamma(u) = u$, the model describes Hammersley process where the distribution of particle position is shown to be a Poisson distribution for continuous time dynamics. In their work, authors considered jump rate $\gamma = 1$, which is independent of the gap variable $u_i$ and jump length distribution as Eq. 1.27. The dynamics is governed by

$$x_i' = y x_i + (1 - y) x_i, \tag{1.28}$$

where $y \in [0, 1]$ and is drawn from the distribution $\phi(y)$. This model is called as Asymmetric Random Average Processes (ARAP).

*Continuous time dynamics:* For continuous time dynamics, for any form of $\phi(y)$, the two-point correlation function of gap variables $\langle u_i u_j \rangle$ factorizes at steady state and the variance in gap variable is given by

$$\sigma^2(u) = \langle u^2 \rangle - \langle u \rangle^2 = \frac{\mu_2}{\rho^2(\mu_1 - \mu_2)}, \tag{1.29}$$

where $\rho$ is particle density and $\mu_n$ is the $n^{th}$ moment of the distribution $\phi(y)$. For uniform $\phi(y)$ and $\langle u_i \rangle = 1$, assuming the pairwise independence of the gap variable $u_i$, the moments of the gap variables are calculated and it is shown that the probability distribution of the gap variable $P(u)$ is a gamma distribution

$$P_\eta(u) = \frac{\eta^\eta}{\Gamma(\eta)} u^{\eta - 1} \exp(-\eta u), \tag{1.30}$$

where $\eta = 1/2$ for continuous time dynamics.

*Discrete time dynamics:* The discrete time dynamics of ARAP is given by

$$u_i(t + 1) = u_i(t) - \delta_i(t) + \delta_{i+1}(t), \tag{1.31}$$

where $\delta_i = y_i u_i$. $y$ is a random variable having a distribution $\phi(y)$. For any form of $\phi(y)$, the two-point correlation function of gap variables $\langle u_i u_j \rangle$ again factorizes at steady state and the variance in gap variable is given by

$$\sigma^2(u) = \langle u^2 \rangle - \langle u \rangle^2 = \frac{\mu_2 - \mu_1^2}{\rho^2(\mu_1 - \mu_2)}, \tag{1.32}$$

where $\rho$ is particle density and $\mu_n$ is the moments of the distribution $\phi(y)$. For uniform $\phi(y)$ and $\langle u_i \rangle = 1$, assuming the pairwise independence of the gap variable $u_i$, the moments of the gap variables are calculated and it is shown that the probability distribution of the gap variable $P(u)$ is a gamma distribution as in Eq. 1.30, where $\eta = 2$ for discrete time dynamics.

Later, in the year 2002, F. Zielen and A. Schadschneider [12] revisited ARAP having continuous mass vaiables $m_i$ on a periodic lattice with $L$ sites with parallel dynamics. They studied this model varying the fraction density $\phi(y)$. As a result, they found a class of density function which yield product measure steady state for ARAP. They calculated $P(m)$, the probability distribution of single site mass $m$ exactly, which turns out to be a gamma distribution. In addition, it was found that mean field ansatz works extremely well for this class of $\phi(y)$. They showed that even if product measure does not hold at steady state, mean field approximation provides a very good approximation for this class of fraction density function $\phi(y)$.

### 1.3.3 *Conserved - mass transport models and particle systems in one dimension*

Rajesh and Majumdar [8] introduced a mass transport model on a discrete lattice system of size $L$ with periodic boundary conditions. At each site $i$, there resides mass variable $m_i \geq 0$. $m_i$ could be discrete or continuous. Total mass $M = \sum_i m_i$ remains conserved. Average single site mass is given by $\rho = M/L$. At each time step, a random fraction $y_i$ of mass $m_i$ is chosen and transferred to its nearest neighbor with probability $p$. If the mass transfer occurs in one preferred direction then the system is called asymmetric system. In symmetric mass transport systems, the random fraction of the mass will transfer to any one of the two neighbors with probability $1/2$.

*Asymmetric mass transfer:* The limit $p = 1$ corresponds to discrete time dynamics and is governed by the equation

$$m_i(t+1) = y_{i-1} m_{i-1}(t) + (1 - y_i) m_i(t). \tag{1.33}$$

This is the same model as studied by Coppersmith *et al.* to study force fluctuation in bead packs as previously mentioned. In this work, Rajesh and Majumdar proved rigorously that

steady state joint mass distribution factorises exactly, which means all $n$ point correlations are zero ($n \geq 2$). The single site mass distribution is given by

$$P(m) = \frac{4m}{\rho^2} \exp\left(\frac{-2m}{\rho}\right). \tag{1.34}$$

For $p < 1$, it is shown that steady state joint mass distribution does not factorise exactly. In this case, for $p = 0$ limit, which corresponds to continuous time dynamics, $P(m)$ is calculated under mean field approximation as

$$P(m) = \frac{1}{\sqrt{2\pi\rho m}} \exp\left(-\frac{m}{2\rho}\right). \tag{1.35}$$

Remarkably it is in very good agreement with numerical results. For aribitrary $p$, it remains difficult to calculate $P(m)$ in closed form, but asymptotic behaviors of the distribution was obtained by authors correctly for $p = 0$ and $p = 1$ case. For $p \to 0$, authors reproduced the result reported by Krug *et. al.* [7] for two-point spatial correlation function $C(r) = \langle m(0)m(r)\rangle$ and found $C(r) = \rho^2$ for $r > 0$.

*Symmetric mass transfer:* In symmetric mass transfer, the dynamics is governed by the following equation,

$$m_i(t+1) = (1 - y_i)m_i(t) + \frac{1 + s_{i-1}}{2} y_{i-1} m_{i-1}(t) + \frac{1 + s_{i+1}}{2} y_{i+1} m_{i+1}(t), \tag{1.36}$$

where $y_i$ is a random variable having a distribution $\phi(y) = (1 - p)\delta(y) + p$ and $s_i$ can be either $+1$ or $-1$ with probability $1/2$. In this model, it is shown that product measure is exact when $p = 0$ limit (continuous time dynamics) is reached. Using mean field approximation, $P(m)$ is calculated and it is given by Eq. 1.35. Otherwise, for arbitrary $p > 0$, steady state joint mass distribution is not factorized. $P(m)$ calculated under mean field calculation is significantly different from that obtained from numerical simulation. Two point spatial correlation function was also calculated in this case. At $p = 0$ limit, $C(r) = \rho^2$ but for arbitrary $p > 0$, symmetric model has nontrivial spatial structure.

For discrete mass variable and asymmetric particle transfer, under mean field approximation, particle distribution $P(m)$ was calculated for random sequential limit and parallel limit. In this discrete mass model also, mean field approximation seems to be exact only for random sequential case.

### 1.3.4 *Conserved-mass models with stickiness and chipping*

S. Bandyopadhyay and P. K. Mohanty [14] in their way to characterize mass transport models where steady state joint mass distribution is not factorized, introduced *stickiness parameter* $\lambda$

to the mass transfer models studied by Rajesh and Majumdar [8]. Their model is defined on a discrete lattice system of size $L$ and total mass $M$ on a periodic boundary. Sites contain a non negative continuous mass variable which can evolve asymmetrically or symmetrically depending on the dynamics.

In *asymmetric mass transfer* case, called as Asymmetric Sticky Chipping Model (ASCM), $\lambda$ fraction of mass $m_i$ sticks to the site $i$ and $(1-\lambda)$ fraction of mass is chipped off. Then, a random fraction $y_i$ of that chipped of mass $(1-\lambda)m_i$ is transferred to the right nearest neighbor and rest comes back to the departing site $i$. For $\lambda = 0$, this model boils down to the asymmetric mass trasfer model studied by Rajesh and Majumdar in [8]. In *symmetric mass transfer*, called as Symmetric Sticky Chipping Model (SSCM), $\lambda$ fraction of mass $m_i$ sticks to the site $i$ and $(1-\lambda)$ fraction of mass is chipped off. A random fraction $y_i$ of that chipped of mass, $(1-\lambda)m_i$, is transferred to the right nearest neighbor $i+1$ and rest goes to left nearest neighbor $i-1$. In their work, Bandyopadhyay and Mohanty showedx that in the presence of stickiness $\lambda \neq 0$, ASCM and SSCM have product measure state neither for random sequential dynamics nor for parallel dynamics. They used perturbation approach around $\lambda = 0$ to calculate $P(m)$ under mean field approximation and found convincing result which was numerically verified for ASCM. On the contrary, in case of SSCM parallel update, their approach to calculate $P(m)$ fails and analytic and numerical results differ significantly due to the presence of finite spatial correlation.

### 1.3.5 *Wealth Distribution Model:*

A large class of models have been proposed in the last few decades to explain realistic wealth exchange in social sciences [19–21]. These models are defined on a one dimensional system of $L$ sites having continuous wealth variable $m_i$. Total wealth of the system $M$ remains conserved. A pair of two agents $i$ and $j$ are randomly selected and allowed to trade between themselves. Each of them save a fraction $\lambda$ of their wealth to themselves and rest of the wealth $(1-\lambda)m_k$ is going to be shuffled. A random fraction $y$ of the total trade off wealth $(1-\lambda)(m_i+m_j)$ goes to one agent and the other $(1-y)$ fraction goes to the other agent. Though, the steady state joint mass distribution is not known, single site distribution of wealth has been obtained in this model. For homogeneous system, $\lambda$ is same for all of the agents and single agent wealth distribution is described by gamma distribution

$$P_\eta(m) = \frac{1}{\Gamma(\eta)}\left(\frac{\eta}{\langle m\rangle}\right)^\eta m^{\eta-1}\exp\left(-\frac{\eta m}{\langle m\rangle}\right), \tag{1.37}$$

where $\eta$ is a function of $\lambda$. For heterogeneous system, where $\lambda \in [0,1]$ is site dependent random variable, exponential law is a nice approximation for intermediate $m$ value but for

large values of $m$, distribution goes as a power law which is well known Pareto law. The exponent of the power law depends on the distribution of $\lambda$.

### 1.3.6 *Zero Range Process (ZRP)*

Zero Range process was first introduced as an example of interacting particle system by Frank Spitzer [22], which is a very simple model having many physical applications [10]. In one dimension, ZRP is defined on a lattice of $L$ sites. At each site $i$, $n_i$ number of particles reside where $n_i \geq 0$. A configuration of the system is given by $\mathbb{C} = \{n_i\} = \{n_1, n_2, n_3, \cdots, n_L\}$ A single particle jumps from $i^{th}$ site to $(i+1)^{th}$ site with hop rate $u(n_i)$.

Interestingly, though ZRP is a nonequilibrium steady state system, it has its *steady state measure* given by an exact *factorized* form,

$$P(\{n_i\}) = Z^{-1} \prod_{l=i}^{L} w(n_i) \delta(\sum_i n_i - N), \tag{1.38}$$

where, $Z$ is the normalization constant.

The weight factor $w(n_i)$ of site $i$ which is related to the particle hop rate $u(n_i)$ as

$$u(n_i) = \frac{w(n_i - 1)}{w(n_i)}. \tag{1.39}$$

In other way, $w(n_i)$ are given by the hop rates as

$$w(n) = \prod_{i=1}^{n} u(i)^{-1}, \tag{1.40}$$

for $n > 0$ and $w(0) = 1$. The probability that a given site contains $n$ particles is $P(n)$. We can calculate it fixing the number of particles at the $1^{st}$ site as $n$. So, we can write the expression of $P(n)$ as the following,

$$\begin{aligned} P(n) &= \sum_{n_2, n_3, \cdots, n_L} P(n, n_2.n_3, \cdots, n_L) \delta(\sum_{i=2}^{L} n_i - (N-n)) && (1.41) \\ &= \sum_{n_2, n_3, \cdots, n_L} \frac{1}{Z_{L,N}} w(n) \prod_{l=2}^{L} w(n_i) \delta(\sum_{i=2}^{L} n_i - (N-n)) \\ &= \frac{w(n)}{Z_{L,N}} \sum_{n_2, n_3, \cdots, n_L} \prod_{l=2}^{L} w(n_i) \delta(\sum_{i=2}^{L} n_i - (N-n)) \\ &= \frac{w(n)}{Z_{L,N}} Z_{L-1, N-n}. && (1.42) \end{aligned}$$

As ZRP has a factorized steady state, all higher order particle particle correlation vanishes.

### 1.3.7 *Driven lattice gases:*

S. Katz, J. Lebowitz and H. Spohn introduced a driven lattice gas system [23], which could be used to model fast ionic conductors, to study the microscopic correlation function in nonequilibrium steady state. The system is defined on two dimensional lattice system having $L$ sites on each side. A site $i = \{i_x, i_y\}$ could be occupied with atmost one particle. The occupation variable $\eta_i$ takes value 1 if the site is occupied otherwise it is 0. The total number of particles is $\sum \eta_i = N$. The system is driven by an electric field $\vec{E} = E\hat{x}$ in $x$ direction and the energy of a certain configuration $C$ is given by

$$H(C) = -J \sum_{\langle i,j \rangle} \eta_i \eta_j - E \sum_i i_x \eta_i, \tag{1.43}$$

where the notation $\langle i, j \rangle$ denotes the sum on nearest neighbors. In the absence of the electric field, the system reaches an equilibrium state having Boltzmann distribution. Particle from one site $i$ hops to its empty nearest neighbor $j$ following detailed balance condition,

$$\frac{W_{E=0}(C'C)}{W_{E=0}(CC')} = \exp\big[-\beta H_{E=0}(C) - H_{E=0}(C')\big], \tag{1.44}$$

where $W_{E=0}(CC')$ is the transition rate from configuration $C$ to $C'$ and $\beta$ is inverse temperature of the bath. But, the presence of the electric field creates a macroscopic particle current flowing in the system and thus the system becomes nonequilibrium in nature. The biased exchange rates $W_E(CC')$ are expected to obey local detailed balance condition

$$\frac{W_E(C'C)}{W_E(CC')} = \exp\big[-\beta H(C) - H(C')\big]. \tag{1.45}$$

Under such microscopic evolution, the system reaches a steady state where the stationary distribution is given by $P_N^{(T,E)}(C)$ which is not Boltzmann distribution. The average over the steady state distribution is denoted as

$$\langle g(C) \rangle_N^{(T,E)} = \sum_C g(C) P_N^{(T,E)}(C), \tag{1.46}$$

where $g(C)$ is an arbitrary macroscopic observable which depends on configuration $C$. Authors studied the dependence of structure factor, current on the field strength $E$ and found that a long range order emerges through a phase separation phenomenon while tuning the interaction strength $J$, temperature $1/\beta$ and electric field strength $E$.

Next, we will like to discuss the studies on nonequilibrium thermodynamics, which is a challenging open question addressed by physicists for the last few decades. In search of a consistent nonequilibrium thermodynamics, which in turn describes the statistical mechanics, physicists have prescribed operational, analytical and numerical procedures. We will review their results in short in the next section.

## 1.4 THERMODYNAMIC CHARACTERIZATION OF NONEQUILIBRIUM STEADY STATE:

To extend equilibrium thermodynamics to the nonequilibrium regime, Jou *et. al.* [24] proposed an extended irreversible thermodynamics where they attempted to put down a generalized Gibbs relation applicable to time dependent nonequilibrium systems. On the other hand Eyink *et. al.* prescribed hydrodynamics for driven lattice gas systems [25]. In doing so, they identified separation of length scale and time scale between microscopic variation and macroscopic variation and with that concept, they defined thermodynamic variables for the nonequilibrium system under consideration. Then Oono and Paniconi [26] proposed a phenomenological framework which established the operational concept of extending equilibrium thermodynamical laws to nonequilibrium steady state systems in general focusing on the transitions among steady states.

Hatano and Sasa followed Oono and Paniconi's construction in their work [27], where they studied Langevin dynamics of a brownian particle having a nonequilibrium steady state. The steady state probability distribution is written as $P_s(x, \alpha)$, where $x$ is the position of the brownian particle and $\alpha$ is the set of control parameter. Tuning the control parameter $\alpha$ within an interval of time $t = 0$ to $t = \tau^*$, the system is taken from one steady state to another steady state. Introducing a quantity related to the steady state distribution as

$$\phi(x, \alpha) = -\log P_s(x, \alpha), \tag{1.47}$$

and utilizing Jarzynski-type equality of the form

$$\langle e^{-\beta W} \rangle = e^{-\beta \Delta F}, \tag{1.48}$$

where, $\beta$ is inverse temperature, $W$ is work done on the system and $\Delta F$ is equilibrium free energy difference, authors derived the second law of thermodynamics for this nonequilibrium steady state system as

$$\beta \langle Q_{ex} \rangle + \Delta \langle \phi \rangle \geq 0. \tag{1.49}$$

Here $Q_{ex}$ is called excess heat which refers to the change of the system in the state space [26]. If Shannon entropy is identified as

$$S = -\int dx P_s(x,\alpha)\log P_s(x,\alpha), \tag{1.50}$$

Eq. 1.49 takes the well known form of second law as

$$T\Delta S \geq -\langle Q_{ex}\rangle. \tag{1.51}$$

They also verified fluctuation relation for this system.

Later, Baiesi *et. al.* [28] found a generalized fluctuation dissipation theorem (FDT) for nonequilibrium systems in general. In equilibrium, fluctuation of an observable $O$ is proportional to the response $R_O$ recorded due to external perturbations. The response is expressed by a correlation function of the observable with another variable conjugate to the external perturbation as

$$R_O(t_2-t_1) = \frac{\delta\langle O(t_2)\rangle}{\delta h(t_1)}\bigg|_{h=0} = \langle O(t_2)V(t_1)\rangle. \tag{1.52}$$

For nonequilibrium systems, authors identified a correction term to the equilibrium fluctuation dissipation theorem. They related the probability of a trajectory $w$ given a particular initial state $\mathcal{P}(w)$ of an unperturbed system with the probability of the same trajectory starting from the same initial condition when the system is perturbed $\mathcal{P}^h(w)$ through a local detailed balance condition as

$$\mathcal{P}^h(w) = \exp[-A(w)]\mathcal{P}(w), \tag{1.53}$$

where $A(w) = -\ln[\mathcal{P}^h(w)/\mathcal{P}(w)]$ is the action. The time asymmetric part $S(w)$ of the action $A(w)$ is the excess entropy flux from the system to the environment which arises due to the perturbation. On the other hand, the time symmetric components $T(w)$ denotes the excess in activity, which quantifies the amount of frenesy in the perturbed process. Ensemble average of any observable $O$ is written as $\langle O(w)\rangle = \sum_w \mathcal{P}(w)O(w)$ for unperturbed system. For perturbed system, the ensemble average of the observable is given by $\langle O(w)\rangle^h = \sum_w \mathcal{P}^h(w)O(w)$. Thus, using Eq. 1.53, authors showed that the response due to the perturbation could be expressed as in the following form

$$R_O(t_2-t_1) = \frac{1}{2}\langle O(t_2)V(t_1)\rangle - \frac{1}{2}\langle \tau(w,t_1)O(t_2)\rangle, \tag{1.54}$$

where $\tau(w,s) = \frac{\delta}{\delta h_s} T(w)|_{h_s=0}$, the first order in excess activity in linear response theory. The importance of this result lies in its validity for nonequilibrium systems in general without knowing the dynamics explicitly.

On the other hand, U. Seifert and T. Speck obtained a similar result in their work [29] for nonequilibrium steady state systems. They also found an additive correction term to the equilibrium response function for markovian systems driven to a nonequilibrium steady state. Authors showed that the correction term is related to the total entropy production. They followed various approaches to calculate the response function $R$ and obtained different FDT in a NESS. But, as the response function should only depend on the observable under consideration, they concluded that the different response functions are equivalent to each other though they are linearly independent. Any linear superposition of those response functions gives rise to another variant of response function.

To concretize Oono and Paniconi's concept of operational procedure in defining equilibriumlike thermodynamical variables in nonequilibrium steady state systems, Sasa and coworkers [30, 31] considered systems having a nonequilibrium steady state (such as, heat conducting fluid, driven lattice gas) and examined the validity of basic postulates and laws of thermodynamics such as scaling laws, extensivity or intensivity, or additivity in terms of a variational principle. They had been able to define various thermodynamic quantities such as pressure, chemical potential, free energy in nonequilibrium regime through operational manner explicitly and showed that an equilibriumlike Maxwell relation, obtained from large deviation principle, could hold in such nonequilibrium systems. They also obtained various fluctuation relations, which can be associated to a nonquilibrium free energy function. On the other hand, Bertin *et. al.* and coworkers proceeded somewhat along the above lines and the theory developed by Eyink *et. al.* and outlined an equilibriumlike statistical mechanical approach to define thermodynamic quantities even in nonequilibrum systems. They discussed how an equilibriumlike additivity property could be extended to simple nonequilibrium systems, which do not have any spatial correlations (such as the ZRP). Both the groups of Sasa and Bertin also examined whether zeroth law of thermodynamics holds in nonequilibrium systems when they are kept in contact with each other and exchange a conserved quantity. It was realized that contact dynamics is a very important quantity, which needs to be defined correctly. Later, Pradhan *et. al.* [32–34] numerically checked zeroth law of thermodynamics in the case of driven lattice gases with both repulsive and attractive interactions and also the ZRP. In their work, they affirmed the nontriviality of contact dynamics. They defined excess chemical potential, which depends on the contact dynamics and is *a priori* unknown. In the next subsections, we shall elaborate the above mentioned thermodynamical prescriptions for nonequilibrium steady state systems.

### 1.4.1 *Steady state thermodynamics : Operational approach*

Sasa and Tasaki demonstrated their framework of steady state thermodynamics taking an example of driven lattice gas in two dimension and obtained concrete mathematical result for the system.

Two driven lattice gases $\Lambda_1$ with particle number $N_1$ and $\Lambda_2$ with particle number $N_2$, defined in the same manner as in previous section 1.3.7 are put in a weak contact. The configurations are denoted as $\eta$ for lattice $\Lambda_1$ and $\zeta$ for lattice $\Lambda_2$. External potentials $u_1$ and $u_2$ are applied on the lattices $\Lambda_1$ and $\Lambda_2$ respectively which affect the transition rates at the contact of two lattices but the bulk dynamics of two lattices remain unaffected. The total number of particles of the combined system $N_1 + N_2 = N$ remains conserved. The total energy function is written as

$$H_{tot}^{u_1,u_2} = H_{\Lambda_1}(\eta) + H_{\Lambda_2}(\zeta) + u_1 N_1 + u_2 N_2. \tag{1.55}$$

At contact, for each $j = 0, 1, \cdots L-1$, a particle can hop from site $(j, 0)$ of lattice $\Lambda_1$ to site $(j, 0)$ of lattice $\Lambda_2$. The weak contact between the systems could be realized by assuming a high energy barrier between two systems. A particle from lattice $\Lambda_1$ ($\Lambda_2$) has to cross that fictitous energy barrier to jump to the other lattice $\Lambda_2$ ($\Lambda_1$). Thus the transition rates from system $\Lambda_1$ to system $\Lambda_2$ would be written as

$$\frac{w(\Lambda_1 \to \Lambda_2)}{w(\Lambda_2 \to \Lambda_1)} = \exp[\beta(H_{\Lambda_1} - H_{\Lambda_2})], \tag{1.56}$$

where $H_{\Lambda_1}$ and $H_{\Lambda_2}$ are local energies of the corresponding systems. So, the transition rates could be uniquely identified as $w(\Lambda_1 \to \Lambda_2) = \epsilon \exp(\beta H_{\Lambda_1}), w(\Lambda_2 \to \Lambda_1) = \epsilon \exp(\beta H_{\Lambda_2})$, where $\epsilon$ could be quantified in terms of the high energy barrier as $\epsilon = c \exp(-\beta W)$. This expression will not contain the electric field $\vec{E}$ as the particle hopping occurs in the perpendicular direction of the applied field. It can be shown that, at contact, detailed balance is satisfied for the rates $W[(\eta, \zeta) \to (\eta', \zeta')]$ and $W[(\eta', \zeta') \to (\eta, \zeta)]$, where $(\eta, \zeta)$ denotes the configuration of the combined system. For $\epsilon \to 0$, the particle exchanges between the systems are rare and the systems become nearly uncorrelated so that the steady state distribution of the combined system factorizes as $P^{T,E}_{\Lambda_1,N_1} P^{T,E}_{\Lambda_2,N_2}$ with the constraint of particle number conservation. Then the effective transition rate for a hop from $\Lambda_1$ to $\Lambda_2$ could be written in the following form

$$\begin{aligned} \tilde{W}(N_1 \to N_1 - 1) &= \epsilon \sum_{j=0}^{L-1} \langle \eta_{j,0}(1 - \zeta_{j,0}) \exp\left[\beta\{H_{\Lambda_1}(\eta) - H_{\Lambda_1}(\eta') + u_1\}\right] \rangle, \\ &= \epsilon L \left(1 - \frac{N_2}{V}\right) g(N_1) \exp(\beta u_1). \end{aligned} \tag{1.57}$$

Here $V = L^2$, and $g(N)$ is the average of local quantity over local distribution. Similarly the counter rate from $\Lambda_2$ to $\Lambda_1$ could be written as

$$\tilde{W}(N_1 \to N_1 + 1) = \epsilon L \left(1 - \frac{N_1}{V}\right) g(N_2) \exp(\beta u_2). \tag{1.58}$$

Since hops between the two systems balance each other at steady state, using Eq. 1.57 and 1.58, we have

$$\begin{aligned} \tilde{W}(N_1 \to N_1 - 1) &= \tilde{W}(N_1 \to N_1 + 1), \\ \epsilon L \left(1 - \frac{N_2}{V}\right) g(N_1) \exp(\beta u_1) &= \epsilon L \left(1 - \frac{N_1}{V}\right) g(N_2) \exp(\beta u_2). \end{aligned} \tag{1.59}$$

From Eq. 1.59, we can conclude that there exists an equilibriumlike intensive thermodynamic variable, a chemical potential in this case, which equalizes at steady state for two systems in contact. The chemical potential has the concrete form

$$\mu(\rho) = \frac{1}{\beta} \log \frac{g(\rho L^2)}{1 - \rho}, \tag{1.60}$$

in the infinite $V$ limit where $\rho$ is the particle density. As the form of the chemical potential contains correlation function of local quantities, the generic long range power law correlation, which appears in the driven lattice gases, does not affect it. The transition rates of Eq. 1.57 and 1.58 are called Sasa-Tasaki rates for contact dynamics between two nonequilibrium systems which can produce equilibriumlike thermodynamics consistently.

A similar operational approach was taken to define pressure of such driven lattice gases. Two lattices with same width $l$ and different heights $h$ and $\tilde{h}$ are put in contact with each other. Here $h \gg \tilde{h}$. The smaller system is kept on top of the bigger system and an uniform potential $u$ is applied on the smaller system. When $u = 0$, the combined system reaches a steady state with uniform density $\rho$ everywhere over the system. Then $u$ is slowly varied from 0 to $\infty$. At $u \to \infty$, all particles from smaller system have moved to the bigger system and at the new steady state, $\rho$ is uniform over the bigger system. This operation could be realized in a manner that with the application of the external potential $u$, the volume of the combined system is reduced from $[l \times (h + \tilde{h})]$ to $[l \times h]$. Using the balance condition at the contact and the standard relation of the mechanical work $W = p\Delta V$ done due to pressure $p$ where $\Delta V = l\tilde{h}$, we get the definition of pressure as

$$p(\rho) = \int_0^\rho d\tilde{\rho} \tilde{\rho} \mu'(\tilde{\rho}), \tag{1.61}$$

which is effectively Maxwell's relation. Using the pressure and chemical potential, the steady state free energy density is defined as

$$f(\rho) = -p(\rho) + \rho\mu(\rho) = \int_0^\rho d\tilde{\rho}\mu(\tilde{\rho}). \tag{1.62}$$

The steady state joint probability that the lattice $\Lambda_1$ has $N_1$ particles and the lattice $\Lambda_2$ has $N_2$ particles could be calculated in the weak contact limit with the help of the steady state free energy defined above as

$$\tilde{P}(N_1, N_2) = \text{const.}\exp[-\beta V\{u_1\rho_1 + u_2\rho_2 + f(\rho_1) + f(\rho_2)\}], \tag{1.63}$$

where $\rho_1 = N_1/V$ and $\rho_2 = N_2/V$. In the absence of the external potentials $u_1$ and $u_2$, we get back the Einstein's relation of density fluctuation as

$$\tilde{P}_{u=0}(N_1, N_2) = \text{const.}\exp[-\beta\{F(T, E, V, N_1) + F(T, E, V, N_2)\}]. \tag{1.64}$$

This is an exact stationary state distribution which contains the informations of small as well as large density fluctuations.

### 1.4.2 *Steady state thermodynamics : Theoretical and numerical approach*

Eyink *et. al.* in their work [25] established a thermodynamic structure of driven lattice gases. They hypothetised a factorized structure of configurational probability which needs a free energy like function to be defined. The free energy function acts as large deviation function in thermodynamic limit. Consequently, they were also able to define a chemical potential like variable which is related to that free energy in the equilibriumlike manner. With the help of this prescription, they constructed hydrodynamic structure in bounded models like driven lattice gases. E. Bertin [35, 36] and coworkers extended equilibrium statistical mechanics to nonequilibrium regime using a theoretical approach similar to Eyink *et. al.* [25]. They showed that this framework of equilibriumlike additivity works remarkably well for some special cases where steady state probability distribution is known to be factorized such as ZRP(1.3.6), ARAP (1.3.2) etc, which are unbounded models having no exclusion interaction. They provided definition of intensive thermodynamic variable (ITV) in nonequilibrium systems and examined under which conditions, equalization of ITVs is possible when two nonequilibrium systems are kept in contact.

They considered a general macroscopic system which evolves to a steady state. The system contains some additive quantity which takes part in the dynamics. Dynamics keep the sum of the additive quantities conserved. In general there could be many conserved quantities but

for simplicity, we will consider that the system consisting of $V$ number of lattice sites has only one conserved quantity, say particle number $N = \sum_i n_i$, $i$ is the site index. The particle density is given by $\rho = N/V$. The steady state distribution of a configuration $C = \{n_1, n_2, \cdots, n_V\}$ is written as

$$P(C) \simeq \prod_{i=1}^{V} \frac{w(n_i)}{Z(N)} \delta(\sum_i n_i - N)), \tag{1.65}$$

where $w(n_i)$ is single site weight factor and $Z(N)$ is the normalization constant. In equilibrium systems, $w(n_i)$ is known to be the Boltzmann factor, whereas in case of nonequilibrium systems, it is not known in general. To define intensive thermodynamic parameter, a whole system is divided into two subsystems $S_1$ of size $(N_1, V_1)$ and $S_2$ of size $(N_2, V_2)$ and the subsystems are allowed to exchange particles. The total particle number $N_1 + N_2 = N$ is kept conserved. The configuration of the combined system is defined as $C : \{C_1, C_2\}$ so that the probability of configuration $C$ is $P_{C_1,C_2}$. The joint probability of subsystem particle numbers $P(N_1, N_2)$ is given by a factorized large deviation form

$$P(N_1, N_2) \simeq \frac{\exp[-V_1 f_1(\rho_1)] \exp[-V_2 f_2(\rho_2)]}{\exp[F(N)]}, \tag{1.66}$$

where $f_1$ and $f_2$ are the large deviation functions of individual subsystems $S_1$ and $S_2$, which depend on corresponding particle density $\rho_1 = N_1/V_1$ and $\rho_2 = N_2/V_2$ of the subsystems $S_1$ and $S_2$ respectively. Due to the asymptotic factorization property, the logarithm of $P(N_1, N_2)$ satisfies an additive form,

$$\ln P(N_1, N_2) = \ln Z_1(N_1) + \ln Z_2(N - N_1) - \ln Z(N) + \epsilon(N_1, N_2), \tag{1.67}$$

with $Z_1 = \exp[-V_1 f_1(\rho_1)], Z_2 = \exp[-V_2 f_2(\rho_2)], Z = \exp[-V f(\rho)]$ and

$$\left| \frac{\epsilon(N_1, N_2)}{\ln P(N_1, N_2)} \right| \ll 1, \tag{1.68}$$

in the thermodynamic limit.

Following the same track as equilibrium thermodynamics, authors used the rule of maximization of probability $P(N_1, N_2)$ to find the maximum probable value of $N_1 = N_1^*$, which gives the steady state. From Eq. 1.67 and Eq. 1.68 we have

$$\left. \frac{\partial \ln Z_1}{\partial N_1} \right|_{N_1^*} = \left. \frac{\partial \ln Z_2}{\partial N_2} \right|_{(N - N_1^*)}. \tag{1.69}$$

Thus ITV is defined conjugate to the additive quantity $N$ as

$$\mu = \frac{\partial \ln Z}{\partial N}. \tag{1.70}$$

So at steady state, this intensive thermodynamic variable equalizes in the two subsystems. The nonequilibrium systems, which have product measure at steady state, obey the additivity in Eq. 1.67 with a vanishing $\epsilon$ in this case. Interestingly, it has been shown that the additivity is still valid in systems whose steady states are not factorized but given by a matrix product ansatz and models described by transfer matrix method.

Authors demonstrated their formalism to calculate ITVs in two mass transport systems like ZRP (defined in 1.3.6) and pair factorized steady state.

*ITV in Zero Range Process*: Let us consider the single site weight factor $w(n)$ has a simple form

$$w(n) = n^{(\delta-1)}, \tag{1.71}$$

where $\delta > 0$. The partition function is

$$Z(N) = \int \prod_{i=1}^{L} (dn_i n_i^{\delta-1}) \delta(\sum_{i=1}^{L} n_i - N). \tag{1.72}$$

To calculate the integral in Eq. 1.72, we rescale the variable as $n_i = x_i N$. Putting this form in the integration we get,

$$\begin{aligned} Z(N) &= \int \prod_{i=1}^{L} [dx_i N (x_i N)^{\delta-1}] \delta(\sum_{i=1}^{L} x_i N - N), \\ &= \frac{1}{N} \int \prod_{i=1}^{L} [dx_i x_i^{\delta-1} N^{1+\delta-1}] \delta(\sum_{i=1}^{L} x_i - 1), \\ &= \int N^{(L\delta-1)} \prod_{i=1}^{L} [dx_i x_i^{(\delta-1)}] \delta(\sum_{i=1}^{L} x_i - 1), \\ &= K_L N^{(L\delta-1)}, \end{aligned} \tag{1.73}$$

where $K_L$ is a constant independent of N. So the intensive thermodynamic parameter is defined as

$$\mu = \frac{-d \ln Z}{dN}, \tag{1.74}$$

$$= \frac{-(L\delta - 1)}{N}. \tag{1.75}$$

In the thermodynamic limit, we get the chemical potential $\mu = -\frac{\delta}{\rho}$ where $\rho = \frac{N}{L}$ is the average particle density of the system. As this is a mass transport system, the ITV is chemical potential conjugate to the fluctuating additive quantity mass.

*ITV in Pair factorized steady state system*: This is a discrete particle system defined on a periodic lattice of size $L$. This model does not exhibit factorized steady state property, but its steady state has a pair-factorized form[11]. Though the conserved quantity is the total number of particles $N = \sum_{i=1}^{L} n_i$, the particle hopping rate $u$ depends on the number of particles of the departing site and its two neighboring sites unlike in ZRP,

$$u(n_{i-1}, n_i, n_{i+1}) = \frac{g(n_{i-1}, n_i - 1)}{g(n_{i-1}, n_i)} \frac{g(n_i - 1, n_{i+1})}{g(n_i, n_{i+1})}. \tag{1.76}$$

which leads the system to attain a pair-factorized steady state,

$$P(\{n_i\}) = \frac{1}{Z_N} \prod_{i=1}^{N} g(n_i, n_{i+1}) \delta(\sum_{i=1}^{N} n_i - N). \tag{1.77}$$

For a simple choice of $g(m, n)$

$$g(m, n) = (m^\alpha n^\beta + m^\beta n^\alpha)^\gamma, \tag{1.78}$$

with $\alpha, \beta, \gamma \geq 0$, we calculate the partition function taking the scaling form $n_i = N x_i$. The partition function is given by

$$\begin{aligned} Z(N) &= \int \prod_{i=1}^{L} [dx_i N (x_i^\alpha N^\alpha x_{i+1}^\beta N^\beta + x_i^\beta N^\beta x_{i+1}^\alpha N^\alpha)^\gamma] \frac{1}{N} \delta(\sum x_i - 1), \\ &= [N^{L(\gamma(\alpha+\beta)+1)-1}] \tilde{K}_N. \end{aligned} \tag{1.79}$$

So, the ITV is defined as

$$\mu = -\frac{d \ln Z}{dN} = \frac{L[\gamma(\alpha + \beta) + 1] - 1}{N}. \tag{1.80}$$

In thermodynamic limit, where $N \to \infty, L \to \infty$, but $\rho = \frac{N}{L}$ is finite denoting the average particle number density, the chemical potential of the system $\mu$ is given by,

$$\mu = \frac{-[\gamma(\alpha + \beta) + 1]}{\rho}. \tag{1.81}$$

After providing the definition of ITV of a system, authors ask what happens when two such systems are kept in contact. Does corresponding ITV equalize with each other at steady state? To answer this question, two systems are kept in contact and allowed to exchange conserved quantity, say mass. The contact dynamics generates a distribution $\Phi(N_1|N)$ for

the random division of $N$ into two parts, $N_1$ in system 1 and $N - N_1$ in system 2. Under the weak contact assumption, authors argued that if the individual systems obey additivity in Eq. 1.67, intensive parameters for two systems would equalize at steady state. This claim in turn puts a constraint on $\Phi$ to be in a form

$$\Phi(N_1|N) \approx \frac{Z_1(N_1)Z_2(N-N_1)}{Z(N)}. \tag{1.82}$$

But, in general, $\Phi$ does not obey Eq. 1.82 and intensive parameters do not equalize.

To demonstrate this result, two mass transport models are kept in contact keeping the total mass of the combined system conserved. The mass transport models have their own bulk dynamics of the form

$$\phi_\alpha(\tilde{m}|m) = v(\tilde{m})\frac{w_\alpha(m-\tilde{m})}{w_\alpha(m)}, \alpha = 1, 2. \tag{1.83}$$

$v(\tilde{m})$ is taken to be same for both systems. Contact dynamics is also taken in the same form of bulk dynamics. Two sites from two different systems are in contact with each other and thus inhomogeneity is created in the combined system. In this case, additivity in Eq. 1.67 holds and ITVs equalize. The simplest example, for which this proposal works, is ZRP. Authors mentioned that if $v(\tilde{m})$ is not same for the systems in contact, the detailed balance along contact is violated and equalization of ITVs will not be satisfied because, Eq. 1.82 does not hold in that case.

Later, Pradhan *et. al.* renewed the interest in the studies and proceeded to explore numerically the nonequilibrium structure of driven lattice gas and zero range processes for a wide range of parameter values [32, 33]. In the first case of driven lattice gas [32], they put two similar systems of size $(N_1, V_1)$ and $(N_2, V_2)$ in contact with each other and allowed them to exchange particles between them. The total particle number of the combined system $N = N_1 + N_2$ remains fixed. The dynamics of the systems are given according to the specifics mentioned in 1.3.7 where the bulk and contact dynamics follow local detailed balance condition. Through numerical studies, they found that there is an intensive thermodynamic variable which equalizes for two systems in contact at steady state. Thus the chemical potential helps to determine the steady state of the combined system. The chemical potentials of the nonequilibrium systems were measured numerically keeping the nonequlibrium system in contact with an equilibrium system with known chemical potential. Remarkably, they found that zeroth law of thermodynamics holds quite good for such systems. They argued that the existence of a zeroth law could be a consequence of factorized large deviation form of the joint particle number distribution of the two systems as given in Eq. 1.66. The assumption of this factorized form of the joint distribution neglects the spatial correlations present in the system. Consequently, the steady state could be obtained by maximizing $P(N_1, N_2)$

with the constraint of particle number conservation and the chemical potentials, given by $\mu_i = \partial f_i / \partial n_i, (i \in [1,2])$, equalize. Authors showed that, an equilibriumlike fluctuation relation, another consequence of the assumption of factorized joint distribution, also holds very good for driven lattice gases. It was also shown that this thermodynamics structure breaks down at higher density regime due to the presence of long range power law correlation in the driven lattice gases.

In their next work [33], Pradhan and coworkers studied in more detail the cases of driven lattice gas and zero range processes. In the case of zero range process, they considered the contact dynamics same as that proposed by Bertin and coworkers in [36]. Two one dimensional lattice rings having $L_1$ and $L_2$ sites are kept in contact with each other at one point of each of them through which, the systems can exchange particles. Any configuration is denoted by $\mathbb{C} = (\{n_{i_1}\}, \{n_{i_2}\})$. A particle hops from a randomly chosen site $i$ (from $L = L_1 + L_2$ sites) to its next neighbor site $i+1$ with hop rate

$$u_\alpha(n_i) = v_\alpha \frac{w(n_i - 1)}{w(n_i)}, \tag{1.84}$$

with $\alpha = \{1,2\}$. $v_\alpha$ is independent of $n_i$. The functional form of the hop rate is same for the hopping in the bulk and hopping from one ring to another via contact point. But, the factor $v_\alpha$ can be different in those two cases, i.e.

$$v_\alpha = v_\alpha^{(b)} \text{ for the hoppings in the bulk,} \tag{1.85}$$

$$v_\alpha = v_\alpha^{(c)} \text{ for the hoppings at the contact point.} \tag{1.86}$$

While studying the properties of nonequilibrium steady states, two different cases may arise.

***Case1: bulk and contact property are same ($v_\alpha^{(b)} = v_\alpha^{(c)}$ and $v_1^{(c)} = v_2^{(c)}$) [36]***:

The value of $v_1^{(b)}$ and $v_2^{(b)}$ is assigned to be 1 without loss of generality. The steady state probability distribution is

$$P(\{n_{i_1})\}, \{n_{i_2})\}) = \frac{1}{Z_N} \left[ \prod_{i_1=1}^{L_1} w_1(n_{i_1}) \prod_{i_2=1}^{L_2} w_2(n_{i_2}) \right] \delta[(N_1 + N_2) - N], \tag{1.87}$$

where $N_1 = \sum_{i_1=1}^{L_1} n_{i_1}$ and $N_2 = \sum_{i_2=1}^{L_2} n_{i_2}$ are the number of particles of ring 1 and ring 2 and $Z_N$ is normalization constant. The joint probability distribution can be written in a form

$$P(N_1, N_2) = \frac{Z_1(N_1) Z_2(N_2)}{Z(N)}, \tag{1.88}$$

where

$$Z_\alpha(N_\alpha) = \sum_{\{n_{i_\alpha}\}} \prod_{i_\alpha=1}^{L_\alpha} w_\alpha(n_{i_\alpha}) \delta(\sum_{i_\alpha=1}^{L_\alpha} n_{i_\alpha} - N_\alpha). \tag{1.89}$$

The macrostate is obtained by maximizing the joint distribution which gives the intensive thermodynamic parameter as $\mu_\alpha = -\frac{\partial \ln Z_\alpha}{\partial N_\alpha}$.

***Case2: bulk properties are same but the contact properties are not same*** ***($v_1 \neq v_2$)***:

This case is more general than the previous one and one of the main result of Pradhan *et. al.*. In this case, the steady state probability distribution is still given by a factorized form as

$$P(\{n_{i_1})\}, \{n_{i_2})\}) = \frac{1}{Z_N} \left[ \prod_{i_1=1}^{L_1} w_1(n_{i_1}) \prod_{i_2=1}^{L_2} w_2(n_{i_2}) \right] e^{\tilde{\mu_1} N_1} e^{\tilde{\mu_2} N_2} \delta[(N_1 + N_2) - N], \tag{1.90}$$

where $\tilde{\mu_1} = \ln \frac{1}{v_1}$ and $\tilde{\mu_2} = \ln \frac{1}{v_2}$. These terms are called *excess chemical potentials*. The joint probability distribution is

$$P(N_1, N_2) = \frac{Z_1(N_1) Z_2(N_2)}{Z(N)} e^{\tilde{\mu_1} N_1} e^{\tilde{\mu_2} N_2}. \tag{1.91}$$

Maximizing $\ln P(N_1, N_2)$, we get the macrostate,

$$\left( -\frac{\partial \ln Z_1}{\partial N_1} + \tilde{\mu_1} \right) = \left( -\frac{\partial \ln Z_2}{\partial N_2} + \tilde{\mu_2} \right). \tag{1.92}$$

Thus, new intensive parameters have been defined which take equal values at steady state when two systems are kept in contact,

$$\overline{\mu_\alpha} = \left( -\frac{\partial \ln Z_\alpha}{\partial N_\alpha} + \tilde{\mu_\alpha} \right). \tag{1.93}$$

For **case1**, when $v_1 = v_2$, the excess chemical potentials become equal and they are cancelled out from both side of the chemical potential equalization equation and old intensive chemical potentials work good. But in **case2**, where $v_1 \neq v_2$, the new $\overline{\mu_\alpha}$ plays the role of chemical potential and becomes equal at the contact at steady state. Moreover, detailed balance condition indeed gets satisfied for the second case.

Zeroth law of thermodynamics was found to satisfy for a particular set of $\{f_\alpha(n), v_\alpha\}$. But the choice of $v_\alpha$ plays a crucial role in this case. It was shown that while verifying zeroth law, if the values of $v_\alpha$ is slightly changed, it affects the final steady state where zeroth law does not hold. This is the main point of the result that role of contact dynamics is very important to have zeroth law. Consequently, due to the arbitraryness of $v_\alpha$, the chemical potentials can have different functional forms depending on the contact dynamics. Thus, equalization of

intensive variables are assured in terms of excess chemical potentials but zeroth law may not hold.

The authors then tried to extend the idea of excess chemical potential in the case of driven lattice gas systems. But, they concluded that even though a modified large deviation form including the effect of excess chemical potential could be written for the joint particle number distribution for two systems in contact, zeroth law is not assured as the excess chemical potential is *ad hoc* in nature and could be arbitrary.

Recently, Dickman and coworkers [37, 38] addressed this issue of nonequilibrium steady state thermodynamics. They studied two different systems, (i) driven stochastic hardcore lattice gas (no energy function is associated with its configurations and particle hops stochastically to its nearest neighbors), (ii) driven lattice gases, which are known as KLS model (1.3.7) (energy function contains nearest neighbor attractive interaction). In both cases, systems are put in contact with weak coupling strength. Particle/energy exchange occurs from any site of one system to any other site of the other system, which is called *global contact*. In case (i), intensive thermodynamic variable e.g., chemical potential could be defined consistently in terms of particle density and drive strength when the combined system reaches steady state. Here zeroth law is satisfied and steady state densities of the systems are rightly determined. But, in case (ii), zeroth law is violated for arbitrary contact dynamics. Even well known metropolis rate does not work in KLS model. Interestingly, Sasa-Tasaki rate, which is discussed in the previous section, is found to work consistently and an effective definition of chemical potential could be obtained for which zeroth law is satisfied. In his second work on steady state thermodynamics [38], R. Dickman considered driven stochastic lattice gas with nonuniform local exchange of particles between systems in contact. Here extension of steady state thermodynamics is violated because the chemical potential does not equalize in systems at stationary state. It is realized that a proper definition of chemical potential is missing for this set up. In the limit of weak contact, which implies vanishingly small exchange rate, the predictions of steady state thermodynamics is valid. For finite exchange rate, it breaks down due to emergence of nonuniformity of density profile.

## 1.5 MOTIVATION AND PLAN OF THE THESIS

From the above brief review on conserved-mass transport processes, which is a paradigm in nonequilibrium statistical physics, a striking common feature comes into light. In many of these processes, the probability distributions of subsystem masses are described by *gamma distributions* [7, 8, 12–14, 16]. In several other cases, e.g., in cases of wealth distribution in a population [19–21] or force distribution in granular beads [15, 16], the distribution functions are not always exactly known, but remarkably they can often be well approximated

by gamma distributions. Although these models have been studied intensively in the past decades, an intriguing question [39] why the gamma-like distributions arise in different contexts irrespective of different dynamical rules however remained unanswered.

As many of these systems are found to have short-ranged spatial correlations, one could perhaps expect an equilibriumlike additivity property to hold, which could help in characterizing the large-scale thermodynamic structure in these systems. There could be two broad questions, which we aimed at addressing in systems having a nonequilibrium steady state [25, 31, 35]: (i) What are the criteria so that additivity holds? (ii) What are the consequences of additivity? In this thesis work, we mainly focus on the second question whether such systems in general could possess an equilibriumlike thermodynamic structure; however, answer to these two questions are somewhat complementary in the sense that, by addressing question (ii), one could also come at some conclusions about question (i). Our studies essentially help us to classify, and to characterize, the nonequilibrium steady state systems for which additivity holds.

In Chapter 2, we focus on paradigmatic conserved-mass transport processes, which have been discussed in this chapter in section 1.3. We provide a unified statistical mechanics framework to characterize steady state mass fluctuations in these systems assuming an equilibriumlike additivity property holds. We show that, in conserved-mass transport processes, the steady state distribution of mass in a subsystem is uniquely determined from the functional dependence of variance of the subsystem mass on its mean, provided that the joint mass distribution of subsystems is factorized in the thermodynamic limit. The factorization condition is not too restrictive as it would hold in systems with short-ranged spatial correlations. To demonstrate the result, we revisit a broad class of mass transport models and its generic variants, and show that the variance of the subsystem mass in these models is proportional to the square of its mean. This particular functional form of the variance constrains the subsystem mass distribution to be a gamma distribution irrespective of the dynamical rules. thus we have been able to answer the long standing question regarding gamma distribution in this thesis.

In Chapter 3, we proceed with the results of Chapter 2 and we ask what happens when two nonequilibrium systems in steady state are kept in contact and allowed to exchange a quantity, say mass, which is conserved in the combined system. Will the systems eventually evolve to a new stationary state where a certain intensive thermodynamic variable, like equilibrium chemical potential, equalizes following the zeroth law of thermodynamics and, if so, under what conditions is it possible? We argue that an equilibriumlike thermodynamic structure can be extended to nonequilibrium steady states having short-ranged spatial correlations, provided that the systems interact weakly to exchange mass with rates satisfying a balance condition - reminiscent of a detailed balance condition in equilibrium. The short-ranged correlations would lead to subsystem factorization on a coarse-grained level and the

balance condition ensures both equalization of an intensive thermodynamic variable as well as ensemble equivalence, which are crucial for construction of a well-defined nonequilibrium thermodynamics. This proposition is proved and demonstrated in various conserved-mass transport processes having nonzero spatial correlations.

In Chapter 4, we focus on conserved lattice gas systems, specifically fixed energy sandpile models which exhibit absorbing to active phase transitions upon tuning particle density $\rho$. We have been able to characterize the steady state mass fluctuations of these systems in active phase using additivity. We find that for unbounded stochastic sandpile models with conserved-mass, in active phase, the scaled variance of subsystem mass $\sigma^2(\rho)$ is proportional to the square of the mass density $\rho$. Thus, the active phase of these paradigmatic fixed energy sandpiles possesses a similar thermodynamic structure as conserved-mass transport processes discussed in Chapter 2. Aiming to characterize the behavior of such systems near criticality, where the active-absorbing phase transition takes place, we study a particular class of fixed energy sandpiles called conserved-mass Manna sandpiles (MS) with continuous-time dynamics. We demonstrate that the MS possesses a remarkable hydrodynamic structure: There is an Einstein relation $\sigma^2(\rho) = \chi(\rho)/D(\rho)$, which connects bulk-diffusion coefficient $D(\rho)$, conductivity $\chi(\rho)$ and mass-fluctuation, or scaled variance of subsystem mass, $\sigma^2(\rho)$. Consequently, density large deviations are governed by an equilibriumlike chemical potential $\mu(\rho) \sim \ln a(\rho)$ where $a(\rho)$ is the activity in the system. Using the above hydrodynamics, we derive two scaling relations: As $\Delta = (\rho - \rho_c) \to 0^+$, $\rho_c$ being critical density, (i) mass-fluctuation $\sigma^2(\rho) \sim \Delta^{1-\delta}$ with $\delta = 0$ and (ii) dynamical exponent $z = 2 + (\beta - 1)/\nu_\perp$, expressed in terms of two static exponents $\beta$ and $\nu_\perp$ for activity $a(\rho) \sim \Delta^\beta$ and correlation length $\xi \sim \Delta^{-\nu_\perp}$, respectively. Our results imply that the conserved MS belong to a distinct universality - *not* that of directed percolation (DP), which, without any conservation law as such, does not obey scaling relation (ii).

# 2

# GAMMALIKE MASS DISTRIBUTIONS AND MASS FLUCTUATIONS IN CONSERVED-MASS TRANSPORT SYSTEMS

## 2.1 INTRODUCTION

Understanding fluctuations is fundamental to the formulation of statistical mechanics. Unlike in equilibrium, where fluctuations are obtained from the Boltzmann distribution, there is no unified principle to characterize fluctuations in nonequilibrium. In this work, we provide a statistical mechanics framework to characterize steady state mass fluctuations in conserved-mass transport processes.

In this chapter [1], we explain in particular why mass transport processes often exhibit gammalike distributions. Our main result is that, in the thermodynamic limit, the functional dependence of variance of subsystem mass on its mean uniquely determines the probability distribution of the subsystem mass, provided that (i) total mass is conserved and (ii) the joint probability distribution of masses in subsystems has a factorized form as given in Eq. 2.2. In other words, if the conditions (i) and (ii) are satisfied, the probability distribution $P_v(m)$ of mass $m$ in a subsystem of size $v$ can be determined from the functional form of the variance $\sigma_v^2 \equiv \psi(\langle m \rangle)$ where $\langle m \rangle$ the mean. In fact, $\psi(\langle m \rangle)$ in systems with short-ranged spatial correlations can be calculated by integrating the two-point spatial correlation function. An important consequence of the main result is the following. When the variance of subsystem mass is proportional to the square of its mean, i.e., $\psi(\langle m \rangle) = \langle m \rangle^2 / v\eta$ with a parameter $\eta$ that depends on the dynamical rules of a particular model, the subsystem mass distribution is a *gamma* distribution,

$$P_v(m) = \frac{1}{\Gamma(v\eta)} \left( \frac{v\eta}{\langle m \rangle} \right)^{v\eta} m^{v\eta - 1} e^{-v\eta m / \langle m \rangle}, \tag{2.1}$$

1 The work reported here is based on the paper "Gammalike mass distribution and mass fluctuation in conserved-mass transport processes", Sayani Chatterjee, Punyabrata Pradhan and P. K. Mohanty, Physical Review Letters, 112, 030601 (2014)

where $\Gamma(\eta) = \int_0^\infty m^{\eta-1}\exp(-m)dm$ the gamma function. Indeed, we find that $\psi(\langle m\rangle)$ is proportional to $\langle m\rangle^2$ in a broad class of mass transport models, which explains why these models exhibit gamma distributions.

It might be surprising how the variance alone could determine the probability distribution $P_v(m)$ as an analytic probability distribution function is uniquely determined only if *all* its moments are provided. However, the result can be understood from the fact that, for a system satisfying the above conditions (i) and (ii), there exists an equilibriumlike chemical potential and consequently a fluctuation-response relation that relates mass fluctuation to the response due to a change in chemical potential. This relation, analogous to equilibrium fluctuation dissipation theorems, provides a unique functional dependence of the chemical potential on mean mass and constrains $P_v(m)$ to take a specific form. In section 2.2, we provide the analytical proof of our result, in section 2.3, we take a few examples of conserved-mass transport processes and verify our result with the help of analytics and simulations. Lastly, in section 4.4, we summarize the scope of this work and conclude.

## 2.2 PROOF

Let us consider a mass transport process on a lattice of $V$ sites with continuous mass variables $m_i \geq 0$ at site $i = 1, \ldots, V$. With some specified rates, masses get fragmented and then the neighboring fragments of mass coalesce with each other. At this stage, we need not specify details of the dynamical rules, only assume that the total mass $M = \sum_{i=1}^{V} m_i$ is conserved. We partition the system into $\nu$ subsystems of equal sizes $v = V/\nu$ and consider fluctuation of mass $M_k$ in $k$th subsystem. We assume that the joint probability $\mathcal{P}(\{M_k\})$ of subsystems having masses $\{M_1, M_2, \ldots M_\nu\} \equiv \{M_k\}$ has a factorized form in steady state,

$$\mathcal{P}(\{M_k\}) \simeq \frac{\prod_{k=1}^{\nu} w(M_k)}{Z(M,V)}\delta\left(\sum_{k=1}^{\nu} M_k - M\right), \tag{2.2}$$

where weight factor $w(M_k)$ depends only on mass $M_k$ of $k$th subsystem and

$$Z(M,V) = Z(M,v\nu) = \prod_{k=1}^{\nu}[\int dM_k w(M_k)]\delta(\sum_{k=1}^{\nu} M_k - M) \tag{2.3}$$

the partition sum.

Distribution $P_v(m)$ of mass $M_k = m$ in the $k$th subsystem of size $v$ is obtained by summing over all other subsystems $k' \neq k$, i.e.,

$$\begin{aligned} P_v(m) &= w(m)\frac{\prod_{k'\neq k}\left[\int dM_{k'} w(M_{k'})\right]}{Z(M,V)}\delta\left(\sum_k M_k - M\right), \\ &= w(m)\frac{Z(M-m,V-v)}{Z(M,V)}. \end{aligned} \tag{2.4}$$

Taking logarithm in both sides of the above equation we expand $\ln Z(M-m,V-v)$ in leading order of $m, v$ in the thermodynamic limit $m \ll M, v \ll V; M, V \gg 1$ with mass density $\rho = M/V$ finite,

$$\begin{aligned} \ln Z(M-m,V-v) &\simeq \ln Z(M,V) - \left(\frac{\partial \ln Z}{\partial M}\right)\Big|_V m - \left(\frac{\partial \ln Z}{\partial V}\right)\Big|_M v \\ &\simeq \ln Z(M,V) + (\mu m) - pv, \end{aligned}$$

where $\mu = -\frac{\partial \ln Z}{\partial M}$ and $p = \frac{\partial \ln Z}{\partial V}$. Thus we get the subsystem mass distribution as

$$P_v(m) = w(m)\frac{Z(M-m,V-v)}{Z(M,V)} = \frac{w(m)e^{\mu(\rho)m}}{\mathcal{Z}(\mu)}, \tag{2.5}$$

where the normalization constant is given by

$$\mathcal{Z}(\mu) = \int_0^\infty w(m)\exp(\mu m)dm = \exp(pv). \tag{2.6}$$

The chemical potential is identified as

$$\mu(\rho) = \frac{df(\rho)}{d\rho}, \tag{2.7}$$

with $Z(M,V) = \exp[-Vf(\rho)]$ [9, 12, 33, 36].

Using two equalities for mean of the subsystem mass and its variance

$$\langle m\rangle = v\rho = \frac{\partial \ln \mathcal{Z}}{\partial \mu}, \tag{2.8}$$

$$\sigma_v^2(\langle m\rangle) = (\langle m^2\rangle - \langle m\rangle^2) = \frac{\partial^2 \ln \mathcal{Z}}{\partial \mu^2}, \tag{2.9}$$

a fluctuation-response relation is obtained in the following form

$$\frac{d\langle m\rangle}{d\mu} = \sigma_v^2(\langle m\rangle). \tag{2.10}$$

For a homogeneous system, the mean and the variance should be independent of $i$. Moreover, when mass is conserved, the variance is a function of mean mass $\langle m \rangle$ or equivalently density $\rho$, i.e., $\sigma_v^2(\langle m \rangle) = \psi(\langle m \rangle)$ . The analogy between Eq. 2.10 and the fluctuation dissipation theorems in equilibrium is now evident. Now Eqs. 2.7 and 2.10 can be integrated to obtain $Z(M, V) = \exp(-Vf(\rho))$ and then its Laplace transform

$$\tilde{Z}(s, V) = \int_0^\infty Z(M, V) e^{-sM} dM = \int_0^\infty e^{-Vf(\rho) - sM} dM. \tag{2.11}$$

On the other hand, taking Laplace transform of Eq. 2.3 on both sides, we get,

$$\begin{aligned} \int_0^\infty Z(M, V) \exp(-sM) dM &= \int_0^\infty \int \prod_{k=0}^{\nu} dM_k w(M_k) \delta(\sum_k M_k - M) \exp(-sM) dM \\ \tilde{Z}(s, V) &= \prod_k \int w(M_k) \exp(-sM_k) dM_k = \tilde{w}(s)^\nu, \end{aligned} \tag{2.12}$$

which gives the Laplace transform of the weight factor $w(m)$

$$\tilde{w}(s) = [\tilde{Z}(s, V)]^{1/\nu}.$$

One can calculate $\tilde{w}(s)$ straightforwardly using the Laplace transform of $Z(M, V)$. Then taking its inverse Laplace transform, we get the weight factor $w(m)$ and use it in Eq. 2.5 to get $P_v(m)$. Using standard statistical mechanical theory of large deviation, the general form of the logarithm of the subsystem mass distribution, in leading order of subsystem mass $m$ and volume $v$, can be alternatively written as [40]

$$P_v(m) \propto e^{[-vf(m/v) + \mu(\rho)m]}. \tag{2.13}$$

We demonstrate this procedure explicitly in a specific case where the variance of mass in a subsystem of size $v$ is proportional to the square of its mean, i.e.,

$$\sigma_v^2(\langle m \rangle) \equiv \psi(\langle m \rangle) = \frac{\langle m \rangle^2}{v\eta}, \tag{2.14}$$

with $\eta$ a constant depending on parameters of a particular model. By integrating Eq. 2.10 w.r.t. $\langle m \rangle = v\rho$ and using Eq. 2.7 we get

$$\mu(\rho) = -\frac{\eta}{\rho} - \alpha \; ; \; f(\rho) = -\eta \ln \rho - \alpha\rho - \beta. \tag{2.15}$$

The integration constants $\alpha$ and $\beta$ do not appear in the final expression of mass distribution. Finally, we get the partition sum

$$Z(M,V) = \exp[-Vf(\rho)] = (M/V)^{\eta V} \exp\{(\alpha M + \beta V)\}.$$

Its Laplace transform

$$\tilde{Z}(s,V) = e^{\beta V} \frac{\Gamma(\eta V + 1)}{[V^{\eta V}(s-\alpha)^{(\eta V+1)}]}$$

can be written as

$$\tilde{Z}(s,V) \simeq \frac{e^{\beta V}\sqrt{2\pi\eta V}(\eta V)^{\eta V} e^{-\eta V}}{V^{\eta V}(s-\alpha)^{(\eta V+1)}} = \frac{\text{const.}}{(s-\alpha)^{(\eta V+1)}}, \tag{2.16}$$

using asymptotic form of the gamma function

$$\Gamma(z+1) \simeq \sqrt{2\pi z} z^z e^{-z}$$

for large $z$. The constant term in the numerator is independent of $s$ and thus $[\tilde{Z}(s, v\nu)]^{1/\nu}$ gives

$$\tilde{w}(s) = \frac{\text{const.}}{(s-\alpha)^{(v\eta+1/\nu)}} = \frac{\text{const.}}{(s-\alpha)^{v\eta}} \tag{2.17}$$

in the thermodynamic limit $\nu \to \infty$. Consequently its inverse Laplace transform is

$$w(m) \propto m^{v\eta-1} e^{\alpha m}. \tag{2.18}$$

The weight factor $w(m)$, along with Eqs. 2.5 and 2.15, leads to $P_v(m)$ which is a gamma distribution as in Eq. 2.1. This completes the proof for the functional form $\psi(x) \propto x^2$. In general, different classes of mass distributions can be generated for other functional forms of $\psi(x)$ The mass distributions for discrete-mass models can be derived quite straightforwardly. Note that the distribution $P_v(m)$ serves as the large deviation function for mass in a large subsystem.

Though the above proof relies on the strict factorization condition Eq. 2.2, the results are not that restrictive and are applicable to systems when the joint subsystem mass distribution is *nearly* factorized. In fact, the near-factorization of the joint mass distribution can be realized in a wide class of systems as long as correlation length $\xi$ is finite, i.e., spatial correlations are *not* long-ranged. In that case, subsystems of size much larger than $\xi$ can be considered statistically independent and thus well described by Eq. 2.2 [25, 32, 35].

We now illustrate the results in the context of a broad class of mass transport models where exact or near factorization condition holds.

### 2.3.1 *Driven Lattice Gas : Pair Factorized Steady State (DLG-PFSS)*

First we consider driven lattice gases (DLG) on a one dimensional ($1D$) periodic lattice of $L$ sites with discrete masses or number of particles $m_i \in (0, 1, 2, \dots)$ at site $i$ where the total mass $M$ is conserved. A particle hops only to its right neighbor with rate $u(m_{i-1}, m_i, m_{i+1})$ which depends on the masses at departure site $i$ and its nearest neighbors. For a specific rate

$$u(m_{i-1}, m_i, m_{i+1}) = \frac{g(m_{i-1}, m_i - 1)g(m_i - 1, m_{i+1})}{g(m_{i-1}, m_i)g(m_i, m_{i+1})}, \tag{2.19}$$

the steady state mass distribution of the model is pair-factorized [11], i.e.,

$$\mathcal{P}(\{m_i\}) = \frac{\prod_{i=1}^{L} g(m_i, m_{i+1})}{Z(M, L)} \delta\left(\sum_{i=1}^{L} m_i - M\right), \tag{2.20}$$

where $Z$ normalization constant or the partition sum,

$$Z(M, L) = \sum_{\{m_i\}} \prod_{i=1}^{L} g(m_i, m_{i+1}) \delta\left(\sum_{i} m_i - M\right). \tag{2.21}$$

Unlike a site-wise factorized state, i.e., Eq. 2.2 with $\nu = V$, the pair-factorized steady state does generate finite spatial correlations. Moreover, in this work, we consider a particular class of homogeneous function $g(x, y)$, which has the following dependence on its variables $x$ and $y$ such that,

$$g(\Lambda x, \Lambda y) = \Lambda^{\delta} g(x, y), \tag{2.22}$$

where $\delta$ is a real constant parameter. Explicit calculation of correlation function $C(r) = \langle m_i m_{i+r} \rangle - \rho^2$ is possible, but somewhat tedious [41]. However, for our purpose of checking additivity in these models, it is not necessary as the dependence of the correlation function $C(r)$ on density $\rho$ can be obtained, in the limit of large density, through the following scaling analysis. The expectation $\langle m_i m_j \rangle$ can be written as

$$\langle m_i m_j \rangle = \sum_{\{m_k\}} P[\{m_k\}] m_i m_j \simeq \left[\prod_k \int_0^{\infty} dm_k\right] P[\{m_k\}] m_i m_j, \tag{2.23}$$

where the $\sum_{\{m_k\}}$ is approximated by an integral $\left[\prod_k \int dm_k\right]$. Therefore, using Eqs. 2.20 and 2.21, we get

$$\langle m_i m_j \rangle \simeq \frac{\left[\prod_k \int_0^\infty dm_k g(m_k, m_{k+1})\right] m_i m_j \delta\left(\sum_k m_k - M\right)}{\left[\prod_k \int_0^\infty dm_k g(m_k, m_{k+1})\right] \delta\left(\sum_k m_k - M\right)}, \tag{2.24}$$

which, upon rescaling of variables $m_k = \rho \tilde{m}_k$, gives

$$\langle m_i m_j \rangle = \frac{\rho^L \rho^{\delta L} \rho^2 (1/\rho)}{\rho^L \rho^{\delta L} (1/\rho)} \frac{\left[\prod_k \int_0^\infty d\tilde{m}_k g(\tilde{m}_k, \tilde{m}_{k+1})\right] \tilde{m}_i \tilde{m}_j \delta\left(\sum_k \tilde{m}_k - L\right)}{\left[\prod_k \int_0^\infty d\tilde{m}_k g(\tilde{m}_k, \tilde{m}_{k+1})\right] \delta\left(\sum_k \tilde{m}_k - L\right)}. \tag{2.25}$$

Here we have used $g(\rho\tilde{m}_k, \rho\tilde{m}_{k+1}) = \rho^\delta g(\tilde{m}_k, \tilde{m}_{k+1})$ (i.e., Eq. 2.22), $M = \rho L$ and $\delta\left(\sum_k m_k - M\right) \equiv (1/\rho)\delta\left(\sum_k \tilde{m}_k - L\right)$. Simplifying the above expression,

$$\langle m_i m_j \rangle = \frac{\left[\prod_k \int_0^\infty d\tilde{m}_k g(\tilde{m}_k, \tilde{m}_{k+1})\right] \tilde{m}_i \tilde{m}_j \delta\left(\sum_k \tilde{m}_k - L\right)}{\left[\prod_k \int_0^\infty d\tilde{m}_k g(\tilde{m}_k, \tilde{m}_{k+1})\right] \delta\left(\sum_k \tilde{m}_k - L\right)} \rho^2 \equiv A(r)\rho^2, \tag{2.26}$$

where

$$A(r) = \frac{\prod_k \left[\int_0^\infty dm'_k g(m'_k, m'_{k+1})\right] m'_i m'_{i+r} \delta\left(\sum_k m'_k - L\right)}{\prod_k \left[\int_0^\infty dm'_k g(m'_k, m'_{k+1})\right] \delta\left(\sum_k m'_k - L\right)}$$

depends on relative distance $r = |i - j|$ but is independent of $\rho$. Therefore the truncated correlation function can be written as

$$C(r) = (\langle m_0 m_r \rangle - \rho^2) = [A(r) - 1]\rho^2 \equiv \frac{\rho^2}{\tilde{\eta}(r)}, \tag{2.27}$$

where we denote $1/\tilde{\eta}(r) \equiv [A(r) - 1]$. The variance $\sigma_v^2$ of mass $m$ in a subsystem of size $v \ll 1$ can be written as

$$\sigma_v^2 \simeq v \int_0^\infty C(r) dr = v\frac{\rho^2}{\eta} = \frac{\langle m \rangle^2}{v\eta}, \tag{2.28}$$

where we denote $1/\eta \equiv \int 1/\tilde{\eta}(r) dr$ which is a constant.

We now simulate DLG for two specific cases with $g(x, y) = (x^\delta + y^\delta + cx^\alpha y^{\delta-\alpha})$ : Case I. $\delta = 1, c = 0$ and Case II. $\delta = 2, c = 1$ and $\alpha = 1.5$. We then calculate the variance $\sigma_v^2 \equiv \psi(\langle m \rangle)$ as a function of mean mass $\langle m \rangle$. As shown in Fig. 2.1(a), in both the cases, $\psi(\langle m \rangle) \propto \langle m \rangle^2$ as in Eq. 2.14 with $\eta \simeq 2.0$ and $\eta \simeq 3.0$ respectively. For these values of $\eta$, corresponding $P_v(m)$ obtained from simulations are also in excellent agreement with Eq. 2.1 as seen in Fig. 2.1(b).

*Single site mass distribution* - For very small subsystems which are comparable to the correlation length $\xi$, the joint distribution of masses does not factorize due to presence of finite spatial correlations.

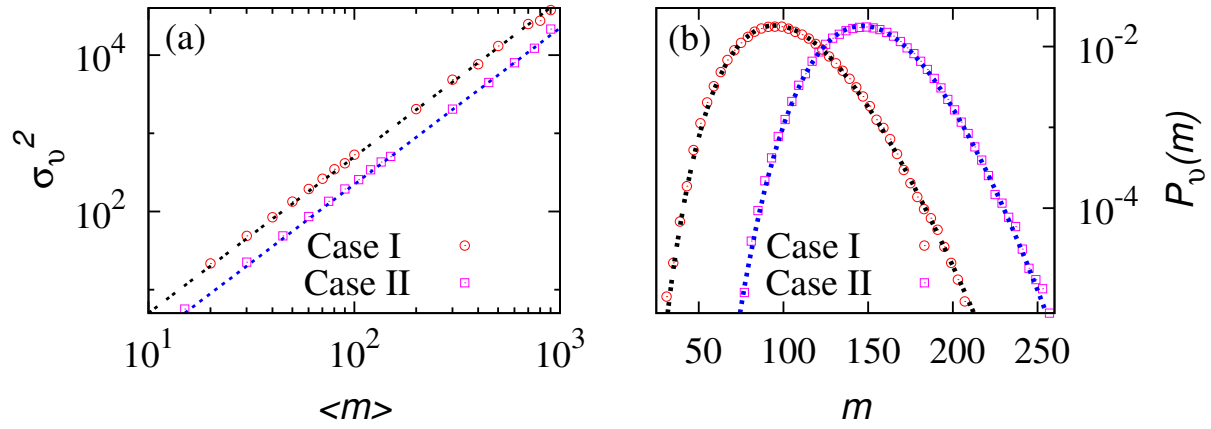


Figure 2.1: Pair-factorized steady state: Variance $\sigma_v^2$ of subsystem mass *vs.* its mean $\langle m \rangle$ [panel (a)], subsystem mass distribution $P_v(m)$ [panel (b)] *vs.* mass $m$ Case I. $\delta = 1$, $c = 0$ and $v = 10$ (red circles) and Case II. $\delta = 2$, $c = 1$, $\alpha = 1.5$ and $v = 15$ (magenta squares); $\rho = 10$ and $L = 2000$ in both the cases. Points - simulations, thick lines - gamma distributions (Eq. 2.1).

In Fig. 2.2 we plot the single-site (i.e., a subsystem of size $v = 1$) mass distribution $P_1(m)$ as a function of mass $m$ for $L = 2000$ and $\rho = 10$. Clearly, the simulation result deviates from the gamma distribution with $\eta = 2$, especially at the right tail.

*Clusterwise Factorized Steady State* - The pair-factorized steady state can be generalized to states where $g(m_i, m_{i+1}, \ldots, m_{i+K})$ is a function of $(K+1)$ variables, i.e., masses in a cluster of $(K+1)$ sites instead of 2 sites in the pair-factorized steady state. We consider a system on a periodic one dimensional (for simplicity) lattice of $L$ sites with total $M$ particles, where the joint probability distribution $\mathcal{P}(\{m_i\})$ in steady state has a product of $(K+1)$-site clusters

$$\mathcal{P}(\{m_i\}) = \frac{\prod_{i=1}^{L} g(m_i, m_{i+1}, \ldots, m_{i+K})}{Z(M,L)} \delta\left(\sum_{i=1}^{L} m_i - M\right), \tag{2.29}$$

with $m_i$ mass at $i$th site having discrete values $m_i = 0, 1, 2, \ldots, M$ and $Z$ the partition sum. As in the case of PFSS systems, the joint distribution of masses in this case also is not factorized on the single-site level as the function $g(m_i, m_{i+1}, \ldots, m_{i+K})$ depends on masses at $K$ neighboring sites and therefore generates finite spatial correlations. We consider only the cases where $g(m_i, m_{i+1}, \ldots, m_{i+K})$ is a homogeneous function,

$$g(\Lambda m_i, \Lambda m_{i+1}, \ldots, \Lambda m_{i+K}) = \Lambda^{\delta} g(m_i, m_{i+1}, \ldots, m_{i+K}), \tag{2.30}$$

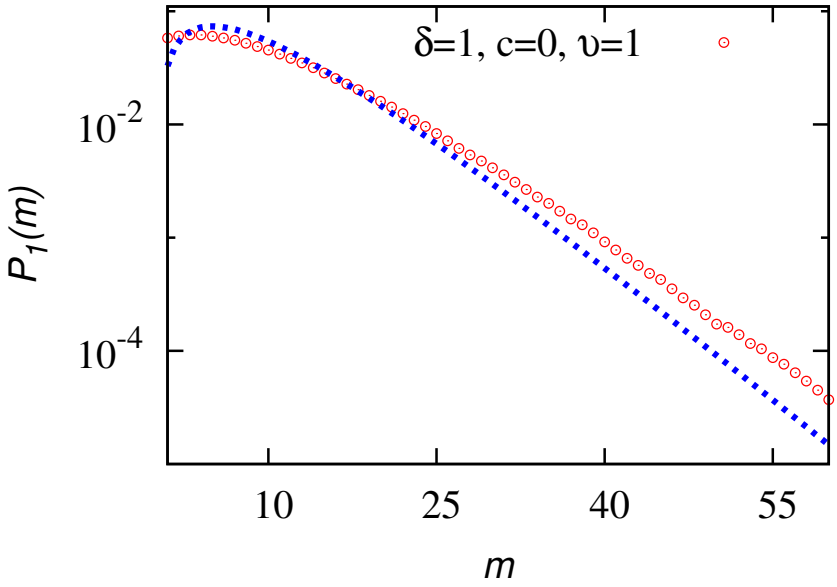


Figure 2.2: Pair-factorized steady state: Single-site mass distribution $P_1(m)$ *vs.* mass $m$ for $\rho$, $L = 2000$, $\delta = 1$, $c = 0$. Red circles - simulation, blue dotted line - gamma distribution with $\eta = 2$ and $v = 1$.

with $\delta$ real. Now using Eqs. 2.29, 2.30 and rescaling $m_k = \rho m'_k$, we find that $\langle m_i m_{i+r}\rangle$ can be written, as $\langle m_i m_{i+r}\rangle \simeq A(r)\rho^2$ where

$$A(r) = \frac{\prod_k \left[\int_0^\infty dm'_k g_k(\{m'_k\}_K)\right] m'_i m'_{i+r} \delta\left(\sum_k m'_k - L\right)}{\prod_k \left[\int_0^\infty dm'_k g_k(\{m'_k\}_K)\right] (m'_k, m'_{k+1}) \delta\left(\sum_k m'_k - L\right)}, \tag{2.31}$$

$g_k(\{m'_k\}_K) \equiv g(m_k, m_{k+1} \ldots, m_{k+K})$ and sum over mass variables replaced by integrals. Clearly, $A(r)$ depends on relative distance $r$ but is independent of $\rho$. We can calculate variance $\sigma_v^2 = v\rho^2/\eta$, which has a form as in Eq. in 2.28 with $\eta^{-1} = \sum_{r=-\infty}^{\infty}[A(r) - 1]$, or $\sigma_v^2 = \langle m\rangle^2/v\eta$. In this case, subsystem mass distribution $P_v(m)$ can be described by gamma distribution.

### 2.3.2 *Mass Chipping Models (MCM)*

#### 2.3.2.1 *Asymmetric Mass Chipping Model*

Next we consider a generic variant of paradigmatic mass transport processes, called *mass chipping models* (MCM) [7, 8, 12–14]. These models are based on mass conserving dynamics with linear mixing of masses at neighboring sites which ensures that $\sigma_v^2 \simeq \langle m\rangle^2/v\eta$ when the two-point correlations are negligible. Note that, factorizability of steady state necessarily implies vanishing of two-point correlations, but not *vice versa*. However, when higher order correlations are also small, which is usually the case in these models, the steady state is

nearly factorized and the resulting $P_v(m)$ can thus be well approximated by gamma distribution for any $v$ (including $v = 1$). We demonstrate these results considering mainly the asymmetric mass transfer in MCM; the symmetric case is then discussed briefly.

In $1D$, asymmetric MCM is defined as follows. On a periodic lattice of size $L$ with a mass variable $m_i \geq 0$ at site $i$, first $(1-\lambda)$ fraction of mass $m_i$ is chipped off from site $i$, leaving the rest of the mass at $i$. Then a random fraction $y_i$ of the chipped-off mass $(1-\lambda)m_i$ is transferred to the right neighbor and the rest comes back to site $i$. At each site, the chipping process occurs with probability $p$; thus the extreme limits $p = 0$ and 1 correspond respectively to random sequential (i.e., continuous-time dynamics) and parallel update rules. Effectively, at time $t$, mass $m_i(t)$ at site $i$ evolves following a *linear* mixing-dynamics

$$m_i(t+1) = m_i(t) - (1-\lambda)[\gamma_i m_i(t) - \gamma_{i-1} m_{i-1}(t)], \tag{2.32}$$

where $\gamma_i = \delta_i y_i$ with $\delta_i$ and $y_i$ are independent random variables drawn at each site $i : \delta_i = 1$ or 0 with probabilities $p$ and $1-p$ respectively and $y_i$ is distributed according to a probability distribution $\phi(y_i)$ in $[0,1]$. Squaring and averaging both sides at steady state ignoring two point correlation we get,

$$\begin{aligned}\langle m_i^2\rangle &= \langle m_i^2\rangle + (1-\lambda)^2\langle\delta_i^2\rangle\langle y_i^2\rangle\langle m_i^2\rangle + (1-\lambda)^2\langle\delta_{i-1}^2\rangle\langle y_{i-1}^2\rangle\langle m_{i-1}^2\rangle \\ &\quad -2(1-\lambda)\langle\delta_i\rangle\langle y_i\rangle\langle m_i^2\rangle - 2(1-\lambda)^2\langle\delta_i\rangle\langle\delta_{i-1}\rangle\langle y_i\rangle\langle y_{i-1}\rangle\langle m_i\rangle\langle m_{i-1}\rangle \\ &\quad +2(1-\lambda)\langle\delta_{i-1}\rangle\langle y_{i-1}\rangle\langle m_i\rangle\langle m_{i-1}\rangle. \end{aligned} \tag{2.33}$$

So, replacing suffices $(i-1)$ by $i$ and putting $\langle m_i\rangle = \rho$ we get,

$$\begin{aligned}\langle m_i^2\rangle &= \langle m_i^2\rangle + 2(1-\lambda)^2\langle\delta_i^2\rangle\langle y_i^2\rangle\langle m_i^2\rangle - 2(1-\lambda)\langle\delta_i\rangle\langle y_i\rangle\langle m_i^2\rangle - 2(1-\lambda)^2\langle\delta_i\rangle^2\langle y_i\rangle^2\rho^2 \\ &\quad +2(1-\lambda)\langle\delta_i\rangle\langle y_i\rangle\rho^2. \end{aligned} \tag{2.34}$$

Now, $\delta_i$ takes value 1 with probability $p$ and 0 with probability $(1-p)$. So, the first two moments of the distribution $P(\delta_i)$ of $\delta_i$ are given by,

$$\langle\delta_i\rangle = \sum_0^1 \delta_i P(\delta_i) = p, \qquad \langle\delta_i^2\rangle = \sum_0^1 \delta_i^2 P(\delta_i) = p.$$

Considering, $\mu_k = \int_0^1 y^k \phi(y) dy$ moments of $\phi(y)$,

$$\begin{aligned}\langle m_i^2\rangle &= \langle m_i^2\rangle + 2(1-\lambda)^2 p\mu_2\langle m_i^2\rangle - 2(1-\lambda)p\mu_1\langle m_i^2\rangle - 2(1-\lambda)^2 p^2\mu_1^2\rho^2 \\ &\quad +2(1-\lambda)p\mu_1\rho^2, \\ [2p\mu_1 - 2(1-\lambda)p\mu_2]\langle m_i^2\rangle &= [2p\mu_1 - 2(1-\lambda)p^2\mu_1^2]\rho^2, \\ [2\mu_1 - 2(1-\lambda)\mu_2]\langle m_i^2\rangle &= [2\mu_1 - 2(1-\lambda)p\mu_1^2]\rho^2, \end{aligned}$$

we obtain the second moment of single site mass $m_i$ in the following form

$$\langle m_i^2 \rangle = \frac{\mu_1 - p\mu_1^2(1-\lambda)}{\mu_1 - \mu_2(1-\lambda)}\rho^2. \tag{2.35}$$

Thus, the variance in single site mass can be calculated as following

$$\begin{aligned} \sigma_i^2 &= \langle m_i^2 \rangle - \rho^2, \\ &= \left[\frac{\mu_1 - p\mu_1^2(1-\lambda)}{\mu_1 - \mu_2(1-\lambda)} - 1\right]\rho^2, \\ &= \frac{(1-\lambda)(\mu_2 - p\mu_1^2)}{[\mu_1 - (1-\lambda)\mu_2]}\rho^2 = \frac{\rho^2}{\eta}, \end{aligned} \tag{2.36}$$

with,

$$\eta = \frac{\mu_1 - (1-\lambda)\mu_2}{(1-\lambda)(\mu_2 - p\mu_1^2)}. \tag{2.37}$$

For uniform distribution $\phi(y) = 1$, $\mu_1 = \frac{1}{2}$ and $\mu_2 = \frac{1}{3}$, which gives

$$\eta = \eta(\lambda, p) = \frac{2(1+2\lambda)}{(1-\lambda)(4-3p)}. \tag{2.38}$$

Moreover, in these models, as the two-point correlation $\langle m_i m_{i+r} \rangle \simeq \rho^2$ for $|r| > 0$, the variance of subsystem mass is given by $\sigma_v^2 \simeq v\sigma_1^2 = \langle m \rangle^2 / v\eta$.

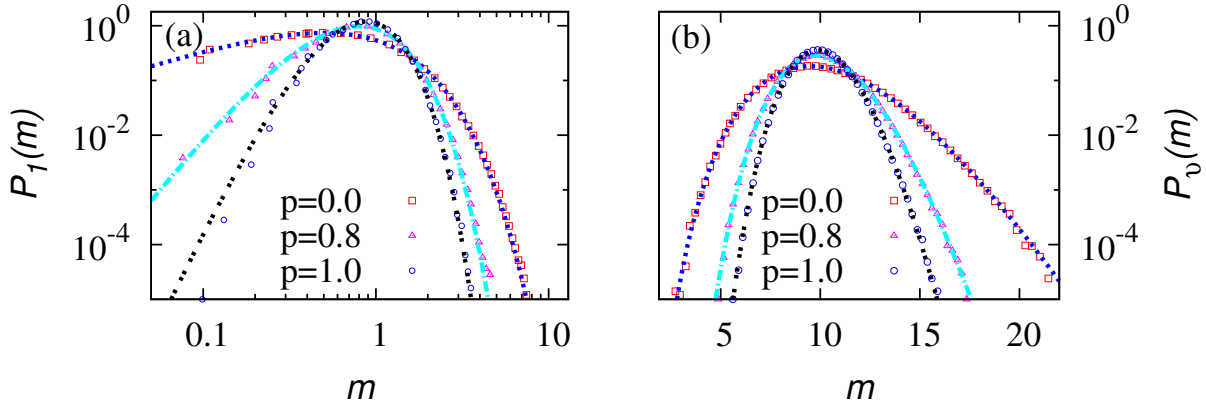


Figure 2.3: Mass chipping models: Single site mass distribution $P_1(m)$ [panel (a)], subsystem mass distributions $P_v(m)$ [panels (b)] *vs.* mass $m$ with $\lambda = 1/2$ and $p = 0$ (red squares), 0.8 (magenta triangles) and 1 (blue circles). Points - simulations, thick lines - gamma distributions (Eq. 2.1) for panel (a): $\rho = 1$, $v = 1$ and $L = 1000$ and panel (b): $\rho = 1$, $v = 10$ and $L = 1000$.

A special case of asymmetric MCM with $\lambda = 0$ and $p = 1$ is the '$q$' model of force fluctuations [15, 16] which has a factorized steady state for a class of distribution $\phi(y)$ [12]. In this case, $P_1(m)$ can be immediately obtained by using $\eta = (\mu_1 - \mu_2)/(\mu_2 - \mu_1^2)$ (from Eq. 2.37) and $v = 1$ in Eq. 2.1. The mass distribution is in perfect agreement with that obtained earlier [12] using generating function method. As a specific example, let us consider

$$\phi(y) = \frac{y^{a-1}(1-y)^{b-1}}{B(a,b)} \tag{2.39}$$

with $B(a,b) = \int_0^1 x^{(a-1)}(1-x)^{(b-1)}dx = \Gamma(a)\Gamma(b)/\Gamma(a+b)$. The first moment is calculated as

$$\begin{aligned} \mu_1 &= \int_0^1 y\phi(y)dy = \int_0^1 \frac{y^a(1-y)^{b-1}}{B(a,b)}dy = \frac{B(a+1,b)}{B(a,b)}, \\ &= \frac{\Gamma(a+1)\Gamma(b)\Gamma(a+b)}{\Gamma(a+b+1)\Gamma(a)\Gamma(b)} = \frac{a}{(a+b)}, \end{aligned} \tag{2.40}$$

and the second moment is given by

$$\begin{aligned} \mu_2 &= \int_0^1 y^2\phi(y)dy = \int_0^1 \frac{y^{(a+1)}(1-y)^{b-1}}{B(a,b)}dy = \frac{B(a+2,b)}{B(a,b)}, \\ &= \frac{\Gamma(a+2)\Gamma(b)\Gamma(a+b)}{\Gamma(a+b+2)\Gamma(a)\Gamma(b)} = \frac{ab}{(a+b)^2(a+b+1)} + \frac{a^2}{(a+b)^2}. \end{aligned} \tag{2.41}$$

Thus, putting these two moments in the expression of $\eta$ obtained by Zielen *et. al* we get $\eta = a + b$. Corresponding mass distributions is in agreement with that obtained in [13]. For $\lambda = 0$ and $p < 1$, the generalized asymmetric MCM becomes the asymmetric random average process [7, 12, 13]. Now, when $y$ is uniformly distributed in $[0,1]$ the steady state is not factorized and exact expression of $P_1(m)$ is not known [8]. However, since the two-point correlations vanish [8], we assume the steady state to be nearly factorized and obtain $P_1(m)$, a gamma distribution with $\eta = 2/(4-3p)$. We verified numerically that this simple form agrees with the actual $P_1(m)$ remarkably well except for small $m \ll \rho$.

For generic $\lambda$ and $p$ and for a uniform $\phi(y) = 1$ for $y \in [0,1]$, the steady state is not factorized [14] and the spatial correlations in general are nonzero. Consequently, no closed form expression of the mass distribution is known, except in a mean-field approximation for $\lambda = 1/2$ and $p = 0$ [14]. However, the spatial correlations are small and gamma distribution provides in general a good approximation of $P_v(m)$. In Fig. 2.3 (a), $P_1(m)$ versus $m$ is plotted for $\lambda = 1/2$, $\rho = 1$ and for various $p = 0, 0.8$ and 1. One can see that $P_1(m)$ agrees quite well with Eq. 2.1 with respective values of $\eta = 2$, 5, and 8. The deviation for small values of $m \ll \rho$ is an indication of the absence of strict factorization on the single-site level. In Fig. 2.3 (b), distribution $P_v(m)$ of mass $m$ in a subsystem of volume $v = 10$ is plotted as a function

of $m$ and it is in excellent agreement with Eq. 2.1 almost over five orders of magnitude. Note that, although Eq. 2.2 does not strictly hold on the single-site level, it holds extremely well for subsystems - a feature observed in these models for generic values of parameters.

#### 2.3.2.2 *Symmetric Mass Chipping Model*

In symmetric MCM's, with parallel update rules, a fraction $\lambda$ of mass $m_i$ at site $i$ is retained at the site and fraction $(1-\lambda)$ of the mass is randomly and symmetrically distributed to the two nearest neighbor sites [14]: $m_i(t+1) = \lambda m_i(t) + (1-\lambda)y_{i-1}m_{i-1}(t) + (1-\lambda)(1-y_{i+1})m_{i+1}(t)$ where $y_i$ uniformly distributed in $[0,1]$. For $\lambda = 0$, the steady state is factorized [14] and $P_1(m)$ is exactly given by Eq. 2.1 with $\eta = 2$. Clearly, when $\lambda = 0$, both symmetric and asymmetric MCM's with parallel updates result in $\eta = 2$, which explains why $P_1(m)$ in these two cases are the same [14]. $P_1(m)$ with other update rules are not described by Eq. 2.1, due to the presence of finite spatial correlations.

### 2.3.3 *Mass Exchange Model (MEM)*

Our results are also applicable to models of energy transport [42] and wealth distributions [19–21, 43, 44] defined on a $1D$ periodic lattice of size $L$. Here, $(1-\lambda)$ fraction of the sum $m^s(t) = m_i(t) + m_{i+1}(t)$ of individual masses (equivalent to 'energy' or 'wealth') at nearest-neighbor sites $i$ and $i+1$ is redistributed :

$$m_i(t+dt) = \lambda m_i(t) + y(1-\lambda)m^s(t) \tag{2.42}$$

$$m_{i+1}(t+dt) = \lambda m_{i+1}(t) + (1-y)(1-\lambda)m^s(t) \tag{2.43}$$

where $y$ is uniformly distributed in $[0,1]$. In this process the total mass remains conserved. Squaring and taking average on both side of this equation at steady state and using the mean field approximation $\langle m_i m_j\rangle \approx \langle m_i\rangle\langle m_j\rangle = \rho^2$, we get,

$$\begin{aligned}\langle m_i^2\rangle &= \lambda^2\langle m_i^2\rangle + 2\lambda(1-\lambda)\langle y\rangle[\langle m_i^2\rangle + \langle m_i\rangle^2] + \langle y^2\rangle(1-\lambda)^2[2\langle m_i^2\rangle + 2\langle m_i\rangle^2], \\ &= \lambda^2\langle m_i^2\rangle + \lambda(1-\lambda)[\langle m_i^2\rangle + \langle m_i\rangle^2] + \frac{2}{3}(1-\lambda)^2[\langle m_i^2\rangle + \langle m_i\rangle^2].\end{aligned} \tag{2.44}$$

So, we get the second moment of single site mass $m_i$,

$$\begin{aligned}\langle m_i^2\rangle[1-\lambda^2-\lambda(1-\lambda)-\frac{2}{3}(1-\lambda)^2] &= [\lambda(1-\lambda)+\frac{2}{3}(1-\lambda)^2]\langle m_i\rangle^2, \\ [1+\lambda-2\lambda^2]\langle m_i^2\rangle &= [(1-\lambda)(\lambda+2)]\langle m_i\rangle^2, \\ \langle m_i^2\rangle &= \frac{(\lambda+2)}{(2\lambda+1)}\langle m_i\rangle^2.\end{aligned} \tag{2.45}$$

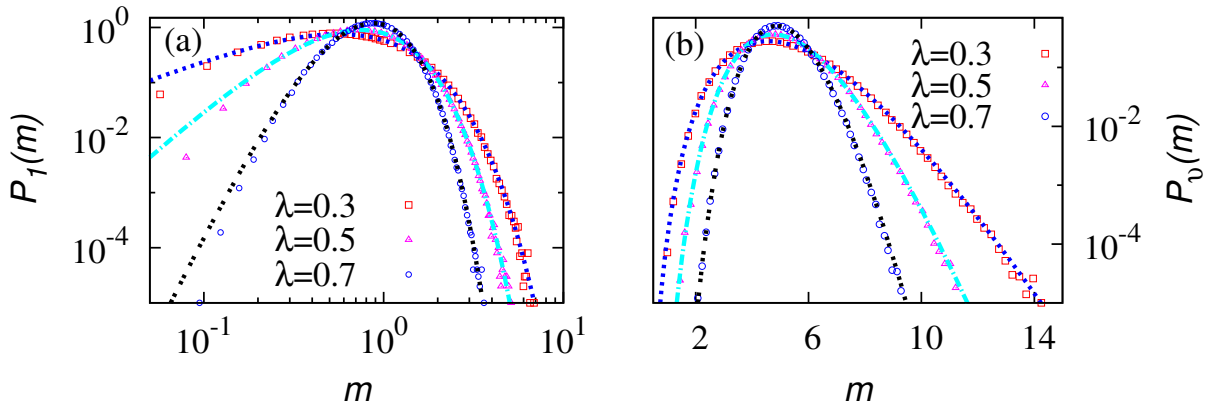


Figure 2.4: Wealth distribution models: Single site mass distribution $P_1(m)$ [panel (a)], subsystem mass distribution $P_v(m)$ [panel (b)] *vs.* mass $m$ with $\lambda = 0.3$ (red squares), 0.5 (magenta triangles) and 0.7 (blue circles). Points - simulations, thick lines - gamma distributions (Eq. 2.1), for panel (a): $\rho = 1$, $v = 1$ and $L = 1000$ and panel (b): $\rho = 1$, $v = 5$ and $L = 1000$.

Thus we obtain the variance in single site mass $m_i$ as,

$$\begin{aligned} \sigma_i^2 &= \langle m_i^2 \rangle - \langle m_i \rangle^2, \\ &= \left[ \frac{(\lambda+2)}{(2\lambda+1)} - 1 \right] \rho^2 = \frac{(1-\lambda)}{(2\lambda+1)} \rho^2 = \frac{\rho^2}{\eta}, \end{aligned} \tag{2.46}$$

where,

$$\eta(\lambda) = 1 + \frac{3\lambda}{(1-\lambda)}, \tag{2.47}$$

which is in agreement with that found earlier numerically [21]. For $\lambda = 0$, i.e., Kipnis-Marchioro-Presutti model in equilibrium [42], the steady state is factorized and $P_1(m) = \exp(-m/\rho)/\rho$ (with $\eta = v = 1$) is exact. For non-zero $\lambda$, as the spatial correlations are small, the mass distributions, to a good approximation, are gamma distributions. In Fig. 2.4(a), $P_1(m)$ versus $m$ is plotted for $\lambda = 0.3$, 0.5 and 0.7 with $\rho = 1$ and $L = 1000$. Except for $m \ll \rho$, $P_1(m)$ agrees well with Eq. 2.1. For a subsystem of size $v = 5$, the distribution $P_v(m)$, plotted in Fig. 2.4 (b) for the same parameter values as in the single-site case, are in excellent agreement with Eq. 2.1 for almost over five orders of magnitude.

## 2.4 SUMMARY

In this work, we argue that subsystem mass fluctuation in driven systems, with mass conserving dynamics and short-ranged spatial correlations, can be characterized from the functional dependence of variance of subsystem mass on its mean. As described in Eq. 2.2, such systems

could effectively be considered as a collection of statistically independent subsystems of sizes much larger than correlation length, ensuring existence of an equilibriumlike chemical potential and consequently a fluctuation-response relation. This relation along with the functional form of the variance, which can be calculated from the knowledge of only two-point spatial correlations, uniquely determines the subsystem mass distribution. We demonstrate the result in a broad class of mass transport models where the variance of the subsystem mass is shown to be proportional to the square of its mean - consequently the mass distributions are gamma distributions which have been observed in the past in different contexts. From a general perspective, this work could provide valuable insights in formulating a nonequilibrium thermodynamics for driven systems.

# 3

# ZEROTH LAW OF THERMODYNAMICS FOR NONEQUILIBRIUM STEADY STATES IN CONTACT

## 3.1 INTRODUCTION

Zeroth law is the cornerstone of equilibrium thermodynamics. It states that, if two systems are separately in equilibrium with a third one, they are also in equilibrium with each other [45]. An immediate consequence of the zeroth law is the existence of state functions - a set of intensive thermodynamic variables (ITV) which equalize for two systems in contact. For example, if two systems are allowed to exchange a conserved quantity, say mass, they eventually achieve equilibrium where chemical potential becomes uniform throughout the *combined* systems. The striking feature of this thermodynamic structure is that all equilibrium systems form equivalence classes where each class is specified by a particular ITV. Then a system, an element of a particular class, is related to any other system in the class by a property that they have the same value of the ITV.

We ask whether a similar thermodynamic characterization is possible in general for systems having a nonequilibrium steady state (NESS). Can equalization of an ITV, governing "equilibration" between two steady state systems in contact, be used to construct such equivalence classes? The answer is nontrivial; in fact, it is not even clear if such a formulation is at all possible [24–26, 30, 31, 37, 46–51]. In this chapter, we find an affirmative answer to this question, which can lead to a remarkable thermodynamic structure where a vast class of systems having a NESS form equivalence classes, equilibrium systems of course included.

There have been extensive studies in the past to find a suitable statistical mechanical framework for systems having a NESS [24–26, 30, 31, 35, 37, 46, 51–55]. Though the studies have not yet converged to a universal picture, it has been realized that suitably chosen mass exchange rates at the contact could possibly lead to proper formulation of a nonequilibrium thermodynamics [31–33, 35, 36, 51]. An appropriate contact dynamics is crucial because, without it, properties of mass fluctuations in a system would be different, depending on whether the system is in contact (grandcanonical) or *not* in contact (canonical) with other system; in other words, without an appropriate contact dynamics, canonical and grandcanonical ensembles

would not be equivalent [33, 56]. The situation is analogous to that in equilibrium where equivalence of ensembles, a basic tenet of equilibrium thermodynamics, is ensured by the mass exchange rates which satisfy detailed balance with respect to the Boltzmann distribution. However in nonequilibrium, in the absence of a priori knowledge of microscopic steady state structure, the intriguing questions, (a) whether there indeed exist a class of exchange rates which could lead to the construction of a well-defined nonequilibrium thermodynamics and (b) how the rates could be determined, are still unsettled.

Previous studies addressed some of these issues. However, the exact studies [35, 36] were mostly confined to a special class of models, called zero range processes. These models have product-measure or factorized steady state and therefore do not have any spatial correlations. In other studies, a class of lattice gas models with nonzero spatial correlations were considered [31, 32, 34, 37, 38] and, for some particular choice of mass exchange rates, zeroth law was found to be obeyed. However, the mass exchange rates, even in the limit of slow exchange, alters the fluctuation properties of the individual systems, leading to the breakdown of equivalence between canonical and grandcanonical ensembles.

In this chapter [1], we formulate necessary and sufficient condition for which equilibrium thermodynamics can be consistently extended to *weakly interacting* nonequilibrium steady state systems having *nonzero* spatial correlations. Under this condition, zeroth law is obeyed and "equilibration" between two systems (labeled by $\alpha = 1, 2$) in contact can be characterized by equalization of an intensive thermodynamic variable which is inherently associated with the respective isolated system. To obtain such a thermodynamic structure, we require the following condition: Mass exchange from one system to the other should occur weakly across the contact with the exchange rates satisfying

$$\frac{u_{12}(\epsilon)}{u_{21}(\epsilon)} = e^{-\Delta F}, \tag{3.1}$$

a reminiscent of detailed balance condition in equilibrium. Here $u_{\alpha\alpha'}(\epsilon)$ is the rate with which a mass of size $\epsilon$ is transferred from system $\alpha$ to $\alpha'$, and $\Delta F$ is the change in a nonequilibrium free energy of the contact regions. In the limit of weak interaction between systems, the mass exchange rates are not necessarily small, but only that the mass exchange process do not affect the dynamics in the individual systems. Now, Eq. 3.1 requires a free energy function inherent to individual isolated system to exist, which, we argue, is the case in a system having short-ranged spatial correlations. This free energy function can in principle be obtained from a fluctuation-response relation, analogous to fluctuation-dissipation theorems in equilibrium.

1 The work reported here is based on the paper "Zeroth law of thermodynamics for nonequilibrium steady states in contact", Sayani Chatterjee, Punyabrata Pradhan and P. K. Mohanty, Physical Review E, 91, 062136 (2015)

The notion of weak interaction is crucial to construct a well-defined nonequilibrium thermodynamics. Also in equilibrium, one implicitly assumes weak interaction where interaction energy between systems is taken to be vanishingly small so that bulk dynamics in an individual system remain unaffected by the other system which may be put in contact with the former. Likewise, weakly interacting nonequilibrium systems imply that dynamics in the individual systems remain unaffected even when two systems are kept in contact. The weak interaction limit, which essentially demands vanishing of correlations between two systems across the contact, is however not guaranteed by mere slow exchange of masses and *vice versa*. We demonstrate how the weak interaction limit can actually be achieved.

The organization of the chapter is as follows. In section 3.2.1, we discuss why an additivity property as in Eq. 3.8 is required for constructing a well-defined thermodynamic structure for nonequilibrium systems. In section 3.2.2, we show that the coarse-grained balance condition (see Eq. 3.1) on mass exchange rates ensures the desired additivity property. In section 3.3, through various previously studied models and their variants, we illustrate how the mass exchange rates can be explicitly constructed so that the balance condition Eq. 3.1 is satisfied. In section 3.4, we discuss that generic mass exchange rates, even in the limit of slow exchange, leads to the breakdown of equivalence between canonical and grandcanonical ensembles. At the end, in section 3.5 we summarize with a few concluding remarks and open issues.

## 3.2 THEORY

### 3.2.1 *General considerations*

Let us consider two systems $\alpha = 1, 2$ of size $V_\alpha$, having mass variables $\mathbf{m}_\alpha \equiv \{m_i \geq 0\}$ defined at the sites $i \in V_\alpha$. Each of the systems, while not in contact with each other (we refer to the situation as *canonical ensemble*), has a nonequilibrium steady state distribution

$$\mathcal{P}_\alpha(\mathbf{m}_\alpha) = \frac{\omega_\alpha(\mathbf{m}_\alpha)}{W_\alpha(M_\alpha, V_\alpha)} \delta\left(M_\alpha - \sum_{i \in V_\alpha} m_i\right), \tag{3.2}$$

where $\omega_\alpha(\mathbf{m}_\alpha)$ is the steady state weight of a microscopic configuration $\mathbf{m}_\alpha$ and

$$W_\alpha(M_\alpha, V_\alpha) = \int d\mathbf{m}_\alpha \omega_\alpha(\mathbf{m}_\alpha) \delta\left(M_\alpha - \sum_{i \in V_\alpha} m_i\right),$$

is the partition sum ($\int d\mathbf{m}_\alpha$ implies integral over all mass variables $m_i$ with $i \in V_\alpha$). The delta function ensures conservation of mass $M_\alpha = \sum_{i \in V_\alpha} m_i$, or mass density $\rho_\alpha = M_\alpha / V_\alpha$, of individual systems. The microscopic weight $\omega_\alpha(\mathbf{m}_\alpha)$ is the time-independent solution of Master equation governing the time evolution of the system in the configuration space of $\mathbf{m}_\alpha$

and in most cases is *not* known. On the other hand, when the systems 1 and 2 are in contact, mass exchange from one system to the other at the contact region breaks conservation of $M_{1,2}$ whereas the total mass $M = M_1 + M_2$ of the combined system remains conserved. We refer this situation as a *grandcanonical ensemble*.

To have a consistent thermodynamic structure, it is necessary that individual systems themselves have well defined canonical free energy functions, $F_{1,2}$ for systems $\alpha = 1$ or 2. Moreover, this free energy function should not change due to the contact between the two systems. That is, free energy of the combined system $F = F_1 + F_2$ is obtained by adding the corresponding canonical free energies of the individual systems and the macrostate, or the maximum probable state, is obtained by minimizing the total free energy function. This additivity property has the following immediate consequences: (i) Equalization of an intensive thermodynamic variable, (ii) a fluctuation-response relation and (iii) zeroth law; all of them follows from standard statistical mechanics [45].

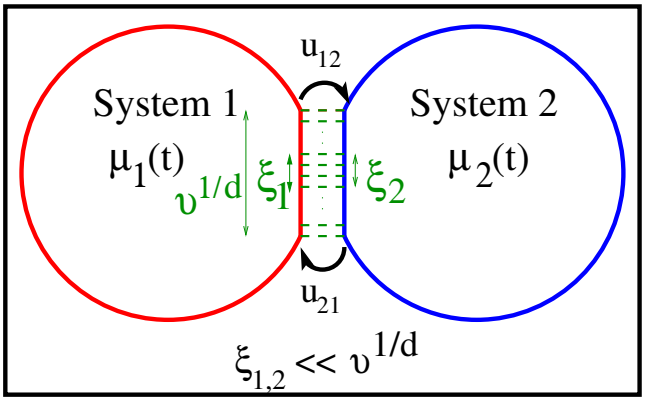


Figure 3.1: Schematic representation: "Equilibration" of two steady state systems in contact. Intensive thermodynamic variables $\mu_1(t)$ and $\mu_2(t)$, chemical potentials of systems 1 and 2 at time $t$, eventually equalize in the steady state, $\mu_1(t = \infty) = \mu_2(t = \infty)$. The size of the contact region $v^{1/d}$, $v$ the volume of the contact region in $d$ dimension, is much larger than the individual correlation length $\xi_\alpha$.

First we discuss the macroscopic properties of systems in canonical ensemble and how a free energy function can be defined consistently for nonequilibrium systems. We consider an individual system $\alpha$ divided into two subsystems, each of which being much larger than spatial correlation length $\xi_\alpha$ and total mass $M_\alpha$ being conserved. As subsystems much larger than the correlation lengths would be statistically independent in the thermodynamic limit, the steady state subsystem mass distribution can be written as product of some weight factors which depend only on mass of the individual subsystem [25, 35]. Thus, when $\xi_{1,2} \ll v \ll V_{1,2}$, we could view each individual system $\alpha$ composed of two statistically independent (apart from the constraint of total mass conservation provided by a delta function) macroscopically large subsystems - contact region (of size $v$ and mass $M_\alpha^c$) and the

rest, i.e., the bulk (of size $V_\alpha - v$ and mass $M_\alpha^b = M_\alpha - M_\alpha^c$) - whose steady state weights are factorized, i.e., product of two coarse-grained weights, as reflected in the partition sum

$$W_\alpha(M_\alpha, V_\alpha) \simeq \int dM_\alpha^c W_\alpha(M_\alpha - M_\alpha^c) W_\alpha(M_\alpha^c). \tag{3.3}$$

Or equivalently, the joint probability distribution of subsystem masses will have a factorized form

$$\begin{aligned} P(M_\alpha^c, M_\alpha^b) &\simeq \frac{W_\alpha(M_\alpha^c) W_\alpha(M_\alpha^b)}{W_\alpha(M_\alpha, V_\alpha)} \delta\left(M_\alpha - M_\alpha^c - M_\alpha^b\right) \\ &= \frac{e^{-[F_\alpha(M_\alpha^c) + F_\alpha(M_\alpha^b)]}}{e^{-F_\alpha(M_\alpha)}} \delta\left(M_\alpha - M_\alpha^c - M_\alpha^b\right), \end{aligned} \tag{3.4}$$

which is maximized to obtain macrostate of the systems (i.e., the maximum probable state). These considerations immediately lead to the existence of a canonical free energy $F_\alpha \equiv -\ln W_\alpha$ in the steady state. The total steady state free energy $F_\alpha(M_\alpha, V_\alpha)$ of the two subsystems is additive and is obtained by minimizing the sum of free energy of the bulk (of volume $V - v$) and that of the contact region (of volume $v$),

$$F_\alpha(M_\alpha, V_\alpha) = \inf_{M_\alpha^c} [F_\alpha(M_\alpha^c, v) + F_\alpha(M_\alpha - M_\alpha^c, V_\alpha - v)]. \tag{3.5}$$

The additivity property in Eq. 3.4 and the above minimization of total free energy implies existence of an intensive thermodynamic variable, called chemical potential,

$$\mu_\alpha(\rho_\alpha) = \frac{\partial F_\alpha}{\partial M_\alpha} = \frac{\partial f_\alpha}{\partial \rho_\alpha}, \tag{3.6}$$

which takes the same value for any subsystems (macroscopically large). In the above equation, we have defined a nonequilibrium free energy density function $f_\alpha(\rho_\alpha) = F_\alpha / V_\alpha$.

It should be noted that the nonequilibrium free energy function is defined in such a way that the principle of free energy minimization automatically holds. Interestingly, for a steady state system having a conserved-mass, this free energy function as well as chemical potential can be calculated from subsystem mass fluctuations (as illustrated later in various models) and therefore has practical importance, e.g., describing phase coexistence [34, 40], etc.

We next consider grandcanonical ensemble - a situation where mass exchange takes place between two systems through contact regions (see Fig. 3.1) each with volume $v$ (taken same for both systems for simplicity) which is much larger than finite spatial correlation length $\xi_\alpha$ but otherwise *arbitrary*. We demand that the canonical description where $M_1$ and $M_2$ are individually conserved, must be equivalent to the grandcanonical ensemble where only total mass $M = M_1 + M_2$ is conserved. That is, the microscopic weight of the combined

system must be a product of the individual canonical microscopic weights and therefore the probability of a microscopic configuration of the combined system should be given by

$$\mathcal{P}(\mathbf{m}_1, \mathbf{m}_2) = \frac{\omega_1(\mathbf{m}_1)\omega_2(\mathbf{m}_2)}{W(M)} \delta\left(M - M_1 - M_2\right), \tag{3.7}$$

with the the partition sum of the combined system being

$$W(M, V) = \int dM_1 W_1(M_1, V_1) W_2(M - M_1, V_2).$$

So the the joint distribution of individual system masses is also factorized and can be written as the product of the individual canonical weights,

$$\begin{aligned} P(M_1, M_2) &= \frac{W_1(M_1, V_1) W_2(M_2, V_2)}{W(M, V)} \\ &\times \delta\left(M - M_1 - M_2\right), \end{aligned} \tag{3.8}$$

and thus additivity is ensured for the combined systems. That is, total free energy $F(M, V) \equiv -\ln W(M, V)$ of the combined system in the steady state is given by

$$F(M, V) = \inf_{M_1} [F_1(M_1, V_1) + F_2(M - M_1, V_2)],$$

which is the sum of individual canonical free energies. This implies that the chemical potential equalizes upon contact, i.e., $\mu_1(\rho_1) = \mu_2(\rho_2)$.

### 3.2.2 *Proof of the balance condition*

Now we show how, in the weak interaction limit, the balance condition in Eq. 3.1 ensures additivity property in Eq. 3.8 - the main result of this work. Let mass exchange occur at the contact with rate $u_{\alpha\alpha'}(\epsilon)$ where a mass $\epsilon$ is transferred from system $\alpha$ to $\alpha'$. The rate may depend on both the mass values at the two contact regions (the mass dependence not explicitly shown in $u_{\alpha\alpha'}$). Mass conservation in the individual systems is then broken in this process ($M_\alpha \to M_\alpha - \epsilon$ and $M_{\alpha'} \to M_{\alpha'} + \epsilon$), generating a mass flow. To attain stationarity, average mass current $J_{12}(\epsilon)$ generated by all possible microscopic exchanges corresponding the rates $u_{12}$, where the chipped off mass $\epsilon$ flows from system 1 to 2, must be balanced by the reverse current $J_{21}(\epsilon)$. Though the net steady state current $|J_{\alpha\alpha'}(\epsilon) - J_{\alpha'\alpha}(\epsilon)|$ from one system to the other (across the contact) is exactly zero, the individual systems can still be far away from equilibrium and can have nonzero steady state mass currents in the bulk.

Since the total mass $M = M_1 + M_2$ of the combined system is conserved, the current balance condition $J_{12}(\epsilon) = J_{21}(\epsilon)$ can be written, using only one of the mass variables, say $M_1$, as

$$\begin{aligned} P(M_1, M - M_1)U_{12}(M_1, \epsilon) &= P(M_1 - \epsilon, M - M_1 + \epsilon) \\ &\times \quad U_{21}(M - M_1 + \epsilon, \epsilon). \end{aligned} \tag{3.9}$$

Here $U_{\alpha\alpha'}(x, y)$ is an effective rate with which mass $y\epsilon$ is transferred from system $\alpha$, having mass $x$, to $\alpha'$. The current balance, along with Eq. 3.8, gives

$$\frac{U_{12}(M_1, \epsilon)}{U_{21}(M - M_1 + \epsilon, \epsilon)} = e^{-\Delta F}, \tag{3.10}$$

where $\Delta F = \sum_{\alpha=1}^{2}(F_\alpha|_{\text{final}} - F_\alpha|_{\text{initial}})$ difference in free energy of the combined system. Or equivalently, we write the above ratio of effective exchange rates as

$$\frac{U_{12}(M_1, \epsilon)}{U_{21}(M - M_1 + \epsilon, \epsilon)} = e^{(\mu_\alpha - \mu_{\alpha'})\epsilon}, \tag{3.11}$$

where $\mu_\alpha = \partial F_\alpha / \partial M_\alpha$ is a nonequilibrium chemical potential (see Eq. 3.6) which is inherently associated with the individual system $\alpha$.

Next we obtain a condition on the actual microscopic exchange rate $u_{12}(\epsilon)$. We first use the expression of current $J_{\alpha\alpha'}(\epsilon) = \langle u_{\alpha\alpha'} \rangle$ as the average mass transfer rate from system $\alpha$ to $\alpha'$ and write $J_{12}(\epsilon) = \int\int d\mathbf{m}_1 d\mathbf{m}_2 \mathcal{P}(\mathbf{m}_1, \mathbf{m}_2) u_{12}(\epsilon)$ as given below

$$\begin{aligned} J_{12}(\epsilon) &= \left[\prod_{\alpha=1}^{2} \int d\mathbf{m}_\alpha\right] \mathcal{P}(\mathbf{m}_1, \mathbf{m}_2) u_{12}(\epsilon) \delta(M - \sum_{\alpha=1}^{2} M_\alpha) \\ &= \frac{1}{W(M, V)} \int\int d\mathbf{m}_1 d\mathbf{m}_2 \omega_1(\mathbf{m}_1)\omega_2(\mathbf{m}_2) u_{12}(\epsilon) \\ &\times \quad \delta\left(M_1 - \sum_{i \in V_1} m_i\right) \delta\left(M_2 - \sum_{i \in V_2} m_i\right) \delta(M - \sum_{\alpha=1}^{2} M_\alpha) \\ &\simeq \frac{1}{W(M, V)} \int\int dM_1^c dM_2^c u_{12} W_1(M_1^c) W_2(M_2^c) \\ &\times \quad W_1(M_1 - M_1^c, V_1 - v) W_2(M_2 - M_2^c, V_2 - v). \end{aligned} \tag{3.12}$$

In the last step, we inserted an identity $\int dM_\alpha^c \delta(M_\alpha^c - \sum_{i \in v} m_i) = 1$, where $v$ being denoted here as the contact region in system $\alpha$, and then used the factorization property,

$$\begin{aligned} \int d\mathbf{m}_\alpha w_\alpha(\mathbf{m}_\alpha) \delta\left(M_\alpha - \sum_{i \in V_\alpha} m_i\right) \delta\left(M_\alpha^c - \sum_{i \in v} m_i\right) \\ \simeq W_\alpha(M_\alpha^c, v) W_\alpha(M_\alpha - M_\alpha^c, V_\alpha - v), \end{aligned}$$

as in Eq. 3.3. As demonstrated later in various models in section III, the above factorization property is expected to be valid when the size of the contact region is much larger than the spatial correlation length $\xi_\alpha$ in system $\alpha$, i.e., when $v \gg (\xi_\alpha)^d$ in $d$ dimension. Then, after some straightforward manipulations, we write $U_{12}(M_1, \epsilon) = J_{12}(\epsilon)/P(M_1, M_2)$ as

$$U_{12}(M_1, \epsilon) = \int_\epsilon \int_0 dM_1^c dM_2^c u_{12}(\epsilon) \prod_{\alpha=1}^{2} \frac{W_\alpha(M_\alpha^c) e^{\mu_\alpha M_\alpha^c}}{\mathcal{Z}_\alpha}, \tag{3.13}$$

by using Eq. 3.8 and using the following equality

$$W_\alpha(M_\alpha^c) \frac{W_\alpha(M_\alpha - M_\alpha^c, V_\alpha - v)}{W_\alpha(M_\alpha, V_\alpha)} = \frac{W_\alpha(M_\alpha^c) e^{\mu_\alpha M_\alpha^c}}{\mathcal{Z}_\alpha}$$

where $\mathcal{Z}_\alpha = \int dM_\alpha^c \; W_\alpha(M_\alpha^c) \; e^{\mu_\alpha M_\alpha^c}$. Similarly, the effective reverse exchange rate, corresponding to the transition $\{M_1^c - \epsilon, M_2^c + \epsilon\} \to \{M_1^c, M_2^c\}$, can be written as

$$\begin{aligned} U_{21}(M - M_1 + \epsilon, \epsilon) &= e^{(\mu_2 - \mu_1)\epsilon} \int_\epsilon \int_0 dM_1^c dM_2^c u_{21}(\epsilon) \\ &\times \frac{W_1(M_1^c - \epsilon) e^{\mu_1 M_1^c}}{\mathcal{Z}_1} \frac{W_2(M_2^c + \epsilon) e^{\mu_2 M_2^c}}{\mathcal{Z}_2}. \end{aligned} \tag{3.14}$$

Now, substituting Eqs. 3.13 and 3.14 in Eq. 3.11 and then by equating the integrals which is valid for any functional form of weight factor $W_\alpha(m)$, we get the desired balance condition as in Eq. 3.1,

$$\frac{u_{12}}{u_{21}} = \frac{W_1(M_1^c - \epsilon)}{W_1(M_1^c)} \frac{W_2(M_2^c + \epsilon)}{W_2(M_2^c)} = e^{-\Delta F^c} = e^{-\Delta F}. \tag{3.15}$$

In the last step, we used the free energy of the contact region $F_\alpha^c(M_\alpha^c) = -\ln W_\alpha(M_\alpha^c)$ and equate the change in free energy at the contact $\Delta F^c = \sum_{\alpha=1}^2 \Delta F_\alpha^c$ to the change in total free energy of the combined system $\Delta F$. This is so since the total free energy $F = \sum_{\alpha=1}^2 (F_\alpha^c + F_\alpha^b)$ can be written as a sum of bulk free energy $F_\alpha^b$ and contact free energy $F_\alpha^c$ where $\Delta F_\alpha^b = 0$ (i.e., changes occur only at the contact regions). It is important to note that the balance condition holds only at the contact regions for mass transfer from one system to the other. However, there is no detailed balancing in the bulk, except when both the systems are in equilibrium.

The balance condition in Eq. 3.15 is necessary and sufficient to ensure that the steady state has the required product form as in Eq. 3.7. This is because any contact dynamics which is constrained by the balance condition in Eq. 3.15 indeed satisfies Master equation in the steady state as the mass-current balance condition $J_{12}(\epsilon) = J_{21}(\epsilon)$, used for deriving the balance condition Eq. 3.1, is nothing but the balancing of configuration-space current occurring due to exchange of masses. This completes the proof.

The contact dynamics Eq. 3.15 is a general one and does not uniquely specify the contact dynamics (CD). We discuss two simple choices in this work, which are given below,

$$\text{CD I} \quad : \quad u_{\alpha\alpha'} = u_0 p(\epsilon) \frac{W_\alpha^c(M_\alpha^c - \epsilon)}{W_\alpha^c(M_\alpha^c)}, \tag{3.16}$$

$$\text{CD II} \quad : \quad u_{\alpha\alpha'} = u_0 p(\epsilon) \text{Min}\{1, e^{-\Delta F}\}, \tag{3.17}$$

where $u_0$ an arbitrary constant (not necessarily small) and $p(\epsilon)$ is a probability that mass $\epsilon$ is chosen for exchange. One should note that the limit $u_0 \to 0$ implies slow exchange of masses. The case with $u_0 = 0$ implies no exchange of masses, i.e., the systems are kept isolated. The resemblance between the rate in Eq. 3.17 and the familiar Metropolis rate is indeed striking. In equilibrium, Eq. 3.15 reduces to the condition of detailed balance, albeit on a coarse-grained level. A similar notion of coarse-grained detailed balance was previously envisaged in [36], though in the context of zero range processes which do not have any spatial correlations.

What still remains to be done is to explicitly specify the exchange rates satisfying Eq. 3.15. This requires calculation of the subsystem weight factor $W_\alpha(m, v)$ in a particular system of interest, which can be done following Ref. [57]. The Laplace transform $\tilde{W}_\alpha(s, v) = \int_0^\infty W_\alpha(M_\alpha^c) \exp(-sM_\alpha^c) dM_\alpha^c$ of the subsystem weight factor can be written in terms of the Laplace transform $\tilde{W}_\alpha(s, V_\alpha) = \int_0^\infty W_\alpha(M_\alpha, V_\alpha) \exp(-sM_\alpha) dM_\alpha$ of the individual canonical partition sum $W_\alpha(M_\alpha, V_\alpha)$ as

$$\tilde{W}_\alpha(s, v) = \left[\tilde{W}_\alpha(s, V_\alpha)\right]^{v/V_\alpha}, \tag{3.18}$$

in the limit $V_\alpha \gg v \gg \xi_\alpha^d$ (in $d$ dimensions). The partition sum $W_\alpha(M_\alpha, V_\alpha)$ can be calculated, as follows, from a canonical fluctuation-response relation, i.e., subsystem mass fluctuation when calculated in canonical ensemble with $u_0 = 0$ is related to the change in density $\rho_\alpha$ in response to the change in chemical potential $\mu_\alpha$ (as in Eq. 3.6) as given below

$$\frac{d\rho_\alpha}{d\mu_\alpha} = \psi_\alpha(\rho_\alpha), \tag{3.19}$$

where, for subsystem volume $v \gg \xi_\alpha^d$, the function $\psi_\alpha(\rho_\alpha) = \sigma_v^2/v$ with variance of subsystem mass $\sigma_v^2 = \langle (M_\alpha^c)^2 \rangle - v^2\rho_\alpha^2$. The variance of subsystem mass in system $\alpha$ can be calculated from the knowledge of correlation function $c_\alpha(r)$ as $\sigma_v^2 \simeq v \sum_{r=-\infty}^{r=\infty} c_\alpha(r)$ where $c_\alpha(r) = \langle m_i m_{i+r} \rangle - \rho_\alpha^2$ is the two-point correlation between masses at sites $i$ and $i + r$ [57]. We assumed here that the correlation function $c_\alpha(r)$ is short-ranged or sufficiently rapidly decaying function so that it is integrable, which is usually the case when there is no long-ranged correlations in the systems. Therefore, once the functional dependence of $\psi_\alpha(\rho_\alpha)$ on the respective density is known, the partition sum for individual system $W_\alpha(M_\alpha, V_\alpha) =$

$\exp[-Vf_\alpha(\rho_\alpha)]$, $f_\alpha(\rho_\alpha)$ being nonequilibrium free energy density, can be obtained by first integrating the fluctuation-response relation Eq. 3.19 w.r.t. density $\rho_\alpha$ and then integrating chemical potential as given in Eq. 3.6. Then the subsystem weight factor $W_\alpha(m)$ can be obtained, via inverse Laplace transform, from Eq. 3.18.

We emphasize here that, even when the detailed microscopic weight $\omega_\alpha(\mathbf{m}_\alpha)$ is not known, the subsystem weight factor $W_\alpha(m, v)$ can still be obtained, either analytically or numerically, from the subsystem mass fluctuations or equivalently from the two-point spatial correlation functions; this makes our formulation work both in theory and in practice.

## 3.3 MODELS AND ILLUSTRATIONS

In this section, we illustrate our analytical results in nonequilibrium models studied extensively in the past as well as in their variants. For each of these models, we analytically obtain chemical potential $\mu(\rho_\alpha)$ and the weight factor $W_\alpha(m)$ when the system is isolated (i.e., $u_0 = 0$), and then we explicitly construct the mass exchange rates $u_{\alpha\alpha'}$ so that they satisfy the balance condition Eq. 3.15. Using these rates, we perform simulations (we use both the contact dynamics I and II). Our simulations demonstrate that, when two systems are kept in contact with unequal initial individual chemical potentials, they indeed "equilibrate" where the chemical potentials associated with the respective isolated systems equalize in the final steady state of the combined system.

### 3.3.1 *Zero Range Processes*

For completeness, we first consider zero range processes (ZRP) [10] which have a factorized steady state (FSS). For ZRP, a well-defined thermodynamic structure has been previously constructed [36]. Consider two systems $\alpha = 1, 2$ where their steady state weights

$$\omega_\alpha(\mathbf{m}_\alpha) = \prod_{i \in V_\alpha} h_\alpha(m_i)$$

are simply product of factors $h_\alpha(m_i)$, function of only single-site mass variable. The individual systems exactly satisfy Eq. 3.3 with weights of contact region and the rest of system being $W^c_\alpha = (f_\alpha)^v$ and $W^b_\alpha = (f_\alpha)^{V-v}$, respectively. When mass exchange occurs either with rate CD I (Eq. 3.16) or with rate CD II (Eq. 3.17), it is easy to check that the joint distribution, which satisfies Master equation, is given by

$$\mathcal{P}(\mathbf{m}_1, \mathbf{m}_2) \propto \prod_\alpha \prod_{i \in V_\alpha} \exp[-f_\alpha(m_i)],$$

i.e., product of individual weight factors $\omega_\alpha(\mathbf{m}_\alpha)$ with $f_\alpha(m_i) = -\ln h_\alpha(m_i)$. For FSS, Eq. 3.15 indeed reduces to detailed balancing at the contact, as found in [36].

### 3.3.2 *Finite Range Processes*

Now we consider a more general situation - keeping in contact systems having nonzero *spatial correlations*. To this end, we introduce a broad class of analytically tractable models, for simplicity in one dimension, where a particle (or mass of size $\epsilon$) is transferred stochastically from a site to one of its nearest-neighbors with rates depending on the discrete occupation numbers (or continuous mass variables) of $R$ neighboring sites. These models are direct generalization of the zero range processes [41, 57] and are called here finite range processes, with range $R$. These finite range mass transport processes have a clusterwise factorized steady state (CFSS) where each weight factor depends on the occupation numbers (or mass variables) $m_i$ ($i \in R$) of a cluster of size $R$. We consider two systems $\alpha = 1, 2,$, for simplicity on a one dimensional lattice of size $L$, where each system having a CFSS of form

$$\omega_\alpha(\mathbf{m}_\alpha) = \prod_i g_\alpha(m_i, m_{i+1}, \ldots, m_{i+R}),$$

where $g_\alpha$ a function of $R+1$ mass or occupation variables at consecutive $R+1$ sites. Clearly, $R = 0$ corresponds to the factorized steady state (FSS). The CFSS could arise in a variety of mass transport processes where mass chipping rate in the bulk satisfies certain conditions. Below, we consider only the *continuous* mass CFSS.

Unlike ZRP, the joint distribution of masses is not factorized on the single-site level as $g(m_i, m_{i+1}, \ldots, m_{i+R})$ is function of masses at $R+1$ sites and therefore generates finite spatial correlations. In this work, mainly due to analytical tractability, we consider a special form of $g(m_i, m_{i+1}, \ldots, m_{i+R})$ which is a homogeneous function,

$$g(\Gamma m_i, \Gamma m_{i+1}, \ldots, \Gamma m_{i+R}) = \Gamma^\delta g(m_i, m_{i+1}, \ldots, m_{i+R}), \tag{3.20}$$

with $\delta$ real. For this particular form, the two-point correlation function $c(r)$ can be exactly calculated. By rescaling of the mass variable $m_k = \rho m'_k$, correlation of masses $\langle m_i m_{i+r} \rangle$ at sites $i$ and $i+r$ can be written, as $\langle m_i m_{i+r} \rangle = A(r)\rho^2$ where

$$A(r) = \frac{\prod_k \left[\int_0^\infty dm'_k g_k(\{m'_k\}_R)\right] m'_i m'_{i+r} \delta\left(\sum_k m'_k - L\right)}{\prod_k \left[\int_0^\infty dm'_k g_k(\{m'_k\}_R)\right] (m'_k, m'_{k+1}) \delta\left(\sum_k m'_k - L\right)}, \tag{3.21}$$

$g_k(\{m'_k\}_R) \equiv g(m_k, m_{k+1} \ldots, m_{k+R})$ [57]. The function $A(r)$ depends on relative distance $r$, but is independent of $\rho$, and can be exactly calculated using a transfer matrix method [41]. Then we obtain variance in a subsystem of size $v$ as $\sigma_v^2 = v\rho^2/\eta$ with $\eta^{-1} = \sum_{r=-\infty}^{\infty}[A(r) - 1]$. Now

the subsystem weight factor $W_\alpha(m)$ can be exactly calculated, using the method outlined in the end of section II.B, to get a functional form of $W_\alpha(m) = m^{v\eta_\alpha - 1}$.

In the case of nonzero spatial correlations, by considering a system in a coarse-grained level, one can have physical insights into the role of the balance condition Eq. 3.1. Let us divide a system $\alpha$ into $\nu_\alpha = V_\alpha/v$ number of almost *statistically independent* subsystems of equal volume $v$ with subsystem masses labelled by $\mathcal{M}_\alpha \equiv \{\mathcal{M}_{\alpha,j}\}$, provided that the spatial correlation length $\xi_\alpha$ is much smaller than $v^{1/d}$ (in $d$ dimensions). Then the joint probability distribution of the subsystem masses of systems $\alpha$ are factorized:

$$\mathcal{P}(\{\mathcal{M}_1, \mathcal{M}_2\}) \propto \prod_\alpha \prod_{j \in V_\alpha} \exp\left[-F^{(\alpha)}(\{\mathcal{M}_{\alpha,j}\})\right]$$

where free energy $F_\alpha = -\sum_j \ln W_\alpha(\mathcal{M}_{\alpha,j})$ of system $\alpha$ is additive over the subsystems. Now let two such systems 1 and 2 be kept in contact such that mass from one specific subsystem of 1 participate in a microscopic mass-exchange dynamics with its adjacent subsystem of 2 with rates satisfying Eq. 3.15. In a coarse-grained level, as the subsystems could be considered as sites, the systems effectively become a set of sites with an "FSS", where mass exchange occurs between two adjacent sites (here subsystems) with rates satisfying balance condition Eq. 3.15, and therefore the additivity property in Eq. 3.8 holds exactly in the limit of large subsystem volume $v \gg \xi_{1,2}$.

Next, we discuss in detail a special case of the clusterwise factorized steady state with $R = 1$.

### 3.3.3 *Pair Factorized Steady State (PFSS)*

To demonstrate that our results are valid even in the presence of nonzero spatial correlations, we first consider two one-dimensional periodic lattices of $L_\alpha$ sites with continuous mass variable $m_i \geq 0$ at sites $i = 1, 2, \ldots, L_\alpha$. The following mass conserving dynamics in the bulk leads to a CFSS with $R = 1$, usually called pair factorized steady state (PFSS) [11], where mass $\epsilon$ chosen from a distribution $p_b(\epsilon)$ is chipped off from a site $i$ and transferred to its right neighbor with rate

$$u^b_\alpha(\epsilon) = p_b(\epsilon) \frac{g_\alpha(m_{i-1}, m_i - \epsilon)}{g_\alpha(m_{i-1}, m_i)} \frac{g_\alpha(m_i - \epsilon, m_{i+1})}{g_\alpha(m_i, m_{i+1})}, \tag{3.22}$$

which depends on the masses at the departure site and its nearest neighbors, and on the chipped-off mass $\epsilon$. Since, in this case, mass-transfer happens in only one direction in the bulk, there are nonzero bulk currents present in the individual systems. We consider homogenous $g_\alpha(x, y) = \Gamma^{-\delta} g_\alpha(\Gamma x, \Gamma y)$, for which one can exactly calculate $\psi_\alpha(\rho_\alpha) = \rho_\alpha^2/\eta_\alpha$ and

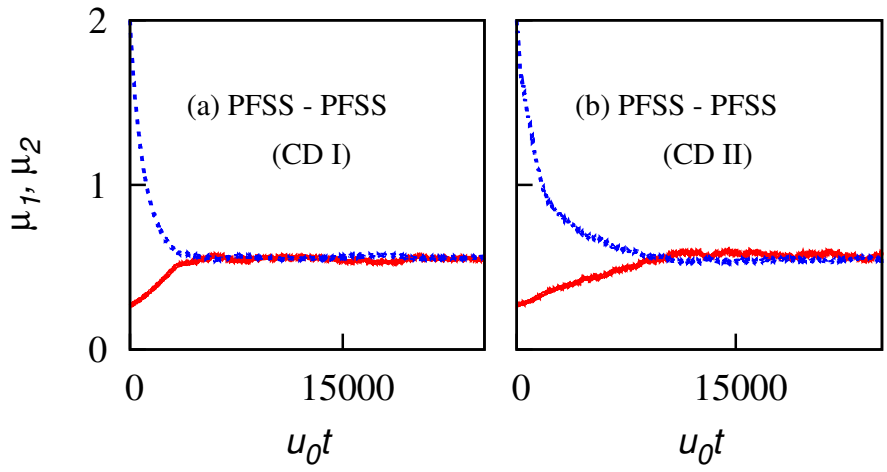


Figure 3.2: "Equilibration" of steady states of two pair factorized models in contact: In (a)-(b), chemical potentials $\mu_1(t)$ and $\mu_2(t)$ of systems 1 (red solid) and 2 (blue dotted) vs. rescaled time $u_0 t$. $\mu_1$ and $\mu_2$, initially chosen to be different, eventually equalize. Densities ($\rho_1$, $\rho_2$) in the final steady states are respectively (3.60, 5.40) in (a), (3.57, 5.43) in (b). In all cases, $p(\epsilon) = p^b(\epsilon) = \exp(-\epsilon)$, $u_0 = 0.1$ and $v = 10$.

values of $\eta_\alpha$ for various microscopic parameters [41]. Then following the method outlined in section II.B, we analytically obtain $W_\alpha(m) = m^{v\eta_\alpha - 1}$ and chemical potential $\mu_\alpha = -\eta_\alpha/\rho_\alpha$ where $\eta_\alpha$ depends on $\delta$. When two such systems are kept in contact, mass conservation in individual system is broken and both density $\rho_\alpha(t)$ and corresponding chemical potential $\mu_\alpha(t)$ evolve until a stationarity is reached where the net mass current from one system to another vanishes and densities are adjusted so that chemical potentials equalize. We simulate using $g_\alpha(x, y) = (x^\delta + y^\delta + cx^\gamma y^{\delta-\gamma})$ and allow the two PFSS with $\eta_1 = 2$ ($\delta = 1$, $c = 0$) and $\eta_2 = 3$ ($\delta = 2$, $c = 1$, $\gamma = 3/2$) to exchange mass following CD I (and CD II in different simulations) with $u_0 = 0.1$, $p(\epsilon) = p_b(\epsilon) = \exp(-\epsilon)$ and $L_1 = L_2 = 1000$. The contact volume $v = 10$ is taken much larger than $\xi_\alpha$ which is here only about a couple of lattice spacings. Simulations in Figs. 3.2(a) and 3.2(b) demonstrate that, starting from arbitrary initial densities, the combined system reaches a stationary state where $\mu_1 = \mu_2$.

The equalization of an ITV, i.e., the above mentioned chemical potential, indeed implies zeroth law which we verify next for three steady states having a PFSS: PFSS1 ($\delta = 1$, $c = 0$; $\eta_1 = 2$), PFSS2 ($\delta = 3$, $c = 0$; $\eta_2 = 4$) and PFSS3 ($\delta = 2$, $c = 1.0$, $\gamma = 3/2$; $\eta_3 = 3$) with CD I. First, PFSS1 with density $\rho_1 \simeq 3.60$ and PFSS2 with density $\rho_2 \simeq 7.25$ are separately equilibrated with a third system PFSS3 with density $\rho_3 \simeq 5.37$. Then, PFSS1 with density $\rho_1$ and PFSS2 with density $\rho_2$ are brought into contact. The two resulting densities after equilibration remain almost unchanged, confirming zeroth law. The zeroth law can be similarly verified for CD II.

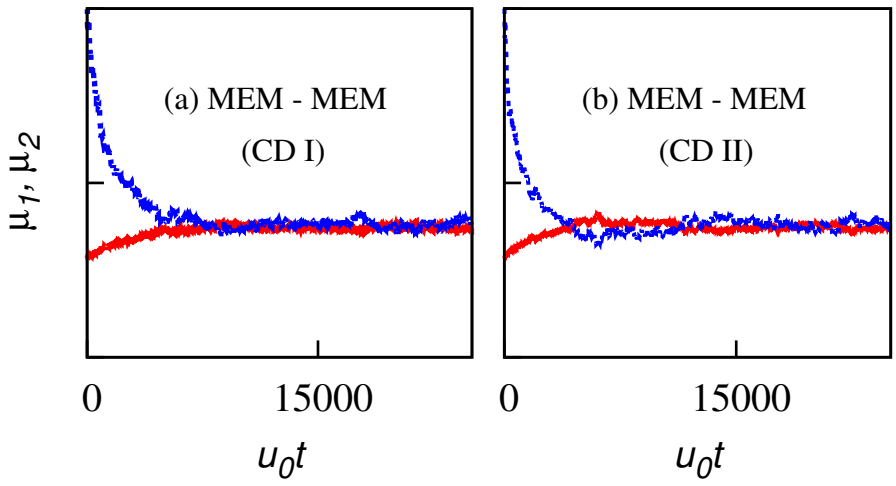


Figure 3.3: "Equilibration" of steady states of two mass exchange models in contact: In (a)-(b), chemical potentials $\mu_1(t)$ and $\mu_2(t)$ of systems 1 (red solid) and 2 (blue dotted) vs. rescaled time $u_0 t$. $\mu_1$ and $\mu_2$, initially chosen to be different, eventually equalize. Densities ($\rho_1$, $\rho_2$) in the final steady states are respectively (5.31, 2.69) in (a), (5.32, 2.68) in (b). In all cases, $p(\epsilon) = p^b(\epsilon) = \exp(-\epsilon)$, $u_0 = 0.1$ and $v = 1$.

There are numerous examples [6–8, 12, 14], where nonequilibrium processes with a conserved-mass show short-ranged spatial correlations, but the exact steady state structures are not known. How does one find a contact dynamics which ensures Eq. 3.8 in these cases? We address the question in a class of widely studied nonequilibrium mass transport processes [19, 42, 43, 58], as another demonstration of how our formulation can be implemented in practice. In these models, we call them mass exchange models (MEM), in one dimension the continuous masses $m_i \geq 0$ and $m_{i+1} \geq 0$ at randomly chosen nearest neighbors $i$ and $i+1$ respectively are updated from time $t$ to $t + dt$ as

$$\begin{aligned} m_i(t+dt) &= \lambda_\alpha m_i(t) + y(1-\lambda_\alpha) m_{sum}(t), \\ m_{i+1}(t+dt) &= \lambda_\alpha m_{i+1}(t) + (1-y)(1-\lambda_\alpha) m_{sum}(t), \end{aligned} \tag{3.23}$$

where, $m_{sum} = m_i + m_{i+1}$ is the sum of nearest neighbor masses, $y$ is a random number uniformly distributed in $[0, 1]$, and $0 < \lambda_\alpha < 1$ a model dependent parameter. As the spatial correlations are nonzero but very small, the subsystem weight factor in the steady states of individual systems can be obtained, to a very good approximation, as $W_\alpha(m) = m^{v\eta_\alpha - 1}$ with $\eta_\alpha = (1 + 2\lambda_\alpha)/(1 - \lambda_\alpha)$ [57]. In Fig. 3.3(a) and 3.3(b), we observe equalization of chemical potentials $\mu_1(t) = -\eta_1/\rho_1(t)$ and $\mu_2(t) = -\eta_2/\rho_2(t)$ (respective ITV in this case) of systems 1 and 2 respectively for both contact dynamics I and II and for $u_0 = 0.1$, $v = 1$, $L_1 = L_2 = 100$

and $p(\epsilon) = p_b(\epsilon) = \exp(-\epsilon)$. The zeroth law can be readily verified for MEM as done in the case of PFSS.

### 3.3.5 *Pair Factorized Steady State and Mass Exchange Models in contact*

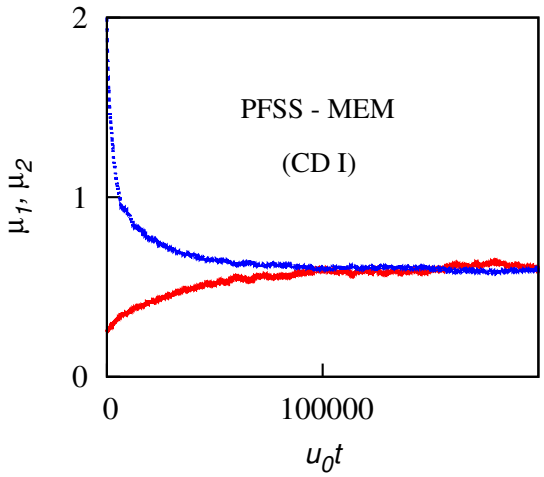


Figure 3.4: "Equilibration" of steady states of one pair factorized and one mass exchange model in contact: chemical potentials $\mu_1(t)$ and $\mu_2(t)$ of systems 1 (PFSS, red solid) and 2 (MEM, blue dotted) vs. rescaled time $u_0 t$. $\mu_1$ and $\mu_2$, initially chosen to be different, eventually equalize. Densities ($\rho_1$, $\rho_2$) in the final steady states are (3.32, 6.68). In all cases, $p(\epsilon) = p^b(\epsilon) = \exp(-\epsilon)$, $u_0 = 0.1$ and $v = 10$

There is no particular difficulty when systems having different kind of bulk dynamics are in contact; equilibration occurs as long as there is a common conserved quantity which is exchanged following Eq. 3.15. We demonstrate this in Fig. 3.4, taking two systems, PFSS and MEM, in contact where mass exchange dynamics at the contact is governed by CD I. In this case, chemical potentials $\mu_1(t)$ and $\mu_2(t)$ eventually equalize and zeroth law follows.

## 3.4 EQUIVALENCE OF ENSEMBLES

In the previous section, we have demonstrated that, when two nonequilibrium systems with short-ranged correlation are allowed to exchange a conserved quantity following a contact dynamics conditioned by Eq. 3.1, they indeed evolve to a stationary state where an intensive thermodynamic variable (ITV), which is inherently associated with the respective isolated system, equalizes. In this thermodynamic construction, zeroth law is obeyed and, at the same time, equivalence of ensembles is also maintained. However, mere equalization of an intensive thermodynamic variable, or validity of zeroth law, does not guarantee the balance

condition Eq. 3.1 and is not enough to construct a consistent nonequilibrium thermodynamics. This is because the ITV which equalizes for systems in grandcanonical ensemble is not necessarily the ITV defined (using additivity property Eq. 3.4) for individual isolated systems in canonical ensemble. To construct a well-defined thermodynamic structure, one must ensure that these two ITVs are indeed the same. That is, one requires that the combined system (grandcanonical ensemble) is statistically equivalent to the individual isolated systems (canonical ensemble).

The requirement of ensemble equivalence, which essentially demands that the contact dynamics must not alter the fluctuation properties in the individual systems, is nothing special in nonequilibrium scenario; it has been an essential ingredient in constructing equilibrium thermodynamics. The proposed balance condition Eq. 3.1 precisely ensures these two aspects - in one hand, it ensures equalization of an intensive thermodynamic variable and, on the other hand, it guarantees ensemble equivalence.

Unlike in equilibrium, when two nonequilibrium systems are brought into contact, the final steady state of the combined system depends, in general, on the absolute values of mass exchange rates, even if the ratio between forward and reverse exchange rates remains unchanged. In these cases too, in the limit of slow mass exchange ($u_0 \to 0$) and weak interaction, there could exist an ITV which equalizes upon contact. However, in spite of equalization of an ITV, as we illustrate in the following subsections, the mass exchange rates which do not satisfy the balance condition Eq. 3.1 lead to the breakdown of ensemble equivalence. That is, mass fluctuation in the isolated systems can be different from that in the combined system and, in that case, an equilibriumlike thermodynamic structure cannot be formulated.

In the examples given below, we consider weakly interacting lattice gases (driven and nondriven both) which exchange masses infinitesimally slowly, i.e., $u_0 \to 0$. The limit of slow exchange is useful in exactly calculating the mass fluctuations as the inhomogeneities which could occur in the contact regions of the individual systems is avoided.

### 3.4.1 *Lattice gases*

We start with $d$-dimensional lattice gases with interacting particles, obeying hardcore exclusion (at most one particle at a site). We consider periodic boundaries, though the following analysis can be straightforwardly extended to other boundary conditions (e.g., reflecting boundary, discussed in the case of nearest-neighbor- exclusion lattice gases in section IV.B). *Internal dynamics*: Particles hop, from one site to its nearest neighbor, inside the individual systems according to some specified rates, e.g., rates satisfying local detailed balance [59] with respect to the Boltzmann distribution $\sim \exp(-\beta E)$ where $\beta$ inverse temperature, $E_\alpha$ energy function of system $\alpha$ and $E = E_1 + E_2$ total energy. *Mass exchange or contact dynamics*:

The rate with which a particle at the contact region (which could be localized, even a point or single-site contact or global contact) jumps from system $\alpha$ to $\alpha'$, provided the contact site in $\alpha$ is occupied and the contact site in $\alpha'$ is unoccupied, is simply a constant $u_0 p_\alpha$. There is no additional constraint on these rates except that $u_0 \to 0$ so that particle exchange occurs very slowly.

Since the transition rates overall do not satisfy detailed balance, the probability of a microscopic configuration of the combined system is not given by the Boltzmann distribution $\sim \exp(-\beta E)$. The particle hopping rates inside the individual systems remain the same irrespective of two systems being in contact or not, which is necessary in realizing the weak interaction limit (which, for a finite $u_0$, is however not sufficient).

The joint probability distribution $P(M_1, M_2)$ of particle numbers $M_1$ and $M_2$ of individual systems, i.e., the large deviation function governing mass or particle-number fluctuations, can be exactly calculated using the general recursion relation Eq. 3.9, with setting $\epsilon = 1$ (i.e., one- particle transfer at a time), as

$$\begin{aligned} P(M_1, M_2) &= P(0, M) \prod_{M_1} \frac{U_{21}(M_2 + 1, 1)}{U_{12}(M_1, 1)} \delta(M - \sum_{\alpha=1}^{2} M_\alpha) \\ &= P(0, M) \left[ e^{\sum_{M_1=0}^{M_1} (\ln U_{21} - \ln U_{12})} \right] \delta(M - \sum_{\alpha=1}^{2} M_\alpha). \end{aligned} \tag{3.24}$$

Now writing the effective mass exchange rates $U_{12} = u_0 p_1 \rho_1 (1 - \rho_2)$ and $U_{21} = u_0 p_2 \rho_2 (1 - \rho_1)$ and integrating over densities, the joint mass distribution can be exactly written in the form as given below,

$$P(M_1, M_2) \propto e^{-[V_1 f_1 + V_2 f_2]} \delta(M - V_1 \rho_1 - V_2 \rho_2), \tag{3.25}$$

where free energy densities $f_1 = \int_0^{\rho_1} \mu_1 d\rho_1$ and $f_2 = \int_{M/V_1}^{\rho_2} \mu_2 d\rho_2$ with chemical potential given by

$$\mu_\alpha(\rho_\alpha) = \ln p_\alpha + \ln \frac{\rho_\alpha}{1 - \rho_\alpha}. \tag{3.26}$$

It is somewhat surprising that the joint mass distribution, as in Eq. 3.24 or 3.25, is actually *independent* of the internal dynamics in each systems. Moreover, the above free energy and chemical potential are nothing but those of a noninteracting hardcore lattice gas. The macrostate, or the maximum probable state, of the combined system with final steady state densities in the individual systems can be obtained by minimizing the total free energy $F = V_1 f_1 + V_2 f_2$, with the constraint $V_1 \rho_1 + V_2 \rho_2 =$ constant. In other words, there exists an intensive thermodynamic variable, we call chemical potential, which indeed equalizes upon contact, i.e., $\mu_1(\rho_1) = \mu_2(\rho_2)$. The equalization of chemical potential essentially signifies the

steady state current balance between two systems across the contact as encoded in Eq. 3.9 and moreover this immediately leads to zeroth law under this particular contact dynamics.

However, in the above construction, clearly there is breakdown of equivalence between canonical and grandcanonical ensembles and, therefore thermodynamically, the construction is not well-defined. We observe that, in this case, the free energy and chemical potential are not the same as those defined in canonical ensemble (see Eq. 3.4) when $u_0 = 0$. In fact, in the canonical ensemble, subsystem particle-number fluctuation in individual systems can have nontrivial properties due to the presence of inter-particle interactions. But, with the above contact dynamics, the particle-number fluctuation in the grandcanonical ensemble is governed by a chemical potential of a noninteracting hardcore lattice gas (see Eq. 3.26), which is so in spite of the presence of inter-particle interaction in the individual systems. The origin of the discrepancy in fluctuations in the two cases with $u_0 = 0$ and $u_0 \to 0$ lies in the fact that mass exchange rates do not satisfy the balance condition Eq. 3.1, which drastically changes the fluctuation properties of the systems in grandcanonical ensembles. That is, unless the balance condition Eq. 3.1 is satisfied by the mass exchange rates, the cases with $u_0 = 0$ and $u_0 \to 0$ are always different.

For example, inequivalence of ensembles arises in the previous studies [31, 32, 34] where two driven lattice gases are allowed to exchange particles with some exchange rates, which were chosen on an *ad hoc* basis. To be specific, let us consider the systems studied in [34], where two lattice gases - a nondriven lattice gas 1 and a driven lattice gas 2 (Katz- Lebowitz-Spohn model [59]), are kept in contact. Particle hopping rates in the bulk as well as the particle exchange rates across the contact both satisfy a local detailed balance [59]. In the limit of slow mass exchange, the ratio of the effective transition rates was found, to a good approximation, to be [34]

$$\frac{U_{12}}{U_{21}} = \frac{e^{\mu_1(\rho_1)}}{e^{\mu_2(\rho_2)}},$$

where $\mu_1(\rho_1)$ and $\mu_2(\rho_2)$ are functions of respective density. By substituting this ratio in Eq. 3.24 and then integrating over densities, one readily obtains the joint distribution $P(M_1, M_2)$ of particle numbers $M_1$ and $M_2$, which has exactly the same form as given in Eq. 3.25. Then, minimizing total free energy function, one can identify $\mu_1(\rho_1)$ and $\mu_2(\rho_2)$ as chemical potentials which equalize in the final steady state after the systems are brought into contact; the equalization of this chemical potential was indeed verified through simulations in [34]. However, the microscopic exchange rates $u_{\alpha\alpha'}$ have not been derived from the canonical fluctuation-response relation Eq. 3.19 and therefore are not constrained by the balance condition Eq. 3.1. Consequently, as in the previous example, these exchange rates lead to the breakdown of ensemble equivalence. That is, free energy function and chemical potential for systems in grandcanonical ensemble are not the same as those for isolated systems in canonical ensemble.

### 3.4.2 *Lattice gases with nearest neighbor exclusion*

Next we consider previously studied athermal hardcore lattice gases, in two dimensions, with nearest neighbor exclusion (NNE) [37, 38]. We study the simplest case where particles can be exchanged through a single-site or point-wise contact ($v = 1$) in each system, which can be readily generalized to other cases, e.g, when particles are exchanged globally ($v = V$) or in higher dimensions. The transition rates for particles hopping inside the individual systems (irrespective of that they are isolated or in contact with each other) can be chosen to be some specific nearest neighbor or next-nearest neighbor (or mixture of both) hopping rates in the presence of a driving field $D$; details of these rates, which can be found in [37, 38], are omitted here as they are not explicitly required in the following analysis as long as the systems exchange particles very slowly.

Let us keep two such lattice gases, systems $\alpha = 1$ and 2, in contact with each other [37, 38] where particles are exchanged as follows. A site is called open if the site as well as all its nearest neighbors are unoccupied. Provided the contact site, say in system 1, is occupied and the contact site in system 2 is open, the particle from system 1 is transferred to system 2 with rate $u_0 \to 0$. The joint distribution $P(M_1, M_2)$ of masses $M_1$ and $M_2$ in the individual systems can be straightforwardly calculated by substituting $U_{\alpha\alpha'}(M_\alpha, \epsilon) = \rho^c_\alpha \rho^{c,\mathrm{op}}_{\alpha'}$ (with $\epsilon = 1$) in Eq. 3.24 where $\rho^c_\alpha$ and $\rho^{c,\mathrm{op}}_{\alpha'}$ are probabilities that contact site is occupied in system $\alpha$ and open in system $\alpha'$, respectively. The probabilities $\rho^c_\alpha(\mathbf{x_c}, \rho_\alpha)$ and $\rho^{c,\mathrm{op}}_\alpha(\mathbf{x_c}, \rho_\alpha)$ are, in principle, functions of the location $\mathbf{x_c}$ of the contact site as well as of the global density $\rho_\alpha$ in system $\alpha$.

Then the joint distribution has the same form as given in Eq. 3.25 where free energy densities can be written as $f_1(\rho_1) = \int_0^{\rho_1} \mu_1 d\rho_1$ and $f_2(\rho_2) = \int_{M/V_1}^{\rho_2} \mu_2 d\rho_2$ with chemical potentials given by

$$\mu_\alpha(\rho_\alpha) = \ln\left(\frac{\rho^c_\alpha}{\rho^{c,\mathrm{op}}_\alpha}\right). \tag{3.27}$$

The macrostate is obtained by minimizing total free energy function $F = V_1 f_1(\rho_1) + V_2 f_2(\rho_2)$ with the constraint $V_1\rho_1 + V_2\rho_2 =$ constant, leading to the existence of an intensive thermodynamic variable, i.e., chemical potential, which indeed equalizes upon contact, $\mu_1(\rho_1) = \mu_2(\rho_2)$. However, the functional form of the chemical potentials does depend on the boundary conditions. Because, a particular boundary condition can make the density profile nonuniform and, consequently, the quantities $\rho^c_\alpha(\mathbf{x_c}, \rho_\alpha)$ and $\rho^{c,\mathrm{op}}_\alpha(\mathbf{x_c}, \rho_\alpha)$ not only depend on density $\rho_\alpha$ but also on the location $\mathbf{x_c}$ of the contact site.

For example, in the case of periodic boundary condition and uniform bulk hopping rates where the system remains homogeneous, chemical potential is given by

$$\mu_\alpha = \ln\left(\frac{\rho_\alpha}{\rho_\alpha^{\rm op}}\right), \tag{3.28}$$

where the density $\rho_\alpha^c(\mathbf{x_c}, \rho_\alpha) = \rho_\alpha$ at the contact site $\mathbf{x_c}$ and the probability $\rho_\alpha^{c,\rm op}(\mathbf{x_c}, \rho_\alpha) = \rho_\alpha^{c,\rm op}(\rho_\alpha)$ of the contact site being open depends only on the bulk density $\rho_\alpha$, i.e., both $\rho_\alpha^c$ and $\rho_\alpha^{c,\rm op}$ do not depend on the location $\mathbf{x_c}$ of the contact. This is exactly the chemical potential which was found in [37], using the concept of virtual exchange, for the pointwise (single-site contact with $v = 1$) as well as for global exchanges ($v = V_\alpha = V_{\alpha'}$).

On the other hand, for hard-wall or reflecting boundary condition (e.g., periodic boundary in $x$ direction and two hard walls placed along $x = 1$ and $x = L$), the density profile becomes nonuniform and the chemical potential then depends on where the contact site is located. For example, if the contact site is located in the bulk, chemical potential has to be calculated with respect to the density and probability of open site in the bulk. That is, even in these cases of nonuniform systems, the existence of the above mentioned chemical potential would then apparently restore an equilibriumlike thermodynamic structure, as formulated in [37, 38] where an ITV equalizes upon contact and zeroth law is obeyed.

In short, in all the above cases of weakly interacting NNE lattice gases with uniform or nonuniform density profiles, there indeed exists, in the limit of slow exchange, an ITV which equalizes upon contact and zeroth law is also obeyed. However, in each of these cases - depending on the boundary conditions and the location of contact site, the functional form of free energy and chemical potential of the individual systems in the grandcanonical ensembles are different. Of course, they are not the same as those defined for the individual isolated systems in canonical ensemble.

## 3.5 SUMMARY AND DISCUSSION

In this chapter, we demonstrate that *weakly interacting* nonequilibrium systems, with short-ranged spatial correlations and having a common conserved quantity, e.g., mass which is exchanged upon contact between two systems, have an equilibriumlike thermodynamic structure in steady state, provided the rates of mass exchange between two systems satisfy a balance condition as given in Eq. 3.1. The size of the contact regions, otherwise arbitrary, should be much larger than correlation lengths, therefore making the contact regions effectively independent of the rest of the systems. The balance condition, reminiscent of equilibrium detailed balance on a coarse-grained level, leads to zeroth law of thermodynamics and fluctuation- response relations analogous to the equilibrium fluctuation- dissipation the-

orems. In other words, for mass exchange rates satisfying the balance condition, one can construct equivalence classes consisting of systems having a nonequilibrium steady state. The systems in each class are specified by the value of an intensive thermodynamic variable, inherently associated with the respective isolated systems, which does not change when any two systems in the class are allowed to exchange mass according to Eq. 3.1.

Following are the two most important aspects in the present study. Firstly, we constructed a well-defined thermodynamic structure, encompassing all (driven or nondriven) steady state systems having *nonzero*, though short-ranged, spatial correlations. Secondly, we have identified the notion of *weak interaction* in constructing such a thermodynamic structure. Note the distinction between the limit of weak interaction and the limit of mere slow mass exchange; the former essentially implies vanishing of spatial correlations between two systems while in contact (ensuring that there is no inhomogeneities at the contact regions) and, moreover, leads to the additivity property as formulated in Eq. 3.8.

In equilibrium, the weak interaction limit directly translates into the infinitesimally small interaction energy between two systems in contact, i.e., sum of the internal energies of the individual systems equals to total internal energy of the combined system. However, in nonequilibrium, the microscopic weights are not determined by energy function and therefore even zero interaction energy could lead to nonzero spatial correlations between two systems while in contact, e.g., when mass exchange rates are finite or nonuniform. In principle, the weak interaction limit can be achieved by keeping the bulk transition rates (i.e., the internal dynamics in the individual systems) unchanged, irrespective of whether the systems are in contact with each other or they are isolated. In weak interaction limit, the systems can exchange mass at finite rate, i.e., weak interaction is possible even when mass exchange rates are finite.

This thermodynamic construction based on additivity may not be valid for the systems having a slow decaying long-ranged spatial correlation, e.g., two-point correlation function decaying as $1/r^d$ (or slower) in $d$ dimensions, which has been observed in a large class of driven systems [60, 61]. In that case, the correlation function is not integrable and therefore the additivity property in Eq. 3.3 presumably breaks down, implying that the fluctuation-response relation in Eq. 3.19 may not exist. Nevertheless, as we demonstrated in this chapter, the results will be applicable to a still wide class of driven systems which have short-ranged correlations. Moreover, even in the presence of long-ranged correlations when the strength of the correlations is weak, the additivity property, to a good approximation, could hold. This possibly explains why driven lattice gases, such as KLS models studied in Refs. [30–32, 37], admit an approximate free energy and chemical potential, thus providing a quite good description of various steady state properties - including description of phase transitions [34] - albeit only in the limit of weak interaction.

It is important to note that the slow exchange of masses do not necessarily imply weak interaction. For example, the nonuniformly driven athermal lattice gas studied in [38] is one where the system is *not* actually weakly interacting, even when mass exchange rates are vanishingly small or slow. In a realistic scenario, finite interaction may be present between two systems while in contact. As an open issue, it remains to be seen whether, in the case of finite interaction, there exists an intensive thermodynamic variable which would equalize upon contact. Also, it would be interesting to explore the validity of additivity property in systems having boundary layers or hard walls, as their presence could alter the fluctuations in the bulk of a system which is otherwise isolated. A related open question [31] is whether the thermodynamic structure based on additivity could be used to connect various physical observables, such as mechanical pressure on a wall [62, 63] or statistical forces on a probe [64], to an intensive thermodynamic variable such as chemical potential. Though addressing these issues in full generality remains a formidable challenge, it would be worthwhile to identify a particular class of driven systems, if any, where connection between 'mechanics' and nonequilibrium thermodynamics could be established on a firmer ground.

We end the discussion with a concluding remark. The problem of constructing a well-defined thermodynamic structure in nonequilibrium, even when spatial correlations are short-ranged, is more subtle than that in equilibrium as, in nonequilibrium, zeroth law alone cannot ensure an equivalence class. Even when zeroth law holds, nonequilibrium ensembles (canonical and grandcanonical) may not be equivalent as the fluctuation properties of systems in grandcanonical ensemble depend on the details of contact dynamics as well as the boundary conditions - which gives insights into the conceptual difficulties in constructing a nonequilibrium thermodynamics, e.g., as attempted in [31–33, 37, 38]. In this scenario, our study provides a general prescription for dynamically generating different equivalent nonequilibrium ensembles and could thus help in formulating a well-defined nonequilibrium thermodynamics for driven systems in general.

# 4

# STATIC AND DYNAMIC CHARACTERIZATION OF CONSERVED LATTICE GASES EXHIBITING ABSORBING PHASE TRANSITION

## 4.1 INTRODUCTION

Absorbing phase transition in conserved lattice gases is one of the well known nonequilibrium critical phenomena, studied intensively in the last two decades. Due to dynamical constraint, these conserved lattice gases cannot get out of some states (once they are reached), which are called absorbing states of the system; other states are called active states. Absorbing to active phase transition is observed upon tuning a parameter, e.g., global particle-number density. Sandpiles were proposed three decades ago as paradigmatic models of "self-organized criticality" (SOC) [65–70] to explain the scale free structure of nature like mountain ranges, river networks, power law distributed activity in earthquake phenomena. Since then, they continued to capture the imagination of physicists and mathematicians alike [71–75]. Sandpiles are defined on discrete lattice sites, associated with discrete nonnegative particles. The dynamics is usually governed by toppling events, where total number of particles is *not* conserved. In the original models, sandpiles are externally driven very slowly by adding a single particle with dissipation at the boundary. Here, slow drive means the time interval between consecutive addition of two particles is large enough so that avalanche of toppling dynamics triggered by the first particle die before adding the next particle. A site becomes active when particle number crosses a threshold value. So, these sandpile models are called threshold activated systems. Particles get transferred from active sites to their nearest neighbors. Thus *avalanche* of activity propagates towards boundary of the system and a particle is lost from boundary sites maintaining a stationary self organized critical state with long-range spatial and temporal correlations. The spatial long-range correlation show up in power law distributed avalanche sizes whereas the temporal one is responsible for giving rise to $1/f$ noise in frequency space. There have been extensive studies of time dependent properties of various nonconserved sandpiles [65–68]. These studies mainly focus on avalanche size distribution and distribution of lifetime of an avalanche. Avalanche

size is measured by the number of toppling occur after addition of a particle. In the critical stationary state, avalanche size distribution has a power law scaling form

$$P(s) = s^{-\tau_s}\mathcal{F}(s/s_0), \tag{4.1}$$

where $\tau$ is a positive exponent and $s_0$ sets the cutoff on the power law behavior. But, this cutoff, related to a characteristic length scale in the system, is due to finite size of the system. So, in thermodynamic limit, avalanche size distribution becomes pure power law. Similar is the case for lifetime distribution of an avalanche which has the finite size scaling form

$$P(t) = t^{-\tau_t}\mathcal{G}(t/t_0). \tag{4.2}$$

Here, $\tau_t$ is another positive exponent. $t_0 \sim L^z$ sets the characteristic time scale, where $z$ is the dynamic exponent. In infinite system size limit, this also shows a power law behavior and thereby, at critical stationary state, system is scale free as it has no characteristic length and time scale. Here, we describe various sandpile models and their universality classes.

*BTW model:* The BTW model [65, 66] is defined on a finite d-dimensional open boundary lattice having $n_i$ number of particles at site $i$. When $n_i \geq 2d$, the site becomes active and particles topple deterministically to the neighboring sites. Each of the $2d$ neighbors gets one particle. When a boundary site topples, particle gets lost from the system. Once toppling starts at a site after addition of a grain, topplings go on till all the sites become stable. BTW sandpile obeys an abelian property, which tells that the final steady state is independent of the order of the toppling occured in the system [76]. Numerical and analytical studies show that the values of the avalanche exponents in two dimensions are given by: $\tau_s \approx 1.22$ and $\tau_t \approx 1.32$ [77, 78].

*Manna sandpile:* Manna sandpile is defined on a $d$-dimensional lattice sites having $n_i$ number of particles at site $i$. The grains are lost at the boundary. Here the toppling rules are stochastic [67]. Whenever $n_i \geq 2$, the site becomes active and 2 particles move independently to any of the nearest neighbor with probability $1/2d$. This model does not obey an abelian property. Values of the avalanche exponents in two dimensions are $\tau_s \approx 1.28$ and $\tau_t \approx 1.47$ [67].

*Oslo ricepile model:* The motivation behind this model came from a real ricepile experiment [68]. Oslo ricepile model is defined on a $d$-dimensional lattice having $n_i$ number of elongated particles at site $i$. Here the toppling rules involve deterministic equal transfer of particles to $2d$ nearest neighbors [68]. But here the critical height $n_c$ is stochastic. It could be either 1 or 2 with equal probability. When $n_i \geq n_c$, the site becomes active and 2 particles move to nearest neighbors. After toppling of a active site, the critical height of that site is reset. Values of the avalanche exponents in two dimensions are $\tau_s \approx 1.26$ and $\tau_t \approx 1.48$ [80].

From the above discussions, one may conclude that the BTW model has its own universality class whereas Manna sandpile and Oslo ricepile belong to Manna universality class [79, 80]. The difference of universality classes is due to the stochasticity in dynamics of Manna and Oslo models.

SOC dynamics possesses two infinitely separated time scales and open boundaries, for which analytical calculations become difficult. Moreover, translational invariance is also absent in these systems due to open boundary. To understand the self organized criticality in more detail in terms of usual language of critical phenomena, people have proposed conserved versions of sandpiles taking the drive rate and dissipation rate zero. Conserved sandpiles are threshold-activated systems of lattice-gases, with sites having non-negative mass or particles (or *height*) and boundary remaining closed. When number of particles at a site crosses a threshold value, the site becomes active and a fixed number of particles are transferred to its neighbors via toppling [81]. In this case, total mass remains constant, without any loss or dissipation. However, local bulk-dynamics is the same as in the original sandpiles. Interestingly, upon tuning global density $\rho$, conserved-mass sandpiles undergo a continuous phase transition between active to absorbing phase at a critical density $\rho_c$ [81–88]. Near criticality, they exhibit scale-invariant structures - reminiscent of that in sandpiles without conservation and maintained at criticality through drive and dissipation [85]. In this case, order parameter of the phase transition is defined as active site density $a(\rho)$ . Near criticality, systems possess scale invariant structure. There are many other models like Restricted Asymmetric Simple Exclusion Processes (RASEP)[89], energy exchange models with activity [90], which also exhibit active absorbing phase transition. There have been intensive studies on universality classes for critical exponents e.g. , order parameter (activity) growth exponent $\beta$ with tuning parameter $(\rho - \rho_c)$, correlation length growth exponent $\nu_\perp$ with system size $L$, dynamic exponent $z$ relating relaxation time $t_r$ and system size $L$ etc. Indeed, sandpiles, and the SOC, produced a wealth of results, through exact [91–96], numerical [67, 77, 84, 86, 97–106] and experimental studies [107, 108]; for reviews, see [85]. Yet, by and large, they resisted attempts to construct a unified statistical mechanics framework. Various static and dynamic properties of the CSS have been studied intensively in the past using simulations [84, 86, 97–101, 104, 105] and continuum field theories [109–112]. However, particle-transport and density-fluctuations, though at the heart of the problem, are far less studied [103–105, 113–115] and lacks general theoretical understanding. Not surprisingly, long-standing question of universality, fiercely debated over past several decades, is not yet settled [69, 86, 102, 110–112, 116–125]. Indeed, it poses a formidable challenge to deal with the issues analytically, precisely because such nonequilibrium many-body systems have nontrivial spatio-temporal correlations; in fact, (quasi-) steady-state probabilities of microscopic configurations are not described by the Boltzmann-Gibbs distributions and *a-priori* not known. In this scenario, one usually resorts to phenomenological field theories, based on symmetries and conservation

laws, or to simulations. However, intricacies in simulations makes it hard to compare with the theories available and hence to draw a definitive conclusion. Thus, it is highly desirable, and quite pressing at this stage, to understand large-scale properties of sandpiles from the underlying microscopic dynamics itself.

In our work, we proceed to characterize the active phase and the critical state of the systems through additivity and macroscopic fluctuation theory. We divide this chapter into two broad sections. In the first section 4.2, we focus on the spatial properties of the systems in the active region which remain uncultivated for ages. In this work, we wish to observe whether our theory of additivity is applicable in the active phases of these models. We proceed to characterize these threshold activated systems through variance in coarse-grained mass and obtain the subsystem mass distribution. In the second section 4.3, we construct a hydrodynamic structure for a class of conserved manna sandpile systems and obtain an equilibriumlike Einstein relation to hold for such systems. This analysis helps us to characterize the scaling properties of the systems near criticality which help us to conclude that Manna sandpiles do not belong to DP universality class. Lastly, in section 4.4, we summarize the main findings of this work and make some concluding remarks.

## 4.2 ADDITIVITY AND PARTICLE NUMBER FLUCTUATION IN CONSERVED LATTICE GASES

In this section, we study particle number fluctuations in the theshold activated systems like driven lattice gases, conserved stochastic sandpiles. When a system is in absorbing state, there is no activity and consequently there is no mass fluctuation, i.e., scaled variance of subsystem mass in the limit of large subsystem size is zero. On the other hand, when a system is in active state, the scaled variance of subsystem mass remains nonzero. In this section, we characterize, using additivity and corresponding fluctuation-response relation, mass fluctuations in the active states for the following conserved lattice gases -

(i) Driven lattice gases having a PFSS, (Sec. 4.2.1)

(ii) Three variants of Manna fixed energy sandpile (FES) model in (Sec. 4.2.2.1), (Sec. 4.2.2.2), and (Sec. 4.2.2.3),

(iii) Manna fixed energy sandpile with height restriction (FES-H) (Sec.4.2.2.4).

### 4.2.1 *Pair factorized steady state (PFSS)*

We consider a pair factorized steady state (PFSS) defined on a one dimensional periodic lattice of $L$ sites having discrete mass (particle) variable $m_i$. There is no hard-core exclusion and total mass $M = \sum_i m_i$ is conserved. The particle hopping rate is taken to be that given in Eq. 2.19 and accordingly the steady-state probability weight is given by Eq. 2.20. As the steady-state probability weight is not a product measure and depends on the masses of pair of nearest neighbor pair of sites, this model has nonzero spatial correlation. Interestingly, for $g(x, y) = x + y$, we have found that the system exhibits absorbing to active phase transition at density $\rho = 1/2$. We study here the mass fluctuation, i.e., the scaled variance in subsystem mass in the active phase using a recently developed transfer-matrix method [41]. If the weight factor $g(m_i, m_{i+1})$ can be written as an inner product of two arbitrary 2 dimensional vectors as

$$g(m_i, m_{i+1}) = \langle f_0(m_i) | f_1(m_{i+1}) \rangle,$$

where $\langle f_0(x)| = (x, 1)$ and $\langle f_1(y)| = (1, y)$, the partition sum in grand canonical ensemble could be written as $\mathcal{Z} = \mathrm{Tr}[T(z)^L]$. Here $T(z)$ is given by

$$T = \sum_{m=0}^{\infty} z^m \begin{bmatrix} m & 1 \\ m^2 & m \end{bmatrix}.$$

So, for $g(x, y) = x + y$, the matrix $T(z)$

$$T = \begin{bmatrix} \sum_{m=0}^{\infty} m z^m & \sum_{m=0}^{\infty} z^m \\ \sum_{m=0}^{\infty} m^2 z^m & \sum_{m=0}^{\infty} m z^m \end{bmatrix} = \begin{bmatrix} \frac{z}{(1-z)^2} & \frac{1}{(1-z)} \\ \frac{z(1+z)}{(1-z)^3} & \frac{z}{(1-z)^2} \end{bmatrix}, \tag{4.3}$$

whose eigenvalues of this matrix are $\lambda_{\pm}$,

$$\lambda_+ = \frac{[z + \sqrt{z(1+z)}]}{(1-z)^2}, \tag{4.4}$$

$$\lambda_- = \frac{[z - \sqrt{z(1+z)}]}{(1-z)^2}. \tag{4.5}$$

In the thermodynamic limit for $L \to \infty$, the particle density as a function of fugacity $z$ is given by

$$\rho(z) = z \frac{\partial}{\partial z} \ln[\lambda_+] = \frac{z}{\sqrt{z(1+z)}} + \frac{z}{2[z + \sqrt{z(1+z)}]\sqrt{z(1+z)}} + \frac{2z}{(1-z)}. \tag{4.6}$$

From Eq. 4.6, we can easily check that there is an absorbing phase transition below a critical particle density $\rho(z = 0) = \rho_c = 1/2$. Taking the limit $z \to 0$, we get an relation $\rho - \rho_c =$

$\sqrt{z}/2$. Using fluctuation-response relation as in Eq. 2.10, we get an expression of the scaled variance $\sigma^2(z) = \lim_{v\to\infty} \sigma_v^2/v$ as given below,

$$\begin{aligned}\sigma^2 &= \frac{z}{\sqrt{z(1+z)}} + \frac{z}{2[z+\sqrt{z(1+z)}]\sqrt{z(1+z)}} + \frac{2z}{(1-z)} - \frac{z^2(1+2z)}{2\sqrt{z(1+z)}^3} \\ &\quad - \frac{2z^2\sqrt{z(1+z)}}{4z(1+z)[z+\sqrt{z(1+z)}]^2} - \frac{z^2(1+2z)}{4z(1+z)[z+\sqrt{z(1+z)}]^2} \\ &\quad - \frac{z^2(1+2z)}{4[\sqrt{z(1+z)}]^3[z+\sqrt{z(1+z)}]} + \frac{2z^2}{(1-z)^2}. \end{aligned} \tag{4.7}$$

It is evident that at criticality ($z = 0, \rho_c = 1/2$), the variance of subsystem mass becomes zero as the dynamics of the system seizes to exist. Near criticality, the $z \to 0$ limit gives $\sigma^2(\rho) = \frac{(\rho-\rho_c)}{2}$.

Next we proceed to calculate the two-point spatial correlation function $C(r)$ for this system using the same transfer matrix $T$ [41]. We have

$$C(0) = \langle m_i^2 \rangle - \rho^2 = \frac{\mathrm{Tr}[T'' T^{L-1}]}{\mathrm{Tr}[T^L]}, \qquad r = 0 \tag{4.8}$$

$$C(r) = \langle m_i m_{i+r} \rangle - \rho^2 = \frac{\mathrm{Tr}[T' T^{r-1} T' T^{L-r-1}]}{\mathrm{Tr}[T^L]}, \qquad r > 0 \tag{4.9}$$

where $T' = dT/d(\ln z)$ and $T'' = d^2T/d(\ln z)^2$. Using Eqs. 4.8 and 4.6, we calculate the single site variance as

$$C(0) = \frac{1 + z[14 + 17z - 8\sqrt{z(1+z)}]}{4(1-z)^2(1+z)}. \tag{4.10}$$

Similarly, we calculate the two-point correlation function using Eqs. 4.9 and 4.6 as

$$C(r) = -\left[\frac{z(1+4z+z^2)}{2(1-z)^2} + \frac{z(1+z)^2}{16(1-z)^2} - \frac{z^2(1+z)}{4} - \frac{(1+4z+z^2)^2}{4(1+z)(1-z)^2}\right]\phi^r, \tag{4.11}$$

where

$$\phi = \frac{\lambda_-}{\lambda_+} = \frac{z - \sqrt{z(1+z)}}{z + \sqrt{z(1+z)}}$$

gives the correlation length of the system $\xi^{-1} = \ln\phi$. Near criticality, at $z \to 0$ limit, the correlation length takes a form $\xi \sim \frac{1}{4(\rho-\rho_c)}$ and diverges as critical particle density is reached. Thus the active absorbing phase transition turns out to be a continuous phase transition occuring in this system. We calculate the scaled variance of subsystem particles number using the correlation functions in Eq. 4.10 and 4.11 following $\sigma_v^2 \simeq vC_0 + 2(v-1)C(1) + 2(v-2)C(2) + \cdots + 2C(v-1)$ and we get back the scaled variance in Eq. 4.7.

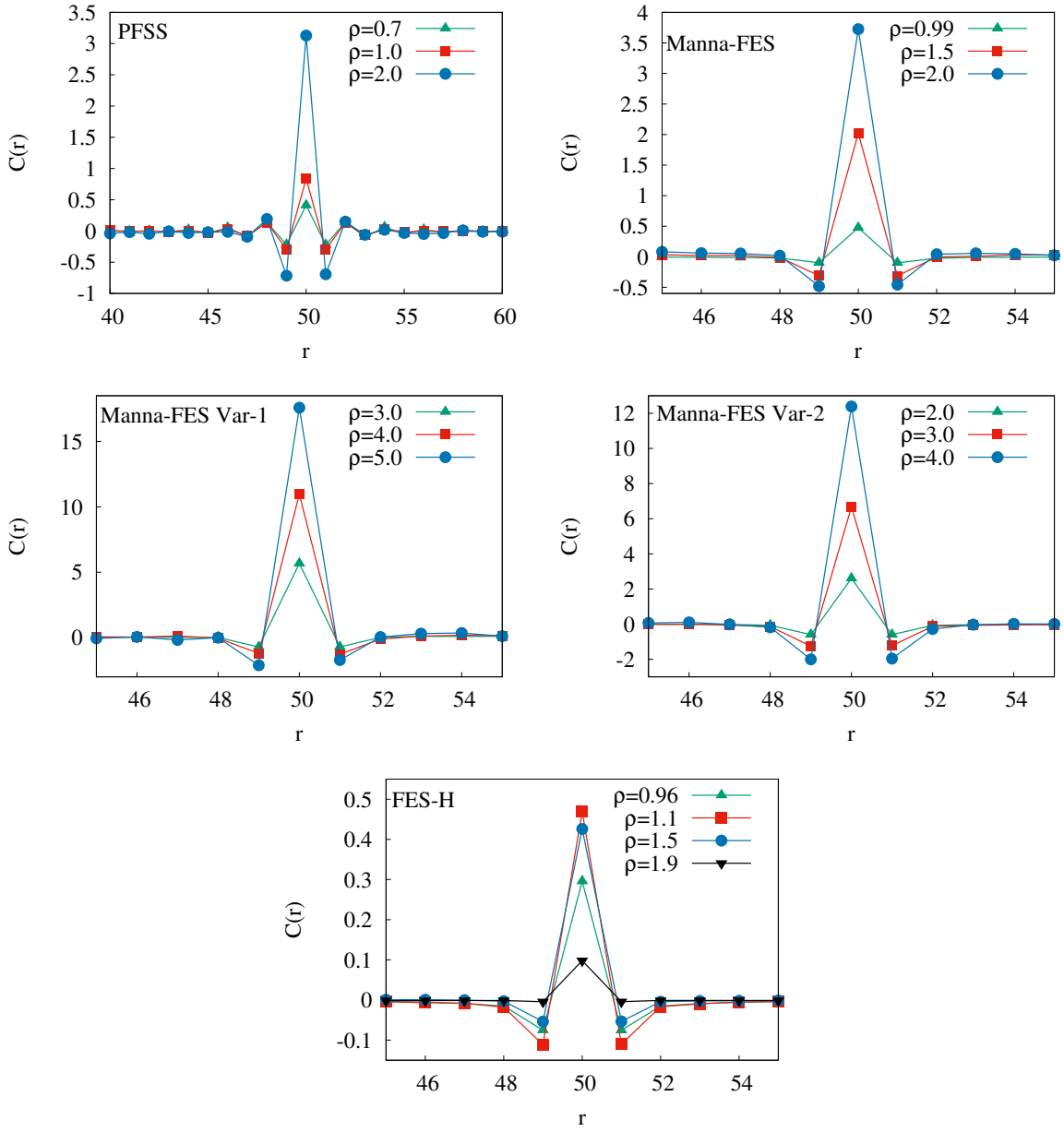


Figure 4.1: Two-point spatial correlation function $C(r)$ is plotted as a function of distance $r$ for different particle density $\rho \gg \rho_c$. In top left panel: DLG-PFSS, in top right panel: Manna-FES, in center left panel: Variant -I of Manna-FES, and in center right panel: Variant - II of Manna-FES, in bottom panel: Manna-FES with height restriction.

It is difficult to explicitly obtain a closed form expression of the scaled variance of subsystem mass as a function of particle density $\rho$ as one has to invert Eqs. 4.6 and 4.7 to get chemical potential $\mu$ as a function of density $\rho$, which however can be exactly done numerically. In Fig. 4.1, upper left panel, we plot the two-point correlation function $C(r)$ as a function of the distance $r$ for different particle densities $\rho = 0.7$ (green filled triangles with solid line), 1.0 (red filled squares with solid line), and 2.0 (blue filled circles with solid line).

In each case, points represent simulations and the solid line represents the analytical result obtained from Eq. 4.6, 4.10, and 4.11. In Fig 4.2, we plot the scaled variance $\sigma^2$ as a function of particle density $\rho$ for the DLG - PFSS (magenta circles with solid line), where magenta circles represent the simulation data and the solid line is the exact computation of scaled variance as a function of density with the help of Eq. 4.6 and 4.7. We see that in large particle density limit, the scaled variance is proportional to the square of the particle density (the red solid line represent the square of particle density).

### 4.2.2 *Fixed energy sandpiles*

#### 4.2.2.1 *Manna model of fixed energy sandpile (Manna-FES):*

We consider a stochastic sandpile model defined on a periodic chain of $L$ lattice sites [84] where $i^{\text{th}}$ site has $m_i \geq 0$ particles. The total number of particles $M = \sum_{i=1}^{L} m_i$ remains conserved and the particle density is given by $\rho = M/L$. A site $i$ is said to be *active* if it has number of particles greater than or equal to 2, i.e., $m_i \geq 2$. Otherwise the site is called inactive. The dynamics involve the toppling of active sites with rate unity. When an active site topples, it sends two particles independently to any of its nearest neighbor sites with probability 1/2. This system undergoes an absorbing to active phase transition when the particle density $\rho$ is tuned. The critical particle density $\rho_c$ has been reported to be 0.9488 [84].

We calculate in simulations the two-point spatial correlation function $C(r) = \langle m_i m_{i+r} \rangle - \rho^2$ for this model in active phase, i.e., for $\rho \gg \rho_c$ . We find that this system has short-ranged spatial correlation with correlation length $\xi$ finite. In Fig. 4.1, upper right panel, we plot the two-point correlation function $C(r)$ as a function of the distance $r$ for different particle densities $\rho = 0.99$ (green filled triangles with solid line), 1.5 (red filled squares with solid line), and 2.0 (blue filled circles with solid line) . This observation leads us to believe that the system would obey the additivity property given in Eq. 2.2 in chapter 2. We take a subsystem of size $v \gg \xi$ and calculate the scaled variance in subsystem mass $\tilde{m} = \sum_{i=1}^{v} m_i$ as $\sigma^2 = \sigma_v^2/v = \frac{\langle \tilde{m}^2 \rangle - \langle \tilde{m} \rangle^2}{v}$ for different $\rho$. As expected, the variance is zero in absorbing phase and it becomes nonzero in active phase as particle number at a site becomes a fluctuating quantity due to the toppling dynamics. We put down a mean field analysis to track the nature of the variance in subsystem mass as a function of mass density.

*Dynamics:* Let us denote $[1 - \delta_{m_i(t),0} - \delta_{m_i(t),1}] = \hat{a}_i$, the occupation probability $\langle (1 - \delta_{m_j,0} - \delta_{m_j,1}) \rangle = \langle \hat{a}_i \rangle = a_i$, i.e. $a_i$ is the probability that a site $i$ is atleast doubly occupied.

$$m_i(t+dt) = \begin{cases} m_i(t)-2 & \text{prob. } \hat{a}_i dt, \\ m_i(t)+1 & \text{prob. } \frac{\hat{a}_{i-1}dt}{2}, \\ m_i(t)+1 & \text{prob. } \frac{\hat{a}_{i+1}dt}{2}, \\ m_i(t)+2 & \text{prob. } \frac{\hat{a}_{i-1}dt}{4}, \\ m_i(t)+2 & \text{prob. } \frac{\hat{a}_{i+1}dt}{4}, \\ m_i(t) & \text{prob. } [1-(\hat{a}_i+\frac{3\hat{a}_{i-1}}{4}+\frac{3\hat{a}_{i+1}}{4})dt], \end{cases} \tag{4.12}$$

We deal with steady-state averages throughout.

***n*-th moment equation:** The time evolution of $n$-th moment $\langle m_i^n \rangle$ can be written as

$$\begin{aligned} \langle m_i^n(t+dt)\rangle = \langle m_i^n(t)\rangle &= \langle [m_i(t)-2]^n\rangle \hat{a}_i dt + \langle [m_i(t)+1]^n\rangle \frac{\hat{a}_{i-1}dt}{2} \\ &+ \langle [m_i(t)+1]^n\rangle \frac{\hat{a}_{i+1}dt}{2} + \langle [m_i(t)+2]^n\rangle \frac{\hat{a}_{i-1}dt}{4} \\ &+ \langle [m_i(t)+2]^n\rangle \frac{\hat{a}_{i-1}dt}{4} \\ &+ \langle m_i^n(t)\rangle [1-(\hat{a}_i+3/4\hat{a}_{i-1}+3/4\hat{a}_{i+1})dt]. \end{aligned} \tag{4.13}$$

**2nd moment equation:** Putting $n=2$ in the above Eq. 4.13, we get,

$$\begin{aligned} \langle m_i^2\rangle &= [\langle m_i^2\hat{a}_i\rangle - 4\langle m_i\hat{a}_i\rangle + 4\langle \hat{a}_i\rangle]dt + [\langle m_i^2\hat{a}_{i-1}\rangle + 2\langle m_i\hat{a}_{i-1}\rangle \\ &+ \langle \hat{a}_{i-1}\rangle]dt/2 + [\langle m_i^2\hat{a}_{i+1}\rangle + 2\langle m_i\hat{a}_{i+1}\rangle \\ &+ \langle \hat{a}_{i+1}\rangle]dt/2 + [\langle m_i^2\hat{a}_{i-1}\rangle + 4\langle m_i\hat{a}_{i-1}\rangle \\ &+ 4\langle \hat{a}_{i-1}\rangle]dt/4 + [\langle m_i^2\hat{a}_{i+1}\rangle + 4\langle m_i\hat{a}_{i+1}\rangle \\ &+ 4\langle \hat{a}_{i+1}\rangle]dt/4 + \langle m_i^2\rangle - \langle m_i^2(\hat{a}_i+3/4\hat{a}_{i-1}+3/4\hat{a}_{i+1})\rangle dt. \end{aligned} \tag{4.14}$$

We find that, the second moment $\langle m_i^2 \rangle$ cancels out from the above equation. Using mean field approximation that all type of two-point correlation vanishes for $i \neq j$ and using $\langle m_i \rangle = \rho$, $\langle m_i \delta_{m_i,1}\rangle = \langle \delta_{m_i,1}\rangle = p_1(\rho)$, we get

$$7a + 4\rho a - 4\rho + 4p_1 = 0, \tag{4.15}$$

which gives us an expression for the occupation probability $a(\rho)$ as following,

$$a(\rho) = \frac{4(\rho - p_1)}{(7+4\rho)}. \tag{4.16}$$

From the above equation of activity, it is evident that at criticality, the activity vanishes, i.e., $a(\rho_c) = 0$. Though the functional form of $p_1(\rho)$ remains undetermined, the vanishing activity at criticality gives the critical mass density

$$\rho_c = p_1(\rho_c). \tag{4.17}$$

**3rd moment equation:** Putting $n = 3$ in the above Eq. 4.13, we get,

$$\begin{aligned}
\langle m_i^3 \rangle \quad = \quad & [\langle m_i^3 \hat{a}_i \rangle - 6\langle m_i^2 \hat{a}_i \rangle + 12\langle m_i \hat{a}_i \rangle - 8\langle \hat{a}_i \rangle]dt \\
& + [\langle m_i^3 \hat{a}_{i-1} \rangle + 3\langle m_i^2 \hat{a}_{i-1} \rangle + 3\langle m_i \hat{a}_{i-1} \rangle + \langle \hat{a}_{i-1} \rangle]dt/2 \\
& + [\langle m_i^3 \hat{a}_{i+1} \rangle + 3\langle m_i^2 \hat{a}_{i+1} \rangle + 3\langle m_i \hat{a}_{i+1} \rangle + \langle \hat{a}_{i+1} \rangle]dt/2 \\
& + [\langle m_i^3 \hat{a}_{i-1} \rangle + 6\langle m_i^2 \hat{a}_{i-1} \rangle + 12\langle m_i \hat{a}_{i-1} \rangle + 8\langle \hat{a}_{i-1} \rangle]dt/4 \\
& + [\langle m_i^3 \hat{a}_{i+1} \rangle + 6\langle m_i^2 \hat{a}_{i+1} \rangle + 12\langle m_i \hat{a}_{i+1} \rangle + 8\langle \hat{a}_{i+1} \rangle]dt/4 \\
& + \langle m_i^3 \rangle - \langle m_i^3 (\hat{a}_i + 3/4\hat{a}_{i-1} + 3/4\hat{a}_{i+1}) \rangle dt.
\end{aligned} \tag{4.18}$$

We find that, the third moment $\langle m_i^3 \rangle$ cancels out from the above equation. Under mean field approximation, we get,

$$(6 - 6a)\langle m_i^2 \rangle = (9a + 12)\rho - 3a - 6p_1. \tag{4.19}$$

Replacing $a(\rho)$ using Eq. 4.16, we get,

$$\langle m_i^2 \rangle = \frac{(14\rho^2 - 10\rho p_1 + 12\rho - 5p_1)}{7 + 4p_1}. \tag{4.20}$$

So, we calculate variance in single site mass $\sigma_1^2 = \langle m^2 \rangle - \rho^2$ as

$$\begin{aligned}
\sigma_1^2 \quad &= \quad \frac{(7 - 4p_1)\rho^2 + (12 - 10p_1)\rho - 5p_1}{(7 + 4p_1)} \\
&= \quad \frac{(\rho - [\frac{-(6-5p_1) + \sqrt{(6-5p_1)^2 + 5(7-4p_1)}}{(7-4p_1)}])(\rho - [\frac{-(6-5p_1) - \sqrt{(6-5p_1)^2 + 5(7-4p_1)}}{(7-4p_1)}])}{(4p_1 + 7)}.
\end{aligned} \tag{4.21}$$

Eq. 4.21 gives us the asymptotic feature of variance. It is indeed true that $\sigma^2 \sim \rho^2$ when $\rho \gg \rho_c$. On the other extreme, when system is at critical point $\rho_c$, $\sigma^2$ becomes zero as the system enters in its absorbing phase. The critical particle density $\rho_c$ could be obtained by making the numerator zero, which gives

$$\rho_c = \frac{-[6 - 5p_1(\rho_c)] + \sqrt{[6 - 5p_1(\rho_c)]^2 + 5[7 - 4p_1(\rho_c)]}}{[7 - 4p_1(\rho_c)]}. \tag{4.22}$$

So, we get two equations for $\rho_c$, which are in fact identical. So, from Eq. 4.17 and 4.22, we get another condition for criticality in terms of $p_1(\rho_c)$

$$p_1(\rho_c) = \frac{-[6-5p_1(\rho_c)] + \sqrt{[6-5p_1(\rho_c)]^2 + 5[7-4p_1(\rho_c)]}}{[7-4p_1(\rho_c)]}. \tag{4.23}$$

The two feasible solutions of the above equation for the probability $p_1(\rho_c)$ are 1 and $\frac{(-7+\sqrt{129})}{8} \approx 0.545$. So, the mean field analysis gives $\rho_c = 1$ or $\frac{(-7+\sqrt{129})}{8} (\approx 0.545)$. At this stage, it would be perhaps appropriate to take the larger value $\rho_c = 1$.

To demonstrate theoretically obtained results, in Fig 4.2, we plot the scaled variance $\sigma^2$ as a function of particle density $\rho$ for the conserved Manna model (green circles with solid line), and we see that in large particle density limit, the scaled variance is indeed proportional to the square of the particle density (the red solid line represent the square of particle density).

We sketch a schematic calculation of subsystem mass distribution $P_v(m) \sim w(m)\exp(\mu m)$ assuming that additivity of Eq. 2.2 holds. We consider a simple form of scaled variance, which may correspond to absorbing phase transition similar to Eq. 4.21,

$$\sigma^2(\rho) \sim c_1\tilde{\rho} + c_2\tilde{\rho}^2, \tag{4.24}$$

where $\tilde{\rho} = \rho - \rho_c$. We take $c_1$ and $c_2$ to be constant; they do not depend on $\rho$. Putting the functional form of variance from the above equation in the fluctuation response relation Eq. 2.10 mentioned in chapter 2, we calculate the chemical potential as

$$\begin{aligned}
\mu(\rho) &= \int \frac{d\rho}{\sigma^2} + \ln\alpha, \\
&= \int \frac{d\tilde{\rho}}{c_1\tilde{\rho} + c_2\tilde{\rho}^2} + \ln\alpha, \\
&= \frac{1}{c_2}\int \frac{d\tilde{\rho}}{(\tilde{\rho}+c_3/2)^2 - (c_3/2)^2} + \ln\alpha, \\
&= \frac{1}{c_1}\ln\frac{\alpha\tilde{\rho}}{\tilde{\rho}+c_3},
\end{aligned} \tag{4.25}$$

where $\ln\alpha$ is integration constant and $c_3 = c_1/c_2$. The corresponding free energy is

$$\begin{aligned}
f(\rho) &= \int \mu d\rho + \beta, \qquad \beta \text{ is integration constant} \\
&= \frac{1}{c_1}\int d\tilde{\rho}\ln\frac{\alpha\tilde{\rho}}{\tilde{\rho}+c_3} + \beta, \\
&= \frac{1}{c_1}[\tilde{\rho}\ln(\alpha\tilde{\rho}) - (\tilde{\rho}+c_3)\ln(\tilde{\rho}+c_3)] + \beta.
\end{aligned} \tag{4.26}$$

Then we proceed to calculate the subsystem weight factor $w_v(m)$ which is needed to calculate $P_v(m)$. With the help of Eq. 4.26, we write the Laplace transform of $w_v(m)$ as [40]

$$\tilde{w}_v(\kappa) = \int dm w_v(m) \exp(-\kappa m) = e^{-\lambda_v(\kappa)}. \tag{4.27}$$

Then, the function $\lambda_v(\kappa)$ is a large deviation function in Laplace space and can be obtained from Legendre transform of free energy density function $f(\rho)$ [126],

$$\lambda_v(\kappa) = v\left[\mathbf{inf}_\rho\{f(\rho) + \kappa\rho\}\right] = v[f(\rho^*) + \kappa\rho^*], \tag{4.28}$$

where $\rho^*(\kappa)$ is the solution of $\kappa = -\mu(\rho^*) = -\frac{1}{c_1}\ln\frac{\alpha(\rho^*-\rho_c)}{[(\rho^*-\rho_c)+c_3]}$. It gives the saddle point $\rho^*$ in the form

$$\rho^* = \rho_c + \frac{c_3}{\alpha e^{c_1\kappa} - 1}. \tag{4.29}$$

Using Eq. 4.28 and 4.29, we have

$$\lambda_v(\kappa) = v\rho_c\kappa - vc_3\kappa + \ln[(\alpha e^{c_1\kappa} - 1)^{vc_3/c_1}] + \text{const.} \tag{4.30}$$

Thus, the Laplace transform of weight factor is calculated as

$$\begin{aligned} \tilde{w}_v(\kappa) &= \text{const.} e^{-v\rho_c\kappa} e^{vc_3\kappa}[e^{c_1(\kappa-\kappa_c)} - 1]^{-vc_3/c_1} \\ &= \text{const.} e^{-v\rho_c\kappa}[1 - \exp\{-c_1(\kappa-\kappa_c)\}]^{-vc_3/c_1}, \end{aligned} \tag{4.31}$$

where $\kappa_c = -\frac{\ln\alpha}{c_1}$. So, when $\kappa \to \kappa_c$ denoting the large $\rho \gg \rho_c$ limit, in leading order of $(\kappa - \kappa_c)$ , $\tilde{w}_v(\kappa)$ is obtained as

$$\tilde{w}_v(\kappa) \simeq \text{const.}(\kappa - \kappa_c)^{-vc_3/c_1}, \tag{4.32}$$

which is in the same form Eq. 2.17 in chapter 2 with $\eta = c_3/c_1$. So, inverse Laplace transform gives the weight factor $w_v(m) = m^{v\eta-1}\exp(m\kappa_c)$. Thus for large $\rho \gg \rho_c$, the subsystem mass distribution is given by a gamma distribution

$$P_v(m) \sim m^{v\eta-1}\exp[\mu(\rho)m], \tag{4.33}$$

where the chemical potential $\mu(\rho) = -\eta/\rho$ for $\rho \gg \rho_c$.

#### 4.2.2.2 *Variant - I of the Manna model:*

We introduce another stochastic sandpile model, which is a variant of the above Manna-FES model. It is defined on a periodic chain of $L$ lattice sites where $i^{\text{th}}$ site has $m_i \geq 0$ particles.

The total number of particles $M = \sum_{i=1}^{L} m_i$ remains conserved and the particle density is given by $\rho = M/L$. Each site has a threshold particle number $m_i^*$ which is either 2 or 3 with probability 1/2. A site is said to be *active* if it has $m_i \geq m_i^* \in [2, 3]$. The dynamics involve the toppling of active sites with rate unity. When an active site topples, it sends two particles independently to any of its nearest neighbor sites with probability 1/2 and then the threshold particle number of the toppling site is reset. This system also undergoes an absorbing to active phase transition when the particle density $\rho$ is tuned where the critical particle density $\rho_c \approx 1.69$.

Numerical calculation of two-point spatial correlation function $C(r) = \langle m_i m_{i+r} \rangle - \rho^2$ for this model in active phase shows that this system has short-ranged spatial correlation with correlation length $\xi$ finite. In Fig. 4.1, lower left panel, we plot the two-point correlation function $C(r)$ as a function of the distance $r$ for different particle densities $\rho = 3.0$ (green filled triangles with solid line), 4.0 (red filled squares with solid line), and 5.0 (blue filled square with solid line). So, we expect additivity property given in Eq. 2.2 to hold for this system. We take a subsystem of size $v \gg \xi$ and calculate the scaled variance in subsystem mass for different $\rho$. As expected, the variance is zero in absorbing states below the critical particle density and it becomes nonzero in active phase. Our simulation shows that when $\rho$ is well above critical density, the scaled variance $\sigma^2$ is proportional to the square of $\rho$. In Fig 4.2, we plot the scaled variance $\sigma^2$ as a function of particle density $\rho$ for this new variant of conserved Manna model (sky-blue triangles with solid line). Interestingly, for this model also, the scaled variance is proportional to the square of particle density when $\rho \gg \rho_c$ (the corresponding simulation data go parallel with the red solid line representing $\rho^2$).

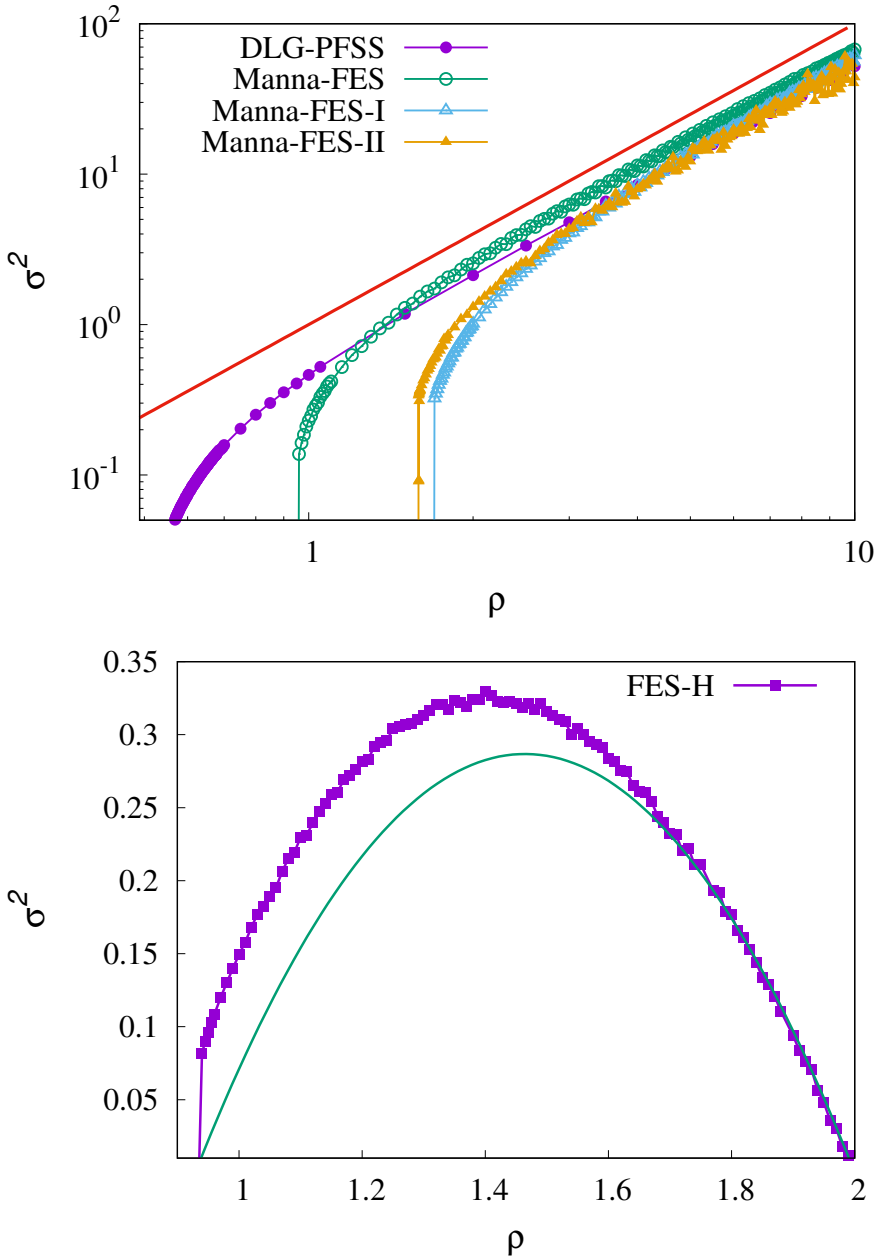


Figure 4.2: The scaled variance $\sigma_v^2/v = \sigma^2$ is plotted as a function of mass density $\rho$. In top panel, for (i) DLG-PFSS, $L = 5000, v = 20$, points - simulations, solid line - exact computation of scaled variance from Eq. 4.6 and 4.7 (ii) Manna-FES, $L = 1000, v = 10$, (iii) Variant - I of Manna-FES, $L = 1000, v = 10$, and (iv) Variant - II of Manna-FES, $L = 1000, v = 10$; points with solid line - simulations. Red solid line : $\rho^2$. In bottom panel, for Manna-FES with height restriction, $L = 1000, v = 10$, Points with solid line - simulations, green solid line : $(\rho - \rho_c)(2.0 - \rho)$

#### 4.2.2.3 *Variant - II of the Manna model:*

We introduce a second variant of the above Manna-FES model. It is defined on a periodic chain of $L$ lattice sites where $i^{\text{th}}$ site has $m_i \geq 0$ particles. The total number of particles

$M = \sum_{i=1}^{L} m_i$ remains conserved and the particle density is given by $\rho = M/L$. Each site has a threshold particle number $m_i^*$ which is either 2 or 3 with probability 1/2. A site is said to be *active* if it has $m_i \geq m_i^* \in [2,3]$. The dynamics involve the toppling of active sites with rate unity. When an active site topples, it sends $m_i^*$ particles independently to any of its nearest neighbor sites with probability 1/2 and then the threshold particle number of the toppling site is reset. This system also undergoes an absorbing to active phase transition when the particle density $\rho$ is tuned where the critical particle density $\rho_c \approx 1.59$.

Numerical calculation of two-point spatial correlation function $C(r) = \langle m_i m_{i+r} \rangle - \rho^2$ for this model in active phase shows that this system has short-ranged spatial correlation with correlation length $\xi$ finite. In Fig. 4.1, lower right panel, we plot the two-point correlation function $C(r)$ as a function of the distance $r$ for different particle densities $\rho = 2.0$ (green filled triangles with solid line), 3.0 (red filled squares with solid line), and 4.0 (blue filled square with solid line). So, we expect additivity property given in Eq. 2.2 to hold for this system. We take a subsystem of size $v \gg \xi$ and calculate the scaled variance in subsystem mass for different $\rho$. As expected, the variance is zero in absorbing states below the critical particle density and it becomes nonzero in active phase. Our simulation shows that when $\rho$ is well above critical density, the scaled variance $\sigma^2$ is proportional to the square of $\rho$. In Fig 4.2, we plot the scaled variance $\sigma^2$ as a function of particle density $\rho$ for this new variant of conserved Manna model (yellow filled triangles with solid line). Interestingly, for this model also, the scaled variance is proportional to the square of particle density when $\rho \gg \rho_c$ (the corresponding simulation data go parallel with the red solid line representing $\rho^2$).

#### 4.2.2.4 *Manna fixed energy sandpile model with height restriction (FES-H):*

We study Manna-FES with height restriction model introduced by Dickman *et. al.* [86]. It is defined on a periodic chain of $L$ lattice sites where $i^{\text{th}}$ site has $m_i \in 0, 1, 2$ particles; i.e. each site may harbour maximum 2 particles. The total number of particles $M = \sum_{i=1}^{L} m_i$ remains conserved and the particle density is given by $\rho = M/L$. Each site has a threshold particle number $m_i^* = 2$. A site is said to be *active* if it has $m_i = m_i^* = 2$. The dynamics involve the toppling of active sites. When an active site topples, it attempts to send two particles independently to any of its nearest neighbor sites chosen with probability 1/2. The attempt succeeds only if the particle number of the chosen neighboring site is $m_j < 2$. Otherwise the attempt fails and the particle to be toppled return back to the departing active site. This system also undergoes an absorbing to active phase transition when the particle density $\rho$ is tuned where the critical particle density $\rho_c \approx 0.929$ [86, 87].

Numerical calculation of two-point spatial correlation function $C(r) = \langle m_i m_{i+r} \rangle - \rho^2$ for this model in active phase shows that this system has short-ranged spatial correlation with correlation length $\xi$ finite. In Fig. 4.1, bottom panel, we plot the two-point correlation func-

tion $C(r)$ as a function of the distance $r$ for different particle densities $\rho = 0.96$ (green filled triangles with solid line), 1.1 (red filled squares with solid line), 1.5 (dark blue filled square with solid line), 1.9 (black filled reverse triangle with solid line). Due to the height restriction present in the system, single site mass fluctuation becomes lesser as mass density approaches 2. As $\xi$ is finite, we expect additivity property given in Eq. 2.2 to hold for this system. We take a subsystem of size $v \gg \xi$ and calculate the scaled variance in subsystem mass for different $\rho$. As expected, the variance is zero in absorbing states below the critical particle density $\rho_c$. Then it becomes nonzero in active phase $\rho_c < \rho < 2.0$, and again the variance starts decreasing to zero as the higher particle density limit $\rho = 2$ is reached. In Fig 4.2 bottom panel, we plot the scaled variance $\sigma^2$ as a function of particle density $\rho$ for Manna-FES with height restriction model (magenta filled squares with solid line). Looking at the feature of the system, a trial function $(\rho - \rho_c)(2 - \rho)$ could be prescribed which fits well with the simulation data at the right arm.

### 4.2.3 *Subsystem particle number distribution in conserved lattice gases*

We now numerically compute, by integrating the FR Eq. 2.10 to obtain $\mu(\rho)$ and $f(\rho)$ [127], probability $P_v(m) \sim \exp[-vh(\hat{\rho})]$ of large deviation in subsystem particle density $\hat{\rho} = m/v$ in subsystem of size $v$ where large deviation function (LDF) is $h(\hat{\rho}) = f(\hat{\rho}) - \mu(\rho)\hat{\rho}$, with $\rho$ being global density. However, the LDF has sub-leading corrections, which can also be obtained here by taking the asymptotic form of $\sigma^2(\rho) \simeq \rho^2/\eta$, which is actually the case in the limit of large density $\rho \gg \rho_c$, with $\eta$ a model-dependent proportionality constant. This particular asymptotic form is quite expected as these stochastic sandpiles, being defined in a unbounded state-space, behaves somewhat like a 'bose gas', with repulsive interactions. In other words, we have $P_v(m) \simeq \text{const.}\exp[-vh(\hat{\rho})]/m$, where the correction term is a $1/m$ factor, at large $m$ (which is effectively a gamma distribution), which means that large-mass behavior of $P_v(m)$, even at lower densities, is effectively determined by large-density behavior of $\sigma^2(\rho)$.

In Fig. 4.3, we have plotted the subsystem particle-number distribution $P_v(m)$ as function of the subsystem particle-number $m$ for DLG-PFSS for different particle densities $\rho = 0.7$ (green filled triangles), 1.0 (red filled squares), and 2.0 (blue filled circles). In the left panel, the solid lines corresponding different particle densities represent the particle-number distributions $P_v(m)$ in Eq. 2.13. In the right panel, the solid lines corresponding different particle densities represent the particle-number distributions $P_v(m)$ in Eq. 2.13 with the logarithmic correction term, which is gamma distribution as in Eq. 2.1.

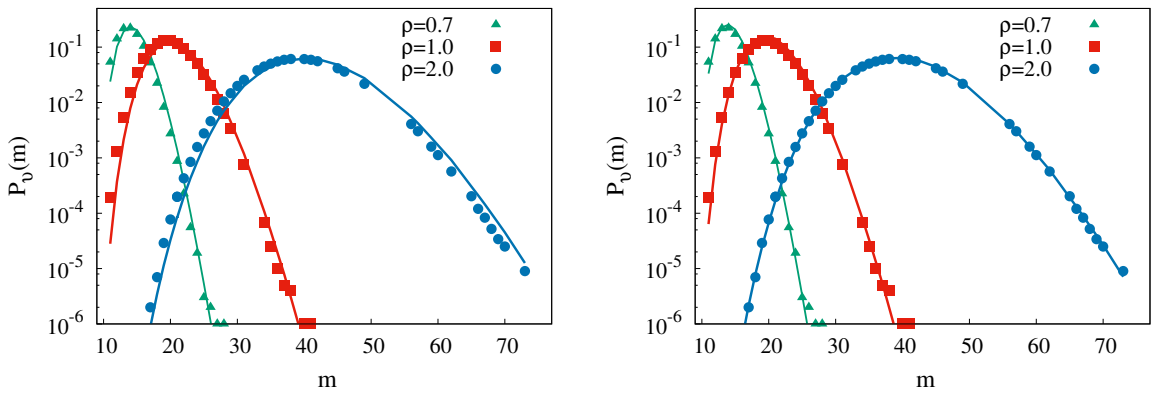


Figure 4.3: DLG-PFSS : The subsystem mass distribution $P_v(m)$ is plotted as a function of subsystem mass $m$ for $L = 5000, v = 20$ and different mass density $\rho$. Left panel: the solid lines represent Eq. 2.13; right panel: the solid lines represent Eq. 2.13 after incorporating a correction term

In Fig. 4.4, we have plotted the subsystem particle-number distribution $P_v(m)$ as function of the subsystem particle-number $m$ for Manna-FES for different particle densities $\rho = 0.99$ (green filled triangles), 1.5 (red filled squares), and 2.0 (blue filled circles). In the left panel, the solid lines corresponding different particle densities represent the particle-number distributions $P_v(m)$ in Eq. 2.13. In the right panel, the solid lines corresponding different particle densities represent the particle-number distributions $P_v(m)$ in Eq. 2.13 with the logarithmic correction term, which is very close to gamma distribution as in Eq. 2.1.

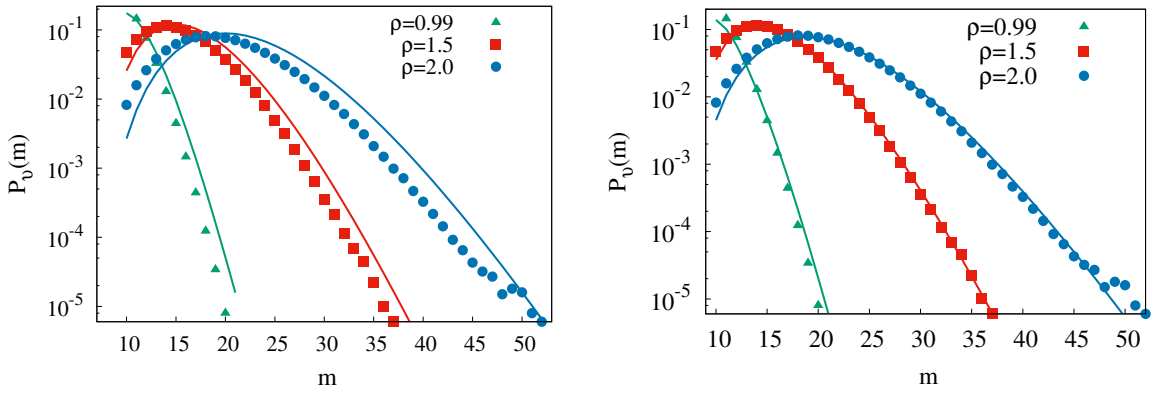


Figure 4.4: Manna - FES: The subsystem mass distribution $P_v(m)$ is plotted as a function of subsystem mass $m$ for $L = 1000, v = 10$ and different mass density $\rho$. Left panel: the solid lines represent Eq. 2.13; right panel: the solid lines represent Eq. 2.13 after incorporating a correction term

In Fig. 4.5, we have plotted the subsystem particle-number distribution $P_v(m)$ as a function of the subsystem particle-number $m$ for variant of Manna-FES - I for different particle densities $\rho = 3.0$ (green filled triangles), 4.0 (red filled squares), and 5.0 (blue solid cir-

cles). In the left panel, the solid lines corresponding different particle densities represent the particle-number distributions $P_v(m)$ in Eq. 2.13. In the right panel, the solid lines corresponding different particle densities represent the particle-number distributions $P_v(m)$ in Eq. 2.13 with a logarithmic correction term, which is indeed very close to gamma distribution in Eq. 2.1.

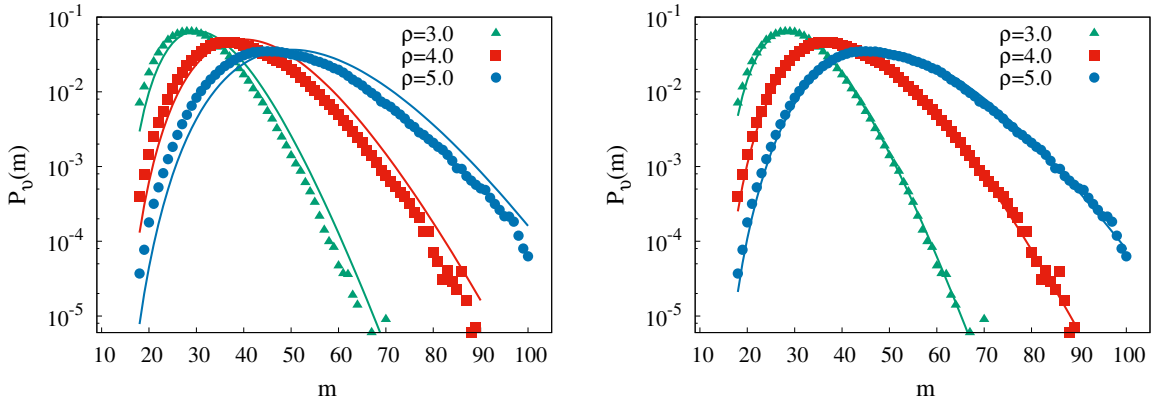


Figure 4.5: Variant - I of Manna-FES: The subsystem mass distribution $P_v(m)$ is plotted against subsystem mass $m$ for $L = 1000, v = 10$ and different mass density $\rho$.Left panel: the solid lines represent Eq. 2.13, right panel: the solid lines represent Eq. 2.13 after incorporating a correction term.

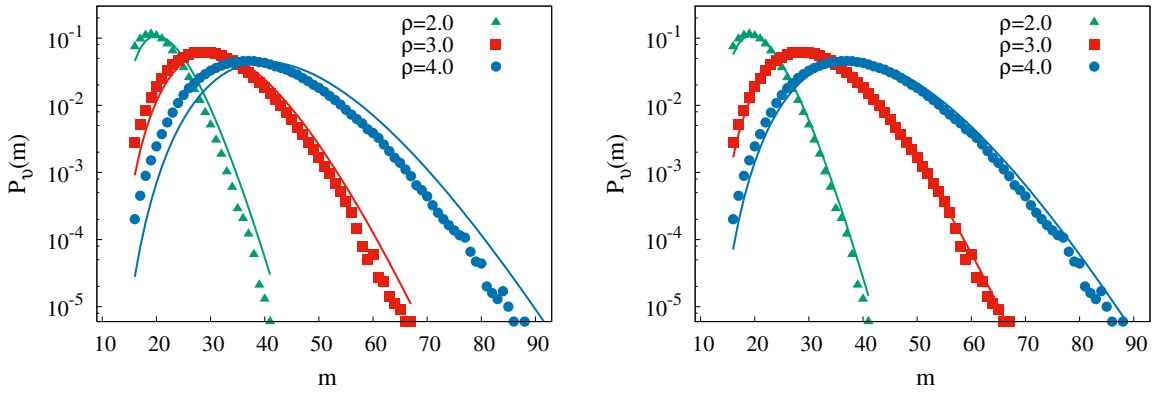


Figure 4.6: Variant - II of Manna-FES: The subsystem mass distribution $P_v(m)$ is plotted against subsystem mass $m$ for $L = 1000, v = 10$ and different mass density $\rho$. Left panel: the solid lines represent Eq. 2.13, right panel: the solid lines represent Eq. 2.13 after incorporating a correction term.

In Fig. 4.6, we have plotted the subsystem particle-number distribution $P_v(m)$ as a function of the subsystem particle-number $m$ for variant of Manna-FES - II for different particle densities $\rho = 2.0$ (green filled triangles), 3.0 (red filled squares), and 4.0 (blue solid circles). In the left panel, the solid lines corresponding different particle densities represent the particle-number distributions $P_v(m)$ in Eq. 2.13. In the right panel, the solid lines correspond-

ing different particle densities represent the particle-number distributions $P_v(m)$ in Eq. 2.13 with a logarithmic correction term, which is indeed very close to gamma distribution in Eq. 2.1.

In Fig. 4.7, we have plotted the subsystem particle-number distribution $P_v(m)$ as a function of the subsystem particle number $m$ for Manna-FES with height restriction for various particle densities. In the top left panel, the distribution is for $\rho = 0.96$, where magenta points represent simulation data, magenta solid line represents the large deviation form obtained assuming additivity (Eq. 2.1). As the system just enters into its active phase, one could naively expect that there exist a collection of noninteracting particles which take part in the dynamics and keep the system in active phase. The yellow solid line in the distribution plot represents corresponding Poisson distribution

$$P(m) = \frac{\exp[-\langle (m - v\rho_c)\rangle]\langle (m - v\rho_c)\rangle^{m-v\rho_c}}{(m - v\rho_c)!}. \tag{4.34}$$

However, contrary to the expectation, the system, which actually has spatial correlations at this particle density $\rho = 0.96$ (Fig 4.1, last panel), the Poisson distribution is not a good approximation for the particle number distribution. Interestingly, we find additivity holds quite well though in this case. In top right panel, the distribution is for $\rho = 1.1$ with magenta points for simulation data, magenta solid line for additivity. The yellow solid line represents the Poisson distribution of collection of noninteracting particles given by Eq. 4.34. In this case also, additivity provides a better approximation than Poisson distribution. In bottom left panel, the particle number distribution is plotted for $\rho = 1.5$ where magenta points are simulation data and magenta solid represents additivity. The yellow solid line represents corresponding Gaussian distribution of the form

$$P(m) = \frac{1}{\sqrt{2\pi\sigma^2}} \exp\left[-\frac{(m - v\rho)^2}{2\sigma^2}\right], \tag{4.35}$$

where $\sigma^2$ is the variance in subsystem particle number obtained from numerical simulation. In this case, particle number distribution is indeed Gaussian distribution and additivity approximates it quite well. Lastly, in bottom right panel, particle distribution is plotted for $\rho = 1.9$ where magenta points are simulation data, magenta solid line is for additivity. In this case, there exists a collection of noninteracting sites, we call them holes, having particle number less than the maximal occupancy number 2. The yellow solid line represents corresponding hole distribution which is expected to be a Poisson distribution due to non-

interacting behavior of the holes prominent from the corresponding two-point correlation in Fig. 4.1, last panel. In this particular case, the Poisson distribution is of the form

$$P(m) = \frac{\exp[-\langle(2v-m)\rangle]\langle(2v-m)\rangle^{2v-m}}{(2v-m)!}. \tag{4.36}$$

We find that additivity still gives a better approximation than the Poisson form.

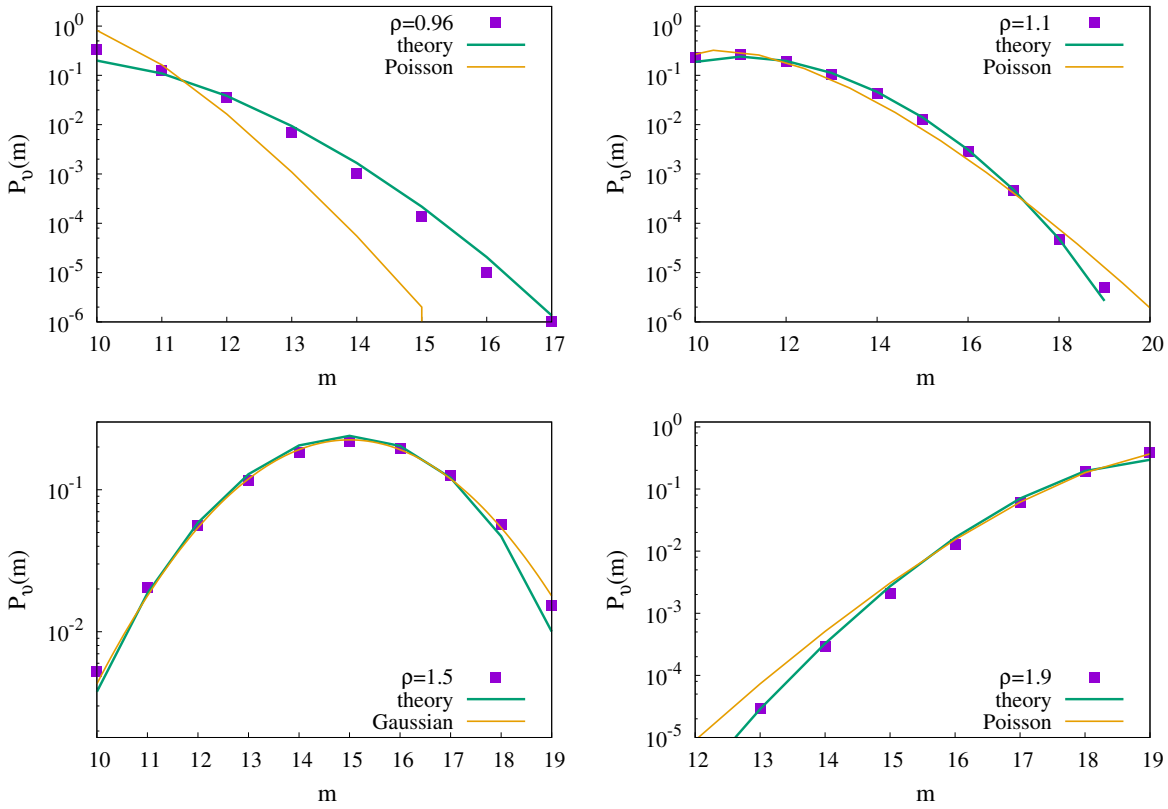


Figure 4.7: Manna-FES with height restriction: The subsystem mass distribution $P_v(m)$ is plotted against subsystem mass $m$ for $L = 1000, v = 10$ and different mass density $\rho$; the green solid lines represent Eq. 2.13, the yellow solid line represents corresponding Poisson or Gaussian distributions.

Thus, in all of these models, we find that particle number distributions obtained from simulations are in good agreement with the theoretical prediction from additivity and thus validate additivity property in active phases in different driven lattice gases exhibiting absorbing phase transition.

In the next section, we proceed to characterize the critical scaling properties of a class of manna sandpiles by obtaining a hydrodynamic descriptions of the conserved-mass Manna sandpiles. The hydrodynamics obtained below strongly supports the results obtained using additivity.

In this section [1], we obtain an exact hydrodynamic structure of the conserved Manna sandpiles (For simplicity, let us rename this model as MS). We demonstrate that the MS possess a 'gradient property' given by Eq.4.42, which we use to uncover a remarkable large-scale structure in the systems, with far-reaching consequences: There is an equilibriumlike Einstein relation,

$$\sigma^2(\rho) = \lim_{v\to\infty} \frac{(\langle m^2\rangle - \langle m\rangle^2)}{v} = \frac{\chi(\rho)}{D(\rho)}, \tag{4.37}$$

which connects scaled variance [or compressibility as in Eq. 4.47] $\sigma^2(\rho)$ of particle-number, or mass, $m$ in a subsystem of volume $v$, the bulk-diffusion coefficient $D(\rho)$ and the conductivity $\chi(\rho)$. Here, the density-dependent transport coefficients $D(\rho)$ and $\chi(\rho)$ are defined from diffusive and drift currents,

$$J_{diff} = -D(\rho)\frac{\partial\rho}{\partial x} \qquad \text{and} \qquad J_{drift} = \chi(\rho)F, \tag{4.38}$$

respectively, where $\partial\rho/\partial x$ is spatial gradient in density and $F$ is a small force applied in the $+$ve $x$-direction. Most crucially, in our theory, the two transport coefficients $D(\rho)$ and $\chi(\rho)$ are related to a macroscopic observable like the activity $a(\rho)$. Consequently, probability distributions of subsystem mass is governed by an equilibriumlike chemical potential $\mu(\rho)$, also related to the activity $a(\rho)$. In particular, for the discrete MS (DMS), we have strikingly simple relations

$$D(\rho) = a'(\rho), \quad \chi(\rho) = a(\rho), \quad \text{and} \quad \mu(\rho) = \ln a(\rho). \tag{4.39}$$

To substantiate our claims, we first directly check the ER [Eq. 4.37] in simulations. Then using the ER, we compute, in the DMS, probabilities of density large-deviations, and the corresponding large deviation function. In all cases, we find good agreement between theory and simulations.

The above hydrodynamic structure has important consequences on critical behaviors of the MS. As $\Delta = (\rho - \rho_c) \to 0^+$, with $\rho_c$ critical density, we obtain two remarkable scaling relations listed following.

(i) Scaled variance $\sigma^2(\rho) \sim (\rho - \rho_c)^{1-\delta}$ with exponent $\delta = 0$; in the DMS near critical point, $\sigma^2(\rho) = (\rho - \rho_c)/\beta$ where the proportionality constant is exactly $1/\beta$ (see inset of Fig. 4.8), with $\beta$ defined from critical behavior of the activity $a(\rho) \sim \Delta^\beta$.

1 This section is based on the paper "Hydrodynamics, density fluctuations and universality in conserved Manna sandpiles", Sayani Chatterjee, Arghya Das, and Punyabrata Pradhan, *submitted*

(ii) Dynamical exponent $z = 2 + (\beta - 1)/\nu_\perp$ is expressed in terms of two static exponents $\beta$ and $\nu_\perp$; exponents $z$ and $\nu_\perp$ are defined from critical behaviors of correlation length $\xi \sim \Delta^{-\nu_\perp}$ and relaxation time $\tau_r \sim \xi^z$.

Indeed, previous estimates of $\beta$, $\nu_\perp$ and $z$ in a broad class of the CSS are in reasonably good agreement with scaling relation (ii) [see Table 1]. Exponents $\beta$, $\nu_\perp$ and $z$ (see Table 1) in directed percolation (DP) [128, 129], having no conservation as such, violate (ii), implying that the conserved MS (and, presumably, the CSS) belong to a distinct universality, *not* that of DP.

### 4.3.1 *Discrete Manna sandpiles (DMS) in one dimension*

We consider the Manna sandpiles (MS), defined in the previous section 4.2.2.1 for simplicity, on a one dimensional (1D) periodic lattice of $L$ sites. In the discrete Manna sandpiles (DMS), a site $i$ is assigned an *unbounded* (unrestricted-height) integer variable $m_i = 0, 1, 2, \ldots$, called number of particles. A site $i$ is *active* if $m_i > 1$. We consider here continuous-time dynamics (random sequential update): A site is chosen at random from a list of $N_a$ number of active sites present in the system and is toppled by independently transferring two particles to any of its nearest neighbors, each with *equal* probability $1/2$; then, these steps are repeated. Total number of particles, or mass, $M = \sum_{i=1}^{L} m_i$ remains *conserved*, with density $\rho = M/L$ fixed. The activity in the system is quantified through active-site density $a(\rho) = \langle N_a \rangle / L$, which depends on density $\rho$. Critical density is found to be $\rho_c \approx 0.95$ [84]. The dynamics of the system is given in Eq. 4.12.

As discussed previously, the conductivity, along with the bulk-diffusion coefficient, plays a crucial role in characterizing fluctuations in the MS. To calculate the conductivity, we define a generalized (biased) version of the MS from the typical unbiased dynamics given by Eq. 4.12]. A constant biasing force $\vec{F}$, coupled to the local particle-number is introduced in the biased dynamics which accordingly modifies the particle-hopping rates in the MS [52, 130, 131]. During a toppling in the biased MS, two particles are transferred, still independently, but each with *unequal* probabilities determined according to the transfer-direction of the particle and the magnitude $F$ of the biasing force field $\vec{F} = F\hat{x}$ present along $\hat{x}$ (similar to stochastic dynamics of a particle of mass $m$ in a gravitational field). So, it is less likely for a

particle to go in the direction opposite to the biasing force. The stochastic time-evolution of $m_i(t)$ in an infinitesimal time-interval $dt$ can be written as

$$m_i(t+dt) = \begin{cases} m_i(t)-2 & \text{prob. } \hat{a}_i(c^F_{i,0}+c^F_{i,+}+c^F_{i,-})dt, \\ m_i(t)+1 & \text{prob. } \hat{a}_{i-1}c^F_{i-1,0}dt, \\ m_i(t)+1 & \text{prob. } \hat{a}_{i+1}c^F_{i+1,0}dt, \\ m_i(t)+2 & \text{prob. } \hat{a}_{i-1}c^F_{i-1,+}dt, \\ m_i(t)+2 & \text{prob. } \hat{a}_{i+1}c^F_{i+1,-}dt, \\ m_i(t) & \text{prob. } [1-\Sigma dt], \end{cases} \tag{4.40}$$

where random variable $\hat{a}_i = 1$ if a site is active and $\hat{a}_i = 0$ otherwise, the modified (biased) particle-hopping rates [52, 130, 131]

$$c^F_{i,\alpha} = c^{F=0}_{i,\alpha} \exp\left[\sum_j \frac{\Delta e_{ij}}{2}\right],$$

the original (unbiased) particle-hopping rates

$$c^{F=0}_{i,0} = \frac{1}{2}, \quad c^{F=0}_{i,+} = c^{F=0}_{i,-} = \frac{1}{4},$$

and

$$\Sigma = [\hat{a}_i(c^F_{i,0}+c^F_{i,+}+c^F_{i,-}) + \hat{a}_{i-1}c^F_{i-1,0} + \hat{a}_{i+1}c^F_{i+1,0} + \hat{a}_{i-1}c^F_{i-1,+} + \hat{a}_{i+1}c^F_{i+1,-}].$$

Here, the modified rates $c^F_{i,0}$, $c^F_{i,+}$ and $c^F_{i,-}$ correspond to transfer of one particle to the left and one to the right, that of both particles to the right and that of both particles to the left, respectively and $\Delta e_{ij} = \Delta m_{i\to j} F(j-i)$ is an 'energy cost' [52, 130, 131] for moving $\Delta m_{i\to j}$ numbers of particles from site $i$ to $j$ (lattice spacing taken to be unity). The case with $F = 0$ corresponds to the unbiased DMS, which is of our interest here.

#### 4.3.1.1 *Hydrodynamics*

First, to calculate conductivity, let us explicitly write, and then expand in linear order of biasing force $F$ (as in linear-response theory), the rates $c^F_{i,0}$, $c^F_{i,+}$ and $c^F_{i,-}$, which correspond to

the transfer of one particle to the left and one to the right, that of both particles to the right and that of both particles to the left, respectively, as given below

$$\begin{aligned} c^F_{i,0} &= c^{F=0}_{i,0} \exp[(F-F)/2] = \frac{1}{2}, \\ c^F_{i,+} &= c^{F=0}_{i,+} \exp(2F/2) \simeq \frac{(1+F)}{4}, \\ c^F_{i,-} &= c^{F=0}_{i,-} \exp(-2F/2) \simeq \frac{(1-F)}{4}. \end{aligned} \tag{4.41}$$

Now using the dynamical rules as in Eq. 4.40 , the infinitesimal-time evolution equation for the first moment $\langle m_i \rangle$ of mass at site $i$ can be written as

$$\begin{aligned} \langle m_i(t+dt) \rangle = \langle [m_i(t)-2]\hat{a}_i \rangle dt + \langle [m_i(t)+1]\hat{a}_{i-1} \rangle \frac{dt}{2} \\ + \langle [m_i(t)+1]\hat{a}_{i+1} \rangle \frac{dt}{2} + (1+F)\langle [m_i(t)+2]\hat{a}_{i-1} \rangle \frac{dt}{4} \\ + (1-F)\langle [m_i(t)+2]\hat{a}_{i+1} \rangle \frac{dt}{4} + \langle m_i(t)(1-\Sigma dt) \rangle. \end{aligned}$$

Thus we obtain the following time-evolution equation for local number-density $\langle m_i(t) \rangle = \rho_i(t)$,

$$\frac{\partial \rho_i}{\partial t} = (a_{i-1} - 2a_i + a_{i+1}) + F\frac{a_{i-1} - a_{i+1}}{2}, \tag{4.42}$$

where the local activity $\langle \hat{a}_i \rangle = a_i$. Note that local diffusive current in Eq. 4.42 can be expressed as gradient (discrete) of a local observable ($a_i$ here), which we call 'gradient property' [130]. As discussed below, the gradient property helps one to immediately identify bulk-diffusion coefficient and conductivity in the DMS. It is expected that, in large spatio-temporal scales, there would exist a local steady-state [130, 131], where local observable, such as $a_i \equiv a[\rho_i(t)]$, is a slowly varying function of space and time and thus function of only local density $\rho_i(t)$. Consequently, taking continuum limit, Eq. 4.42 leads to the desired hydrodynamic evolution of density field $\rho(x,t)$ at position $x$ and time $t$,

$$\frac{\partial \rho(x,t)}{\partial t} = \frac{\partial^2 a(\rho)}{\partial x^2} - F\frac{\partial a(\rho)}{\partial x} \equiv -\frac{\partial J}{\partial x}, \tag{4.43}$$

In the above equation, the local current $J(\rho(x)) = J_{diff} + J_{drift}$ can be broken into two parts: The diffusion current $J_{diff} \equiv -D(\rho)\partial\rho/\partial x$ and the drift current $J_{drift} \equiv \chi(\rho)F$ with the density-dependent bulk-diffusion coefficient and conductivity can be identified as

$$D(\rho) = \frac{da}{d\rho} \equiv a'(\rho) \quad \text{and} \quad \chi(\rho) = a(\rho), \tag{4.44}$$

respectively. The hydrodynamic structure as derived in Eq. 4.43 is exact and is the first important result of this work, constituting the basis of the whole analysis here. Indeed, there are certain similarities between Eq. 4.43 and the previously obtained coarse-grained field theories [81, 110, 112]. However, there are important differences too: Eq. 4.43 here involves only a single field variable, i.e., conserved density field $\rho(x,t)$; the activity $a[\rho(x,t)]$ is not treated here as an independent field variable, rather it evolves through its (nonlinear) dependence on density field.

#### 4.3.1.2 *Macroscopic fluctuation theory*

Now following the prescription of recently developed macroscopic fluctuation theory (MFT) [52, 130], the above hydrodynamics Eq. 4.43 can be readily used to characterize fluctuations, on a coarse-grained level, in the *unbiased* system with $F = 0$, solely in terms of the two transport coefficients $D(\rho)$ and $\chi(\rho)$. To elaborate on this point, we consider a system, which is divided into $\nu = L/l$ large subsystems of size $l \ll L$. Then the joint probability distribution $\mathcal{P}[\hat{\rho}_1, \hat{\rho}_2, \ldots, \hat{\rho}_\nu]$ of the subsystem number-densities $\{\hat{\rho}_\alpha = M_\alpha/l\}$, with $M_\alpha$ being particle-number in $\alpha$th subsystem and $\alpha \in \{1, 2, \ldots, \nu\}$, can be written as a product of subsystem weight-factors [57],

$$\mathcal{P}[\{\rho_\alpha\}] \simeq \prod_\alpha \exp[-\{f(\hat{\rho}_\alpha) - f(\rho) - \mu(\rho)(\hat{\rho}_\alpha - \rho)\}], \tag{4.45}$$

with $\rho = M/L$ being the global density. In a suitable coarse-grained limit, the joint distribution can also be written as $\mathcal{P} \simeq \exp\{-\mathcal{H}[\hat{\rho}(x)]\}$ where $\mathcal{H}[\rho(x)] = \int dx[f(\hat{\rho}(x)) - f(\rho) - \mu(\rho)(\hat{\rho}(x) - \rho)]$ with $f(\rho)$ and $\mu(\rho) = df/d\rho$ being equilibriumlike free-energy density and chemical potential, respectively. According to the MFT, free-energy density $f(\rho)$ can be determined by solving a Hamilton-Jacobi equation [52, 130],

$$\int dx \frac{\partial}{\partial x}\left(\frac{\delta \mathcal{H}}{\delta \hat{\rho}}\right) \chi(\hat{\rho}) \frac{\partial}{\partial x}\left(\frac{\delta \mathcal{H}}{\delta \hat{\rho}}\right) - \int dx \frac{\delta \mathcal{H}}{\delta \hat{\rho}} \frac{\partial J_{diff}}{\partial x} = 0, \tag{4.46}$$

implying $f''(\rho) = (d\mu/d\rho) = D(\rho)/\chi(\rho)$. Now, as the product form of joint subsystem mass distribution $\mathcal{P}[\{\hat{\rho}_\alpha = M_\alpha/l\}]$ in Eq. 4.45 implies a fluctuation-response relation (FR) [57],

$$\frac{d\rho}{d\mu} = \sigma^2(\rho), \tag{4.47}$$

with $\sigma^2(\rho) = \lim_{l\to\infty}(\langle M_\alpha^2\rangle - \langle M_\alpha\rangle^2)/l$, we arrive at the ER Eq. 4.37. In the unbiased MS with $F = 0$, we obtain, using $D(\rho) = a'(\rho)$ and $\chi(\rho) = a(\rho)$, an alternative form of the ER, relating mass-fluctuation and activity,

$$\sigma^2(\rho) = \frac{a(\rho)}{a'(\rho)}. \tag{4.48}$$

The ER Eq. 4.48 is the second important result of this work. By integrating $d\mu/d\rho = a(\rho)/a'(\rho)$, obtained from Eqs. (4.47) and (4.48), one immediately has an equilibriumlike chemical potential $\mu(\rho) = \ln a(\rho) + c$, with $c$ being arbitrary integration constant.

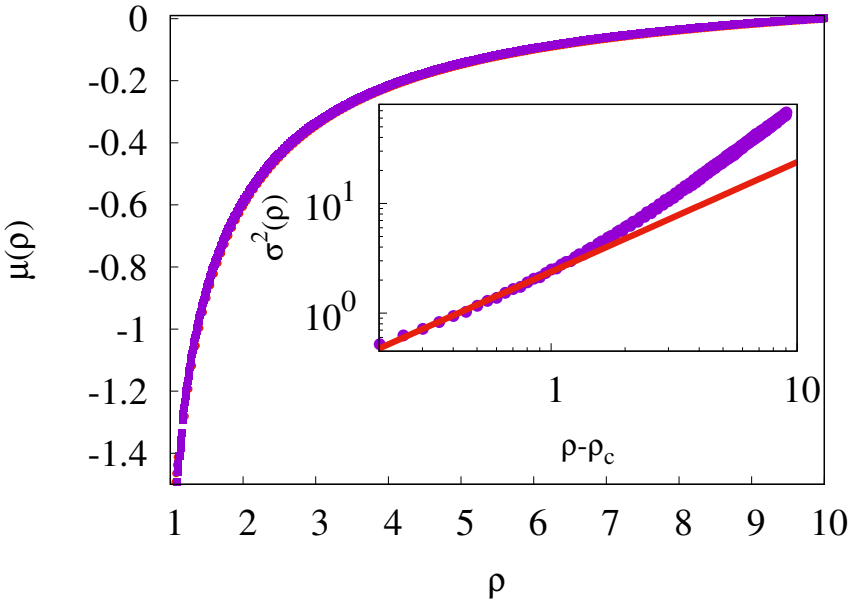


Figure 4.8: Chemical potentials $\mu(\rho) = \int_{\rho_0}^{\rho} a'(\rho)/a(\rho)d\rho$ [red circles; integrating inverse of rhs of Eq. 4.48] and $\mu(\rho) = \int_{\rho_0}^{\rho} 1/\sigma^2(\rho)d\rho$ [magenta squares; integrating inverse of lhs of Eq. 4.48] are plotted as a function of density $\rho$. *Inset:* Scaled variance $\sigma^2(\rho)$ *vs.* $(\rho - \rho_c)$, is plotted (magenta circles) where red line [theory, scaling relation (i)] represents $\sigma^2 = (\rho - \rho_c)/\beta$, with $\rho_c \approx 0.95$ and $\beta \approx 0.42$ [84].

In the following, we check the integrated form of the ER Eq. 4.48 [or, equivalently, Eq. 4.37]. We first calculate from simulations both the scaled variance $\sigma^2(\rho)$ and the activity $a(\rho)$ as a function of density $\rho$. Then we calculate chemical potential in two ways: $\mu(\rho) = \int_{\rho_0}^{\rho} 1/\sigma^2 d\rho$ and $\mu(\rho) = \int_{\rho_0}^{\rho} a'(\rho)/a(\rho)d\rho = [\ln a(\rho) - \ln a(\rho_0)]$ by integrating, w.r.t. $\rho$, inverse of lhs and rhs of Eq. 4.48, respectively. In Fig. 4.8, both the chemical potentials are plotted as a function of $\rho$ and are in excellent agreement with each other, thus verifying the ER for the DMS.

#### 4.3.1.3 *Scaling relations*

The above results have two important consequences on the near-critical behaviors of the DMS.

1. Since chemical potential $\mu(\rho) = \ln a(\rho)$ and the activity $a(\rho) \sim \Delta^{\beta}$ as $\Delta = (\rho - \rho_c) \to 0^+$, we obtain scaling relation (i) Scaled variance

$$\sigma^2(\rho) \sim \Delta^{1-\delta}$$

of subsystem-mass near criticality is proportional to $(\rho - \rho_c)$, with $\delta = 0$ and the proportionality constant is exactly $1/\beta$. So, near criticality, the scaled variance is given by

$$\sigma^2(\rho) = \frac{(\rho - \rho_c)}{\beta}.$$

In the inset of Fig. 4.8, we plot scaled variance $\sigma^2(\rho)$ of subsystem mass as a function of $(\rho - \rho_c)$, which is in quite good agreement with simulations.

2. We obtain another scaling relation as follows. In the unbiased DMS, Eq. 4.43 with $F = 0$ leads to hydrodynamic evolution equation

$$\frac{\partial \rho(x,t)}{\partial t} = \frac{\partial}{\partial x}\left[D(\rho)\frac{\partial \rho}{\partial x}\right].$$

Now, a simple dimensional analysis would imply relaxation time

$$\tau_r \sim \frac{\xi^2}{D} \sim \xi^{2+\frac{(\beta-1)}{\nu_\perp}}$$

with spatial correlation length

$$\xi \sim \Delta^{-\nu_\perp}$$

and the bulk-diffusion coefficient

$$D(\rho) = a'(\rho) \sim \Delta^{\beta-1} \sim \xi^{(1-\beta)/\nu_\perp},$$

both diverging at criticality. Defining dynamic exponent $z$ as $\tau_r \sim \xi^z$, we obtain scaling relation (ii),

$$z = 2 + \frac{(\beta - 1)}{\nu_\perp},$$

where dynamic exponent $z$ is expressed in terms of static exponents $\beta$ and $\nu_\perp$, reminiscent of similar relations in equilibrium critical phenomena [132].

*Density large deviations.*— We now numerically compute, by integrating the FR Eq. 4.47 to obtain $\mu(\rho)$ and $f(\rho)$ [127], probability $P_v(m) \sim \exp[-vh(\hat{\rho})]$ of large deviation in coarse-grained density $\hat{\rho} = m/v$ in subsystem of size $v$ where large deviation function (LDF) is $h(\hat{\rho}) = f(\hat{\rho}) - \mu(\rho)\hat{\rho}$, with $\rho$ being global density. However, the LDF having sub-leading corrections, comes in the same form as discussed in the previous section 4.2.3.

Table 4.1: Previous estimates of $z$ are compared with $z$, calculated from scaling relation (ii) [using previously estimated static exponents $\beta$ and $\nu_\perp$ in (ii)].

| Models: Conserved stochastic sandpiles (CSS) and directed percolation (DP) | $\beta$ | $\nu_\perp$ | $z$ | $z$ from scaling relation (ii) |
|---|---|---|---|---|
| 1D *unrestricted-height* MS, from Ref. [84] | 0.42 | 1.81 | 1.66 | 1.68 |
| 2D *unrestricted-height* MS, from Ref. [97] | 0.64 | 0.82 | 1.57 | 1.56 |
| 1D *restricted-height* MS, from Ref. [87] | 0.29 | 1.36 | 1.50 | 1.48 |
| 2D *restricted-height* MS, from Ref. [103] | 0.64 | 0.82 | 1.51 | 1.56 |
| 1D conserved lattice gas (CLG), from Ref. [98] | 0.63 | 0.78 | 1.52 | 1.53 |
| 2D conserved threshold transfer process (CTTP), from Table 1 in Ref. [103] | 0.64 | 0.80 | 1.53 | 1.55 |
| 1D DP, from Table 1 in Ref. [111] | 0.28 | 1.10 | 1.58 | 1.35 |
| 2D DP, from Table 1 in Ref. [103] | 0.58 | 0.73 | 1.77 | 1.42 |

### 4.3.2 *Two dimensional (2D) Discrete Manna Sandpile (DMS)*

Here we consider the discrete Manna sandpile on a periodic two dimensional lattice. The particle dynamics is generalized in two dimension case. We define a set of random variable

$\hat{a}_{i,j} = 1$ if a site is active and $\hat{a}_{i,j} = 0$ otherwise. Then, the time-evolution of mass $m_{i,j}(t)$ at site $(i,j)$ at time $t$ can be written in an infinitesimal time-interval $dt$.

$$m_{i,j}(t+dt) = \begin{cases} m_{i,j}(t) - 2 & \text{prob. } \hat{a}_{i,j}dt, \\ m_{i,j}(t) + 1 & \text{prob. } \frac{3\hat{a}_{(i-1),j}}{8}dt, \\ m_{i,j}(t) + 1 & \text{prob. } \frac{3\hat{a}_{(i+1),j}}{8}dt, \\ m_{i,j}(t) + 1 & \text{prob. } \frac{3\hat{a}_{i,(j-1)}}{8}dt, \\ m_{i,j}(t) + 1 & \text{prob. } \frac{3\hat{a}_{i,(j+1)}}{8}dt, \\ m_{i,j}(t) + 2 & \text{prob. } \frac{\hat{a}_{(i-1),j}}{16}dt, \\ m_{i,j}(t) + 2 & \text{prob. } \frac{\hat{a}_{(i+1),j}}{16}dt, \\ m_{i,j}(t) + 2 & \text{prob. } \frac{\hat{a}_{i,(j-1)}}{16}dt, \\ m_{i,j}(t) + 2 & \text{prob. } \frac{\hat{a}_{i,(j+1)}}{16}dt, \\ m_{i,j}(t) & \text{prob. } [1 - \Sigma dt] \end{cases} \tag{4.49}$$

where

$$\begin{aligned} \Sigma \;=\; & \hat{a}_{i,j} + \frac{3\hat{a}_{(i-1),j}}{8} + \frac{3\hat{a}_{(i+1),j}}{8} + \frac{3\hat{a}_{i,(j-1)}}{8} + \frac{3\hat{a}_{i,(j+1)}}{8} \\ & + \frac{\hat{a}_{(i-1),j}}{16} + \frac{\hat{a}_{(i+1),j}}{16} + \frac{\hat{a}_{i,(j-1)}}{16} + \frac{\hat{a}_{i,(j+1)}}{16}. \end{aligned} \tag{4.50}$$

In the presence of the biasing force $\vec{F} = F\hat{x}$ in +ve-$x$ direction, the modified particle-hopping [52, 130, 131] rates can be written as $c^{F}_{i,j,\alpha,\alpha'} = c^{F=0}_{i,j,\alpha,\alpha'} \exp\left[\sum_{(i',j')} F\Delta m_{(i,j)\to(i',j')}/2\right]$, where $c^{F}_{i,j,\alpha,\alpha'}$ is the rate for the toppling event at an active site $(i,j)$ where one particle goes

to $\alpha$th direction and the other to $\alpha'$th direction, with $\alpha, \alpha' \in \{+\hat{x}, -\hat{x}, +\hat{y}, -\hat{y}\}$. The rates can be explicitly written in linear order of biasing force $F$ as given below,

$$\begin{aligned}
C^F_{i,j,+x,+x} &= C^{F=0}_{i,j,+x,+x} \exp(2F/2) \simeq \frac{(1+F)}{16}, \\
C^F_{i,j,-x,-x} &= C^{F=0}_{i,j,-x,-x} \exp(-2F/2) \simeq \frac{(1-F)}{16}, \\
C^F_{i,j,+y,+y} &= C^{F=0}_{i,j,+y,+y} = \frac{1}{16}, \\
C^F_{i,j,-y,-y} &= C^{F=0}_{i,j,-y,-y} = \frac{1}{16}, \\
C^F_{i,j,+x,-x} &= C^{F=0}_{i,j,+x,-x} \exp[(F-F)/2] = \frac{1}{8}, \\
C^F_{i,j,+x,\pm y} &= C^{F=0}_{i,j,+x,\pm y} \exp(F/2) \simeq \frac{(1+F/2)}{8}, \\
C^F_{i,j,-x,\pm y} &= C^{F=0}_{i,j,-x,\pm y} \exp(-F/2) \simeq \frac{(1-F/2)}{8}, \\
C^F_{i,j,+y,-y} &= C^{F=0}_{i,j,+y,-y} = \frac{1}{8}.
\end{aligned}$$

Now, the typical dynamics of the biased system could be written in the following form.

$$m_{i,j}(t+dt) = \begin{cases}
m_{i,j}(t) - 2 & \text{prob. } \hat{a}_{i,j} dt, \\
m_{i,j}(t) + 1 & \text{prob. } \frac{(3+F)\hat{a}_{(i-1),j}}{8} dt, \\
m_{i,j}(t) + 1 & \text{prob. } \frac{(3-F)\hat{a}_{(i+1),j}}{8} dt, \\
m_{i,j}(t) + 1 & \text{prob. } \frac{3\hat{a}_{i,(j-1)}}{8} dt, \\
m_{i,j}(t) + 1 & \text{prob. } \frac{3\hat{a}_{i,(j+1)}}{8} dt, \\
m_{i,j}(t) + 2 & \text{prob. } \frac{(1+F)\hat{a}_{(i-1),j}}{16} dt, \\
m_{i,j}(t) + 2 & \text{prob. } \frac{(1-F)\hat{a}_{(i+1),j}}{16} dt, \\
m_{i,j}(t) + 2 & \text{prob. } \frac{\hat{a}_{i,(j-1)}}{16} dt, \\
m_{i,j}(t) + 2 & \text{prob. } \frac{\hat{a}_{i,(j+1)}}{16} dt, \\
m_{i,j}(t) & \text{prob. } [1 - \Sigma dt]
\end{cases} \tag{4.51}$$

where

$$\begin{aligned}
\Sigma &= \hat{a}_{i,j} + \frac{(3+F)\hat{a}_{(i-1),j}}{8} + \frac{(3-F)\hat{a}_{(i+1),j}}{8} + \frac{3\hat{a}_{i,(j-1)}}{8} + \frac{3\hat{a}_{i,(j+1)}}{8} \\
&\quad + \frac{(1+F)\hat{a}_{(i-1),j}}{16} + \frac{(1-F)\hat{a}_{(i+1),j}}{16} + \frac{\hat{a}_{i,(j-1)}}{16} + \frac{\hat{a}_{i,(j+1)}}{16}.
\end{aligned} \tag{4.52}$$

The local density variable $\rho_{i,j}(t) = \langle m_{i,j}(t) \rangle$ at site $(i,j)$ and time $t$ evolves through the following equation (which have 'gradient property'),

$$\begin{aligned} \frac{d\rho_{i,j}}{dt} &= \frac{1}{2}\left[a_{(i+1),j} - 2a_{i,j} + a_{(i-1),j}\right] + \frac{1}{2}\left[a_{i,(j+1)} - 2a_{i,j} + a_{i,(j-1)}\right] \\ &\quad -\frac{F}{4}\left[a_{(i+1),j} - a_{(i-1),j}\right], \end{aligned} \tag{4.53}$$

which, in continuum limit, leads to the desired hydrodynamic time-evolution equation for density field $\rho(\vec{r},t)$ at position $\vec{r} = \{x,y\}$ and time $t$,

$$\frac{\partial \rho(\vec{r},t)}{\partial t} = \frac{1}{2}\nabla^2 a(\rho) - \frac{1}{2}F\frac{\partial a(\rho)}{\partial x} \equiv -\nabla.\vec{J}(\rho(\vec{r})). \tag{4.54}$$

In the above hydrodynamic equation, local current $\vec{J} = \vec{J}_{diff} + \vec{J}_{drift}$ has two parts: diffusive current $\vec{J}_{diff} = -(1/2)\nabla a(\rho) \equiv -D(\rho)\nabla\rho$ and drift current $\vec{J}_{drift} = \chi(\rho)\vec{F}$ where bulk-diffusion coefficient $D(\rho) = a'(\rho)/2$ and conductivity $\chi = a(\rho)/2$; the two transport coefficients are density-dependent in general. Now, following macroscopic fluctuation theory [52, 130], as discussed in the case of the 1D DMS, we recover the Einstein relation (ER) in the 2D DMS,

$$\sigma^2(\rho) = \frac{D(\rho)}{\chi(\rho)} = \frac{a(\rho)}{a'(\rho)}, \tag{4.55}$$

and obtain an equilibriumlike chemical potential

$$\mu(\rho) = \int_{\rho_0}^{\rho} \frac{\chi(\rho)}{D(\rho)} d\rho = \ln a(\rho) - \ln a(\rho_0), \tag{4.56}$$

where mass-fluctuation $\sigma^2(\rho)$ and chemical potential $\mu(\rho)$ in the 1D and 2D DMS have similar dependence on the activity $a(\rho)$; the dependence of the activity $a(\rho)$ on density $\rho$ in the 1D and 2D DMS is of course different.

### 4.3.3 *One dimensional (1D) Continuous Manna sandpile (CMS).*

In this section, we briefly discuss the results in a continuous-mass version of the Manna sandpile [120], which, for simplicity, is defined on a periodic one-dimensional lattice of $L$ sites with $m_i \geq 0$ being a continuous (and unbounded) mass variable assigned to site $i$; generalization to higher dimensions is straightforward (similar to that for the DMS in Sec. II in the SM). We consider here only continuous-time dynamics (random sequential updates). Total mass $M = \sum_{i=1}^{L} m_i$ remains *conserved* in the process, with mass-density $\rho = M/L$ fixed. Provided $m_i \geq 1$, site $i$ becomes *active* and topples with rate unity, by transferring a uniformly

distributed random fraction $y_i \in [0,1]$ of mass $m_i$ to its left nearest neighbor and the rest of the mass to its right nearest neighbor. The system undergoes an active to absorbing phase transition below a critical density $\rho_c \approx 0.66$. The typical dynamics of this system is given in the following.

$$m_i(t+dt) = \begin{cases} m_i(t) - y_i m_i(t) & \text{prob. } \hat{a}_i dt, \\ m_i(t) + y_{i+1} m_{i+1}(t) & \text{prob. } \hat{a}_{i+1} dt, \\ m_i(t) + \tilde{y}_{i-1} m_{i-1}(t) & \text{prob. } \hat{a}_{i-1} dt, \\ m_i(t) & \text{otherwise,} \end{cases} \tag{4.57}$$

where random variable $\hat{a}_i = 1$ if a site is active and $\hat{a}_i = 0$ otherwise, $\tilde{y}_i = (1 - y_i)$.

To calculate the conductivity, we now bias the system by applying a small constant force $\vec{F} = F\hat{x}$, which leads to the following evolution of mass $m_i(t)$ in infinitesimal time interval $dt$,

$$m_i(t+dt) = \begin{cases} m_i(t) - y_i m_i(t) & \text{prob. } \hat{a}_i c_i^F dt, \\ m_i(t) + y_{i+1} m_{i+1}(t) & \text{prob. } \hat{a}_{i+1} c_{i+1}^F dt, \\ m_i(t) + \tilde{y}_{i-1} m_{i-1}(t) & \text{prob. } \hat{a}_{i-1} c_{i-1}^F dt, \\ m_i(t) & \text{otherwise,} \end{cases} \tag{4.58}$$

modified (biased) mass-transfer rates $c_i^F = c_i^{F=0} \exp\left[\sum_j \Delta e_{ij}/2\right]$ from site $i$ to nearest neighbors, with the corresponding unbiased ($F = 0$) mass-transfer rates $c_i^{F=0} = 1$, $\Delta e_{ij} = \Delta m_{i\to j} F(j - i)$ being an 'energy cost' to transfer $\Delta m_{i\to j}$ amount of mass from site $i$ to $j$. Now, by keeping only the terms linear in biasing force $F$,

$$c_i^F = \hat{a}_i \left[1 + \frac{m_i(1-2y_i)}{2} F\right], \tag{4.59}$$

we arrive at the time-evolution equation of local mass-density $\langle m_i(t)\rangle = \rho_i(t)$,

$$\frac{\partial \rho_i}{\partial t} = \left[u_{i-1}^{(1)} - 2u_i^{(1)} + u_{i+1}^{(1)}\right] + F\left[u_{i-1}^{(2)} - u_{i+1}^{(2)}\right], \tag{4.60}$$

where we denote $u_i^{(1)} = \langle m_i \hat{a}_i\rangle/2$ and $u_i^{(2)} = \langle m_i^2 \hat{a}_i\rangle/12$. Here, the 'gradient condition' is still satisfied by the time-evolution equation as the rhs can be written as gradients (discrete) of the two local observables $u^{(1)}$ and $u^{(2)}$. Now, in large spatio-temporal scales where observables are slowly varying functions of space and time, local observables $u^{(\alpha)} = u^{(\alpha)}[\rho_i(t)] \equiv u^{(\alpha)}[\rho(x,t)]$, with $\alpha = 1, 2$, are functions of only local density $\rho(x,t)$. Therefore, in the contin-

uum limit, we obtain, from Eq. 4.60, the hydrodynamic evolution of density field $\rho(x,t)$ at position $x$ and time $t$,

$$\frac{\partial \rho(x,t)}{\partial t} = \frac{\partial^2 u^{(1)}}{\partial x^2} - \frac{\partial u^{(2)}}{\partial x} \equiv -\frac{\partial J}{\partial x}. \tag{4.61}$$

In the above equation, local current $J(\rho(x)) = J_{diff} + J_{drift}$ can be decomposed into two parts: diffusive current $J_{diff} = -\partial^2 u^{(1)}/\partial x^2$ and drift current $J_{drift} = u^{(2)}F$, leading to the expressions for bulk-diffusion coefficient $D(\rho) = du^{(1)}/d\rho$ and conductivity $\chi(\rho) = u^{(2)}$, both of which are density-dependent. Then, using macroscopic fluctuation theory [52, 130], via Eqs. 4.45 and 4.46, we obtain an Einstein relation (ER), as in Eq. 4.37, between scaled variance $\sigma^2(\rho)$ of subsystem mass, bulk-diffusion coefficient $D(\rho)$ and conductivity $\chi(\rho)$.

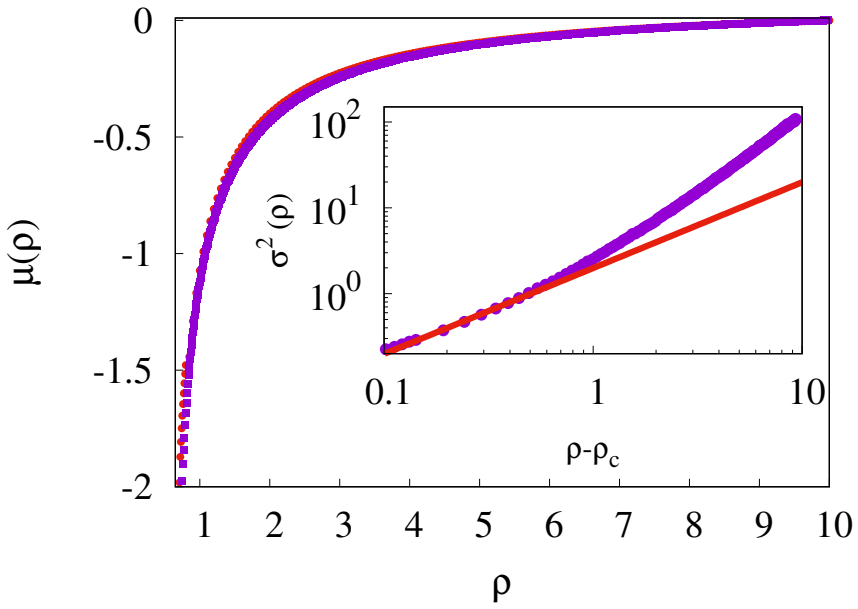


Figure 4.9: Chemical potentials $\mu(\rho) = \int_{\rho_0}^{\rho} D(\rho)/\chi(\rho)d\rho$, with $D(\rho) = du^{(1)}/d\rho$ and $\chi(\rho) = u^{(2)}(\rho)$, and $\mu(\rho) = \int_{\rho_0}^{\rho} 1/\sigma^2(\rho)d\rho$ are plotted as function of density $\rho$ [obtained by integrating inverse of rhs and lhs of Eq. 4.37]. *Inset*: The scaled variance $\sigma^2(\rho)$ is plotted as a function $(\rho - \rho_c)$ with $\rho_c \approx 0.66$ in the continuous Manna sandpile (CMS). Points - simulations, red line - theory [scaling relation (ii) without theoretical determination of the proportionality constant].

In Fig. 4.9, we have plotted chemical potentials $\mu(\rho) = \int_{\rho_0}^{\rho}(1/\sigma^2)d\rho$ and $\mu(\rho) = \int_{\rho_0}^{\rho}(D/\chi)d\rho$, obtained by numerically (simulations) calculating $u^{(1)}(\rho)$ [thus also $du^{(1)}/d\rho$) and $u^{(2)}(\rho)$] as a function of $\rho$ and then numerically integrating the inverse of Eq. 4.37. Both chemical potentials are in excellent agreement with each other, thus verifying the ER in Eq. 4.37] in the CMS.

Now, assuming that, near criticality, singularities in the quantities $u^{(1)}(\rho) = (1/L)\sum_i \langle m_i \hat{a}_i \rangle/2$ and $u^{(2)}(\rho) = (1/L)\sum_i \langle m_i^2 \hat{a}_i \rangle/12$ come from the singular contribution of only the activity $a(\rho) \sim (\rho - \rho_c)^\beta$, i.e., as $\rho \to 0^+$,

$$u^{(1)}(\rho) \simeq \text{const.} a(\rho) \; ; \; u^{(2)}(\rho) \simeq \text{const.} a(\rho),$$

and we recover scaling relations (i) $\sigma^2(\rho) \propto (\rho - \rho_c)$ and (ii) $z = 2 + (\beta - 1)/\nu_\perp$ as in the case of the DMS. Here we use the ER in Eq. 4.37 and the fluctuation-response relation in Eq. 4.47 to have bulk-diffusion coefficient $D(\rho) \sim a'(\rho)$, conductivity $\chi(\rho) \sim a(\rho)$, and consequently chemical potential $\mu(\rho) = \int 1/\sigma^2 d\rho = \int D(\rho)/\chi(\rho) d\rho \sim \ln a(\rho)$. The above analysis is however valid only near criticality. Note that, in the case of the CMS, the proportionality constant in scaling relation (i) however could not be determined. In the inset of Fig. 4.9, we plot scaled variance $\sigma^2(\rho)$ of subsystem mass as a function of $(\rho - \rho_c)$, which is in quite good agreement with simulations.

## 4.4 SUMMARY

We study a few threshold activated systems like fixed energy Manna sandpiles and its variants with continuous time dynamics. We demonstrate that these nonequilibrium steady state systems possess a remarkable thermodynamic structure in active phase. We show, that equilibriumlike additivity property holds quite good in these systems as correlation length is finite in active phases. It has been possible to analyse the unbounded fixed energy manna sandpile under mean field approximation and show that scaled variance in mass is proportional to square of the mass density. The reason behind of this particular asymptotic form could be "Bose Gas" like behavior of these unbounded models. Thus, the large deviation function for subsystem mass distribution could be estimated by gamma distribution. We have checked our results through numerics. We also find that though the functional form of scaled variance could not be obtained, the numerically obtained large deviation functions of height restricted models are well approximated by the analytic form obtained using additivity.

We derive exact hydrodynamic structure of conserved-mass (*fixed-energy*) Manna sandpiles (MS) with continuous-time dynamics (random sequential updates). Interestingly, the MS possess a 'gradient property', where local diffusive current and, therefore, time-evolution of local densities [see rhs of Eq. 4.42], can be written as a gradient (discrete) of local observable like the activity. We use the gradient property, and recently developed macroscopic fluctuation theory (MFT) [52, 130], to uncover a remarkable thermodynamic structure, where bulk-diffusion coefficient $D(\rho)$, conductivity $\chi(\rho)$ and mass fluctuations $\sigma^2(\rho)$ are shown to be connected to the activity $a(\rho)$, through an equilibriumlike Einstein relation

$\sigma^2(\rho) = \chi(\rho)/D(\rho)$ [Eq. 4.37]. In particular, in the discrete MS, we have strikingly simple relations $D(\rho) = a'(\rho)$, $\chi(\rho) = a(\rho)$ and $\sigma^2(\rho) = a(\rho)/a'(\rho)$. Moreover, we compute probabilities of density large deviations, governed by an equilibriumlike chemical potential $\mu(\rho)$ related again to the activity $a(\rho)$. In the discrete MS, we have $\mu(\rho) = \ln a(\rho)$. Our theoretical results are in excellent agreement with simulations and can be generalized to higher dimensions, the other CSS and other update rules (e.g., parallel update), etc.

This particular hydrodynamic structure has far-reaching consequences on critical behaviors of the conserved MS, through two scaling relations (i) and (ii), which, we believe, could help settle the long-standing issue of universality in such systems. As evident from Table 1 in the SM, a broad class of the CSS - restricted-height MS [87], conserved lattice gases (CLG) [98] and conserved threshold transfer processes (CTTP) [99–101] - all obey reasonably well scaling relation (ii), which is manifestly violated for directed percolation (DP), without any conservation law, thus ruling out DP universality for the conserved MS in particular and, presumably, for the CSS in general. However, unlike the MS, many of the CSS, with bounded state-space, can have 'non-gradient' structures in density evolution. The issue of putting the latter assertion regarding universality in the CSS on a firmer ground requires further studies and remains open, and intriguingly poised.

# 5

## SUMMARY AND CONCLUSIONS

- In this thesis work, we formulate a general statistical mechanics framework, which helps us to characterize, in a consistent way, fluctuations in systems having a nonequilibrium steady state. We have studied here conserved-mass transport processes, which are in general governed by fragmentation, diffusion and coalescence of masses. We verify that these conserved-mass transport processes obey an equilibriumlike additivity property, which implies that, if a system is divided into several large subsystems (much larger than the correlation length in the system), the subsystems could be considered statistically almost independent of each other. In other words, the joint probability of subsystem masses could then be written as product of some weight factors, which depend on the individual subsystems and generalize the Boltzman-Gibbs weights to nonequilibrium situations. Our main result says that, provided additivity holds, these weight factors and, consequently, the steady-state distribution of mass in a large subsystem can be determined from the functional dependence of variance of the subsystem mass on its mean.

- Using additivity, we demonstrate why certain mass distributions, e.g., gammalike mass distributions, arise in many of these mass transport processes, irrespective of different dynamical rules in the systems. We show that, the common feature among a broad class of conserved-mass transport processes is that the subsystem mass variance is proportional to square of the average subsystem mass, which immediately implies gammalike subsystem mass distributions.

- We formulate the criteria for nonequilibrium steady-state systems, having nonzero spatial correlation, to obey zeroth law of thermodynamics. We find that when two nonequilibrium steady-state systems are kept in contact and are allowed to exchange a conserved quantity, say mass, the mass exchange rate between the two systems in contact must obey a coarse-grained balance condition. A broad class of model systems are explicitly shown to form equivalence classes with respect to an equilibriumlike chemical potential. Our study provides a general prescription for dynamically generating

different equivalent nonequilibrium ensembles and could thus help in formulating a well-defined nonequilibrium thermodynamics for driven systems in general.

- Using additivity and consequent fluctuation-response relation, we characterize the active phase of a broad class of conserved lattice gases, which exhibit active-absorbing phase transition upon tuning global number density. In the active phase away from criticality, for unbounded systems like conserved manna sandpiles and its variants, the scaled variance of subsystem mass distribution is found to be approximately proportional to square of the number density, which, along with additivity, immediately implies a gammalike distribution for the subsystem masses. This theoretical prediction has been verified in the simulations. We show, that even for conserved manna sandpiles with height restriction, the additivity holds good to an extent and the subsystem mass distribution is well approximated by the theoretical large deviation form obtained from additivity. We also discover a gradient property in conserved mass Manna sandpile, which helps us to uncover a remarkable hydrodynamic structure. Using this hydrodynamic structure we show that an equilibriumlike Einstein relation holds for such nonequilibrium systems. This thermodynamic structure also helps us to obtain certain scaling relations, which provide a better understanding of active-absorbing phase transitions in such conserved stochastic sandpiles.

Overall, in this thesis work, we study a broad class of mass transport processes, which do not satisfy detailed balance, have mass-conserving dynamics and short-ranged spatial correlations (i.e., correlation length is finite). In all these processes, we find that the subsystem mass distributions can be obtained using an equilibriumlike additivity property. That is, mass fluctuations even in these nonequilibrium systems can be characterized by an equilibriumlike free energy function and chemical potential. We believe our work would help in formulating a consistent thermodynamic theory of fluctuations for driven systems in general.

# BIBLIOGRAPHY


[1] S. K. Friedlander, *Smoke, dust and haze: Fundamentals of aerosol behavior* (1977) (cit. on p. 7).

[2] P Meakin, "Droplet deposition growth and coalescence," Reports on Progress in Physics **55**, 157 (1992) (cit. on p. 7).

[3] W. H. White, "On the form of steady-state solutions to the coagulation equations," Journal of Colloid and Interface Science **87**, 204 –208 (1982) (cit. on p. 7).

[4] R. M. Ziff, "Kinetics of polymerization," Journal of Statistical Physics **23**, 241–263 (1980) (cit. on p. 7).

[5] H. Takayasu, "Steady-state distribution of generalized aggregation system with injection," Phys. Rev. Lett. **63**, 2563–2565 (1989) (cit. on p. 7).

[6] S. N. Majumdar, S. Krishnamurthy, and M. Barma, "Nonequilibrium phase transitions in models of aggregation, adsorption, and dissociation," Phys. Rev. Lett. **81**, 3691–3694 (1998) (cit. on pp. 7, 58).

[7] J. Krug and J. García, "Asymmetric particle systems on r," Journal of Statistical Physics **99**, 31–55 (2000) (cit. on pp. 7, 8, 11, 27, 38, 41, 58).

[8] R. Rajesh and S. N. Majumdar, "Conserved mass models and particle systems in one dimension," Journal of Statistical Physics **99**, 943–965 (2000) (cit. on pp. 7, 8, 10, 12, 27, 38, 41, 58).

[9] M. R. Evans, S. N. Majumdar, and R. K. P. Zia, "Factorized steady states in mass transport models," Journal of Physics A: Mathematical and General **37**, L275 (2004) (cit. on pp. 7, 32).

[10] M. R. Evans and T Hanney, "Nonequilibrium statistical mechanics of the zero-range process and related models," Journal of Physics A: Mathematical and General **38**, R195 (2005) (cit. on pp. 7, 13, 54).

[11] M. R. Evans, T. Hanney, and S. N. Majumdar, "Interaction-driven real-space condensation," Phys. Rev. Lett. **97**, 010602 (2006) (cit. on pp. 7, 23, 35, 56).

[12] F. Zielen and A. Schadschneider, "Exact mean-field solutions of the asymmetric random average process," Journal of Statistical Physics **106**, 173–185 (2002) (cit. on pp. 7, 10, 27, 32, 38, 41, 58).

[13]F Zielen and A Schadschneider, "Matrix product approach for the asymmetric random average process," Journal of Physics A: Mathematical and General **36**, 3709 (2003) (cit. on pp. 7, 27, 38, 41).

[14]S. Bondyopadhyay and P. K. Mohanty, "Conserved mass models with stickiness and chipping," Journal of Statistical Mechanics: Theory and Experiment **2012**, P07019 (2012) (cit. on pp. 7, 11, 27, 38, 41, 42, 58).

[15]C. Liu, S. R. Nagel, D. Schecter, S. Coppersmith, S. Majumdar, et al., "Force fluctuations in bead packs," Science **269**, 513 (1995) (cit. on pp. 8, 27, 41).

[16]S. N. Coppersmith, C. h. Liu, S. Majumdar, O. Narayan, and T. A. Witten, "Model for force fluctuations in bead packs," Phys. Rev. E **53**, 4673–4685 (1996) (cit. on pp. 8, 27, 41).

[17]S. Krauss, P. Wagner, and C. Gawron, "Continuous limit of the nagel-schreckenberg model," Phys. Rev. E **54**, 3707–3712 (1996) (cit. on p. 8).

[18]D. Chowdhury, L. Santen, and A. Schadschneider, "Statistical physics of vehicular traffic and some related systems," Physics Reports **329**, 199 –329 (2000) (cit. on p. 8).

[19]V. M. Yakovenko and J. B. Rosser, "Colloquium," Rev. Mod. Phys. **81**, 1703–1725 (2009) (cit. on pp. 12, 27, 42, 58).

[20]Patriarca, M., Heinsalu, E., and Chakraborti, A., "Basic kinetic wealth-exchange models: common features and open problems," Eur. Phys. J. B **73**, 145–153 (2010) (cit. on pp. 12, 27, 42).

[21]M. Patriarca, A. Chakraborti, and K. Kaski, "Statistical model with a standard Γ distribution," Phys. Rev. E **70**, 016104 (2004) (cit. on pp. 12, 27, 42, 43).

[22]F. Spitzer, "Interaction of markov processes," Advances in Mathematics **5**, 246 –290 (1970) (cit. on p. 13).

[23]S. Katz, J. L. Lebowitz, and H. Spohn, "Phase transitions in stationary nonequilibrium states of model lattice systems," Phys. Rev. B **28**, 1655–1658 (1983) (cit. on p. 14).

[24]D Jou, J Casas-Vázquez, and G Lebon, "Extended irreversible thermodynamics," Reports on Progress in Physics **51**, 1105 (1988) (cit. on pp. 15, 45).

[25]G. L. Eyink, J. L. Lebowitz, and H. Spohn, "Hydrodynamics and fluctuations outside of local equilibrium: driven diffusive systems," Journal of Statistical Physics **83**, 385–472 (1996) (cit. on pp. 15, 20, 28, 34, 45, 48).

[26]Y. Oono and M. Paniconi, "Steady state thermodynamics," Progress of Theoretical Physics Supplement **130**, 29 (1998), eprint: `/oup/backfile/Content_public/Journal/ptps/130/10.1143/PTPS.130.29/2/130-29.pdf` (cit. on pp. 15, 16, 45).

[27]T. Hatano and S.-i. Sasa, "Steady-state thermodynamics of langevin systems," Phys. Rev. Lett. **86**, 3463–3466 (2001) (cit. on p. 15).

[28]M. Baiesi, C. Maes, and B. Wynants, "Fluctuations and response of nonequilibrium states," Phys. Rev. Lett. **103**, 010602 (2009) (cit. on p. 16).

[29]U. Seifert and T. Speck, "Fluctuation-dissipation theorem in nonequilibrium steady states," EPL (Europhysics Letters) **89**, 10007 (2010) (cit. on p. 17).

[30]K. Hayashi and S.-i. Sasa, "Thermodynamic relations in a driven lattice gas: numerical experiments," Phys. Rev. E **68**, 035104 (2003) (cit. on pp. 17, 45, 65).

[31]S.-i. Sasa and H. Tasaki, "Steady state thermodynamics," Journal of Statistical Physics **125**, 125–224 (2006) (cit. on pp. 17, 28, 45, 46, 62, 65, 66).

[32]P. Pradhan, C. P. Amann, and U. Seifert, "Nonequilibrium steady states in contact: approximate thermodynamic structure and zeroth law for driven lattice gases," Phys. Rev. Lett. **105**, 150601 (2010) (cit. on pp. 17, 24, 34, 45, 46, 62, 65, 66).

[33]P. Pradhan, R. Ramsperger, and U. Seifert, "Approximate thermodynamic structure for driven lattice gases in contact," Phys. Rev. E **84**, 041104 (2011) (cit. on pp. 17, 24, 25, 32, 45, 46, 66).

[34]P. Pradhan and U. Seifert, "Thermodynamic theory of phase transitions in driven lattice gases," Phys. Rev. E **84**, 051130 (2011) (cit. on pp. 17, 46, 49, 62, 65).

[35]E. Bertin, O. Dauchot, and M. Droz, "Definition and relevance of nonequilibrium intensive thermodynamic parameters," Phys. Rev. Lett. **96**, 120601 (2006) (cit. on pp. 20, 28, 34, 45, 46, 48).

[36]E. Bertin, K. Martens, O. Dauchot, and M. Droz, "Intensive thermodynamic parameters in nonequilibrium systems," Phys. Rev. E **75**, 031120 (2007) (cit. on pp. 20, 25, 32, 45, 46, 53–55).

[37]R. Dickman and R. Motai, "Inconsistencies in steady-state thermodynamics," Phys. Rev. E **89**, 032134 (2014) (cit. on pp. 27, 45, 46, 63–66).

[38]R. Dickman, "Failure of steady-state thermodynamics in nonuniform driven lattice gases," Phys. Rev. E **90**, 062123 (2014) (cit. on pp. 27, 46, 63, 64, 66).

[39]E. Bertin, O. Dauchot, and M. Droz, "Temperature in nonequilibrium systems with conserved energy," Phys. Rev. Lett. **93**, 230601 (2004) (cit. on p. 28).

[40]A. Das, S. Chatterjee, P. Pradhan, and P. K. Mohanty, "Additivity property and emergence of power laws in nonequilibrium steady states," Phys. Rev. E **92**, 052107 (2015) (cit. on pp. 33, 49, 78).

[41]A. Chatterjee, P. Pradhan, and P. K. Mohanty, "Cluster-factorized steady states in finite-range processes," Phys. Rev. E **92**, 032103 (2015) (cit. on pp. 35, 55, 57, 71, 72).

[42]C. Kipnis, C. Marchioro, and E. Presutti, "Heat flow in an exactly solvable model," Journal of Statistical Physics **27**, 65–74 (1982) (cit. on pp. 42, 43, 58).

[43]Chakraborti, A. and Chakrabarti, B. K., "Statistical mechanics of money: how saving propensity affects its distribution," Eur. Phys. J. B **17**, 167–170 (2000) (cit. on pp. 42, 58).

[44]P. K. Mohanty, "Generic features of the wealth distribution in ideal-gas-like markets," Phys. Rev. E **74**, 011117 (2006) (cit. on p. 42).

[45]M. Kardar, *Statistical physics of particles* (Cambridge University Press, 2007) (cit. on pp. 45, 48).

[46]D. Jou and J. Casas-Vázquez, "Possible experiment to check the reality of a nonequilibrium temperature," Phys. Rev. A **45**, 8371–8373 (1992) (cit. on p. 45).

[47]L. F. Cugliandolo, J. Kurchan, and L. Peliti, "Energy flow, partial equilibration, and effective temperatures in systems with slow dynamics," Phys. Rev. E **55**, 3898–3914 (1997) (cit. on p. 45).

[48]A. Barrat, J. Kurchan, V. Loreto, and M. Sellitto, "Edwards' measures for powders and glasses," Phys. Rev. Lett. **85**, 5034–5037 (2000) (cit. on p. 45).

[49]A. Baranyai, "Temperature of nonequilibrium steady-state systems," Phys. Rev. E **62**, 5989–5997 (2000) (cit. on p. 45).

[50]B. Behringer, "Granular materials: taking the temperature," Nature **415**, 594–595 (2002) (cit. on p. 45).

[51]T. S. Komatsu, N. Nakagawa, S.-i. Sasa, and H. Tasaki, "Exact equalities and thermodynamic relations for nonequilibrium steady states," Journal of Statistical Physics **159**, 1237–1285 (2015) (cit. on p. 45).

[52]L. Bertini, A. De Sole, D. Gabrielli, G. Jona-Lasinio, and C. Landim, "Fluctuations in stationary nonequilibrium states of irreversible processes," Phys. Rev. Lett. **87**, 040601 (2001) (cit. on pp. 45, 88, 89, 91, 95, 97, 99, 100).

[53]L. Bertini, A. De Sole, D. Gabrielli, G. Jona-Lasinio, and C. Landim, "Macroscopic fluctuation theory for stationary non-equilibrium states," Journal of Statistical Physics **107**, 635–675 (2002) (cit. on p. 45).

[54]T. S. Komatsu, N. Nakagawa, S.-i. Sasa, and H. Tasaki, "Steady-state thermodynamics for heat conduction: microscopic derivation," Phys. Rev. Lett. **100**, 230602 (2008) (cit. on p. 45).

[55]T. S. Komatsu and N. Nakagawa, "Expression for the stationary distribution in nonequilibrium steady states," Phys. Rev. Lett. **100**, 030601 (2008) (cit. on p. 45).

[56]O. Cohen and D. Mukamel, "Phase diagram and density large deviations of a nonconserving *abc* model," Phys. Rev. Lett. **108**, 060602 (2012) (cit. on p. 46).

[57]S. Chatterjee, P. Pradhan, and P. K. Mohanty, "Gammalike mass distributions and mass fluctuations in conserved-mass transport processes," Phys. Rev. Lett. **112**, 030601 (2014) (cit. on pp. 53, 55, 58, 91).

[58]D. Matthes and G. Toscani, "On steady distributions of kinetic models of conservative economies," Journal of Statistical Physics **130**, 1087–1117 (2008) (cit. on p. 58).

[59]S. Katz, J. L. Lebowitz, and H. Spohn, "Nonequilibrium steady states of stochastic lattice gas models of fast ionic conductors," Journal of statistical physics **34**, 497–537 (1984) (cit. on pp. 60, 62).

[60]P. L. Garrido, J. L. Lebowitz, C. Maes, and H. Spohn, "Long-range correlations for conservative dynamics," Phys. Rev. A **42**, 1954–1968 (1990) (cit. on p. 65).

[61]G. Grinstein, D.-H. Lee, and S. Sachdev, "Conservation laws, anisotropy, and "self-organized criticality" in noisy nonequilibrium systems," Phys. Rev. Lett. **64**, 1927–1930 (1990) (cit. on p. 65).

[62]A. P. Solon, J. Stenhammar, R. Wittkowski, M. Kardar, Y. Kafri, M. E. Cates, and J. Tailleur, "Pressure and phase equilibria in interacting active brownian spheres," Phys. Rev. Lett. **114**, 198301 (2015) (cit. on p. 66).

[63]A. P. Solon, Y Fily, A. Baskaran, M. E. Cates, Y Kafri, M Kardar, and J Tailleur, "Pressure is not a state function for generic active fluids," Nature Physics (2015) (cit. on p. 66).

[64]U. Basu, C. Maes, and K. Neto čný, "How statistical forces depend on the thermodynamics and kinetics of driven media," Phys. Rev. Lett. **114**, 250601 (2015) (cit. on p. 66).

[65]P. Bak, C. Tang, and K. Wiesenfeld, "Self-organized criticality: an explanation of the 1/f noise," Phys. Rev. Lett. **59**, 381–384 (1987) (cit. on pp. 67, 68).

[66]P. Bak, C. Tang, and K. Wiesenfeld, "Self-organized criticality," Phys. Rev. A **38**, 364–374 (1988) (cit. on pp. 67, 68).

[67]S. Manna, "Two-state model of self-organized criticality," Journal of Physics A: Mathematical and General **24**, L363 (1991) (cit. on pp. 67–69).

[68]V. Frette, "Sandpile models with dynamically varying critical slopes," Phys. Rev. Lett. **70**, 2762–2765 (1993) (cit. on pp. 67, 68).

[69]L. P. Kadanoff, S. R. Nagel, L. Wu, and S.-m. Zhou, "Scaling and universality in avalanches," Phys. Rev. A **39**, 6524–6537 (1989) (cit. on pp. 67, 69).

[70]P. Bak, *How nature works: the science of self-organized criticality* (Springer Science & Business Media, 2013) (cit. on p. 67).

[71]S. R. Nagel, "Instabilities in a sandpile," Rev. Mod. Phys. **64**, 321–325 (1992) (cit. on p. 67).

[72]M. Kardar, "Avalanche theory in rice," Nature **379** (1996) (cit. on p. 67).

[73]A. Cipriani, R. S. Hazra, and W. M. Ruszel, "The divisible sandpile with heavy-tailed variables," arXiv preprint arXiv:1610.09863 (2016) (cit. on p. 67).

[74]L. Levine, M. Murugan, Y. Peres, and B. E. Ugurcan, "The divisible sandpile at critical density," in Annales henri poincaré, Vol. 17, 7 (Springer, 2016), pp. 1677–1711 (cit. on p. 67).

[75]L. Levine and Y. Peres, "Scaling limits for internal aggregation models with multiple sources," Journal d'Analyse Mathématique **111**, 151–219 (2010) (cit. on p. 67).

[76]D. Dhar, "Self-organized critical state of sandpile automaton models," Phys. Rev. Lett. **64**, 1613–1616 (1990) (cit. on p. 68).

[77]S. S. Manna, "Large-scale simulation of avalanche cluster distribution in sand pile model," Journal of Statistical Physics **59**, 509–521 (1990) (cit. on pp. 68, 69).

[78]S. Manna, "Critical exponents of the sand pile models in two dimensions," Physica A: Statistical Mechanics and its Applications **179**, 249 –268 (1991) (cit. on p. 68).

[79]H. Nakanishi and K. Sneppen, "Universal versus drive-dependent exponents for sandpile models," Phys. Rev. E **55**, 4012–4016 (1997) (cit. on p. 69).

[80]J. A. B. Fajardo, "Universality in self-organized criticality," PhD thesis (PhD Thesis, Departamento de Electromagnetismo y Fısica de la Materia, Institute Carlos I for Theoretical, and Computational Physics, University of Granada, Spain, 2008) (cit. on pp. 68, 69).

[81]A. Vespignani, R. Dickman, M. A. Muñoz, and S. Zapperi, "Driving, conservation, and absorbing states in sandpiles," Phys. Rev. Lett. **81**, 5676–5679 (1998) (cit. on pp. 69, 91).

[82]A. Chessa, E. Marinari, and A. Vespignani, "Energy constrained sandpile models," Phys. Rev. Lett. **80**, 4217–4220 (1998) (cit. on p. 69).

[83]R. Dickman, A. Vespignani, and S. Zapperi, "Self-organized criticality as an absorbing-state phase transition," Phys. Rev. E **57**, 5095–5105 (1998) (cit. on p. 69).

[84]R. Dickman, M. Alava, M. A. Muñoz, J. Peltola, A. Vespignani, and S. Zapperi, "Critical behavior of a one-dimensional fixed-energy stochastic sandpile," Phys. Rev. E **64**, 056104 (2001) (cit. on pp. 69, 74, 88, 92, 94).

[85]R. Dickman, M. A. Muñoz, A. Vespignani, and S. Zapperi, "Paths to self-organized criticality," Brazilian Journal of Physics **30**, 27–41 (2000) (cit. on p. 69).

[86]R. Dickman, T. Tomé, and M. J. de Oliveira, "Sandpiles with height restrictions," Phys. Rev. E **66**, 016111 (2002) (cit. on pp. 69, 81).

[87]R. Dickman, "Critical exponents for the restricted sandpile," Phys. Rev. E **73**, 036131 (2006) (cit. on pp. 69, 81, 94, 101).

[88]J. Marro and R. Dickman, *Nonequilibrium phase transitions in lattice models* (Cambridge University Press, 2005) (cit. on p. 69).

[89]U. Basu and P. K. Mohanty, "Active-absorbing-state phase transition beyond directed percolation: a class of exactly solvable models," Phys. Rev. E **79**, 041143 (2009) (cit. on p. 69).

[90]Basu, U., Basu, M., and Mohanty, P. K., "Absorbing phase transition in energy exchange models," Eur. Phys. J. B **86**, 236 (2013) (cit. on p. 69).

[91]D. Dhar and R. Ramaswamy, "Exactly solved model of self-organized critical phenomena," Phys. Rev. Lett. **63**, 1659–1662 (1989) (cit. on p. 69).

[92]V. B. Priezzhev, D. Dhar, A. Dhar, and S. Krishnamurthy, "Eulerian walkers as a model of self-organized criticality," Phys. Rev. Lett. **77**, 5079–5082 (1996) (cit. on p. 69).

[93]V. B. Priezzhev, D. V. Ktitarev, and E. V. Ivashkevich, "Formation of avalanches and critical exponents in an abelian sandpile model," Phys. Rev. Lett. **76**, 2093–2096 (1996) (cit. on p. 69).

[94]V. B. Priezzhev, "Structure of two-dimensional sandpile. i. height probabilities," Journal of statistical physics **74**, 955–979 (1994) (cit. on p. 69).

[95]E. Ivashkevich, "Boundary height correlations in a two-dimensional abelian sandpile," Journal of Physics A: Mathematical and General **27**, 3643 (1994) (cit. on p. 69).

[96]D. V. Ktitarev, S. Lübeck, P. Grassberger, and V. B. Priezzhev, "Scaling of waves in the bak-tang-wiesenfeld sandpile model," Phys. Rev. E **61**, 81–92 (2000) (cit. on p. 69).

[97]A. Vespignani, R. Dickman, M. A. Muñoz, and S. Zapperi, "Absorbing-state phase transitions in fixed-energy sandpiles," Phys. Rev. E **62**, 4564–4582 (2000) (cit. on pp. 69, 94).

[98]M. Rossi, R. Pastor-Satorras, and A. Vespignani, "Universality class of absorbing phase transitions with a conserved field," Phys. Rev. Lett. **85**, 1803–1806 (2000) (cit. on pp. 69, 94, 101).

[99]S. Lübeck, "Scaling behavior of the conserved transfer threshold process," Phys. Rev. E **66**, 046114 (2002) (cit. on pp. 69, 101).

[100]S. Lübeck and P. C. Heger, "Universal finite-size scaling behavior and universal dynamical scaling behavior of absorbing phase transitions with a conserved field," Phys. Rev. E **68**, 056102 (2003) (cit. on pp. 69, 101).

[101]S. Lübeck and P. C. Heger, "Universal scaling behavior at the upper critical dimension of nonequilibrium continuous phase transitions," Phys. Rev. Lett. **90**, 230601 (2003) (cit. on pp. 69, 101).

[102]J. A. Bonachela and M. A. Muñoz, "Confirming and extending the hypothesis of universality in sandpiles," Phys. Rev. E **78**, 041102 (2008) (cit. on p. 69).

[103]S. D. da Cunha, L. R. da Silva, G. M. Viswanathan, and R. Dickman, "Activity, diffusion, and correlations in a two-dimensional conserved stochastic sandpile," Journal of Statistical Mechanics: Theory and Experiment **2014**, P08003 (2014) (cit. on pp. 69, 94).

[104]D. Hexner and D. Levine, "Hyperuniformity of critical absorbing states," Phys. Rev. Lett. **114**, 110602 (2015) (cit. on p. 69).

[105]D. Hexner and D. Levine, "Noise, diffusion, and hyperuniformity," Phys. Rev. Lett. **118**, 020601 (2017) (cit. on p. 69).

[106]P. Grassberger, D. Dhar, and P. K. Mohanty, "Oslo model, hyperuniformity, and the quenched edwards-wilkinson model," Phys. Rev. E **94**, 042314 (2016) (cit. on p. 69).

[107]H. M. Jaeger, C.-h. Liu, and S. R. Nagel, "Relaxation at the angle of repose," Phys. Rev. Lett. **62**, 40–43 (1989) (cit. on p. 69).

[108]V. Frette, K. Christensen, A. Malthe-Sorenssen, J. Feder, et al., "Avalanche dynamics in a pile of rice," Nature **379**, 49 (1996) (cit. on p. 69).

[109]T. Hwa and M. Kardar, "Dissipative transport in open systems: an investigation of self-organized criticality," Phys. Rev. Lett. **62**, 1813–1816 (1989) (cit. on p. 69).

[110]M. A. Muñoz, G. Grinstein, R. Dickman, and R. Livi, "Critical behavior of systems with many absorbing states," Phys. Rev. Lett. **76**, 451–454 (1996) (cit. on pp. 69, 91).

[111]J. J. Ramasco, M. A. Muñoz, and C. A. da Silva Santos, "Numerical study of the langevin theory for fixed-energy sandpiles," Phys. Rev. E **69**, 045105 (2004) (cit. on pp. 69, 94).

[112]I. Dornic, H. Chaté, and M. A. Muñoz, "Integration of langevin equations with multiplicative noise and the viability of field theories for absorbing phase transitions," Phys. Rev. Lett. **94**, 100601 (2005) (cit. on pp. 69, 91).

[113]D. Dhar and P. Pradhan, "Probability distribution of residence times of grains in sand-pile models," Journal of Statistical Mechanics: Theory and Experiment **2004**, P05002 (2004) (cit. on p. 69).

[114]P. Pradhan and D. Dhar, "Probability distribution of residence times of grains in models of rice piles," Phys. Rev. E **73**, 021303 (2006) (cit. on p. 69).

[115]S. da Cunha, R. R. Vidigal, L. da Silva, and R. Dickman, "Diffusion in stochastic sandpiles," The European Physical Journal B-Condensed Matter and Complex Systems **72**, 441–449 (2009) (cit. on p. 69).

[116]A. Ben-Hur and O. Biham, "Universality in sandpile models," Phys. Rev. E **53**, R1317–R1320 (1996) (cit. on p. 69).

[117]P. Grassberger, "Are damage spreading transitions generically in the universality class of directed percolation?" Journal of statistical physics **79**, 13–23 (1995) (cit. on p. 69).

[118]P. K. Mohanty and D. Dhar, "Generic sandpile models have directed percolation exponents," Phys. Rev. Lett. **89**, 104303 (2002) (cit. on p. 69).

[119]J. A. Bonachela, H. Chaté, I. Dornic, and M. A. Muñoz, "Absorbing states and elastic interfaces in random media: two equivalent descriptions of self-organized criticality," Phys. Rev. Lett. **98**, 155702 (2007) (cit. on p. 69).

[120]M. Basu, U. Basu, S. Bondyopadhyay, P. K. Mohanty, and H. Hinrichsen, "Fixed-energy sandpiles belong generically to directed percolation," Phys. Rev. Lett. **109**, 015702 (2012) (cit. on pp. 69, 97).

[121]S. B. Lee, "Comment on "fixed-energy sandpiles belong generically to directed percolation"," Phys. Rev. Lett. **110**, 159601 (2013) (cit. on p. 69).

[122]S. B. Lee, "Critical behavior of absorbing phase transitions for models in the manna class with natural initial states," Phys. Rev. E **89**, 062133 (2014) (cit. on p. 69).

[123]S. B. Lee, "Universality class of the conserved manna model in one dimension," Phys. Rev. E **89**, 060101 (2014) (cit. on p. 69).

[124]R. Dickman and S. D. da Cunha, "Particle-density fluctuations and universality in the conserved stochastic sandpile," Phys. Rev. E **92**, 020104 (2015) (cit. on p. 69).

[125]P. Le Doussal and K. J. Wiese, "Exact mapping of the stochastic field theory for manna sandpiles to interfaces in random media," Phys. Rev. Lett. **114**, 110601 (2015) (cit. on p. 69).

[126]H. Touchette, "The large deviation approach to statistical mechanics," Physics Reports **478**, 1 –69 (2009) (cit. on p. 78).

[127]S. Chakraborti, *Private communication*, 2016 (cit. on pp. 82, 94).

[128]M. Henkel, H. Hinrichsen, S. Lübeck, and M. Pleimling, *Non-equilibrium phase transitions*, Vol. 1 (Springer, 2008) (cit. on p. 88).

[129]P. Grassberger, "On phase transitions in schlögl's second model," Zeitschrift für Physik B Condensed Matter **47**, 365–374 (1982) (cit. on p. 88).

[130]L. Bertini, A. De Sole, D. Gabrielli, G. Jona-Lasinio, and C. Landim, "Macroscopic fluctuation theory," Rev. Mod. Phys. **87**, 593–636 (2015) (cit. on pp. 88–91, 95, 97, 99, 100).

[131]A. Das, A. Kundu, and P. Pradhan, "Einstein relation and hydrodynamics of nonequilibrium mass transport processes," Phys. Rev. E **95**, 062128 (2017) (cit. on pp. 88–90, 95).

[132]P. C. Hohenberg and B. I. Halperin, "Theory of dynamic critical phenomena," Rev. Mod. Phys. **49**, 435–479 (1977) (cit. on p. 93).